SSI

SSI 8142-6

October 1982

THE ANALYSIS OF THE EFFECTS OF FRAME RESPONSE ON BASEMENT SHELTERS IN TALL BUILDINGS

FINAL REPORT

for

FEDERAL EMERGENCY MANAGEMENT AGENCY
WASHINGTON, D.C. 20472

Approved for public release; distribution unlimited

Contract No. EMW-C-0570
Work Unit 1128E

SCIENTIFIC SERVICE, INC.

THE ANALYSIS OF THE EFFECTS OF FRAME RESPONSE ON BASEMENT SHELTERS IN TALL BUILDINGS

FEMA Work Unit 1128E. October 1982

SSI 8142-6

UNCLASSIFIED

SECURITY CLASSIFICATION OF THIS PAGE (When Data Entered)

REPORT DOCUMENTATION PAGE		READ INSTRUCTIONS BEFORE COMPLETING FORM
1. REPORT NUMBER 8142-6	2. GOVT ACCESSION NO. AD-A121 609	3. RECIPIENT'S CATALOG NUMBER
4. TITLE (and Subtitle) THE ANALYSIS OF THE EFFECTS OF FRAME RESPONSE ON BASEMENT SHELTERS IN TALL BUILDINGS		5. TYPE OF REPORT & PERIOD COVERED final report
		6. PERFORMING ORG. REPORT NUMBER
7. AUTHOR(s) B.L. Gabrielsen, G.J. Cuzner, J. Hendricks, and T.C. Zsutty		8. CONTRACT OR GRANT NUMBER(s) EMW-C-0570
9. PERFORMING ORGANIZATION NAME AND ADDRESS Scientific Service, Inc. 517 East Bayshore, Redwood City, CA 94063		10. PROGRAM ELEMENT, PROJECT, TASK AREA & WORK UNIT NUMBERS Work Unit 1128E
11. CONTROLLING OFFICE NAME AND ADDRESS Federal Emergency Management Agency		12. REPORT DATE October 1982
		13. NUMBER OF PAGES 156
14. MONITORING AGENCY NAME & ADDRESS(if different from Controlling Office)		15. SECURITY CLASS. (of this report) Unclassified
		15a. DECLASSIFICATION/DOWNGRADING SCHEDULE

16. DISTRIBUTION STATEMENT (of this Report)

Approved for Public Release; Distribution Unlimited

17. DISTRIBUTION STATEMENT (of the abstract entered in Block 20, if different from Report)

18. SUPPLEMENTARY NOTES

19. KEY WORDS (Continue on reverse side if necessary and identify by block number)

basement shelters; blast wave; frame response; reinforced concrete; steel; key worker shelter

20. ABSTRACT (Continue on reverse side if necessary and identify by block number)

This report presents the results of a program to develop a theoretical analysis of the effects of frame response on basement shelters in tall buildings. The objective was to determine the effect on an upgraded basement key worker shelter of the aboveground portion of the structure being subjected to a blast wave that would destroy the building.

Both steel and reinforced concrete frame structures were investigated, with

DD FORM 1 JAN 73 1473 EDITION OF 1 NOV 65 IS OBSOLETE

UNCLASSIFIED

SECURITY CLASSIFICATION OF THIS PAGE (When Data Entered)

20. ABSTRACT (contd)

most emphasis on poured-in-place reinforced concrete beam, slab, and girder type framing and poured-in-place flat-slab and flat-plate construction.

A prediction technique using both hand and computer analysis was developed and tested using a previously demolished 15-story cast-in-place reinforced structure. The analysis indicated that the upgraded basement would have survived even though the aboveground portion of the structure was exposed to 50 psi.

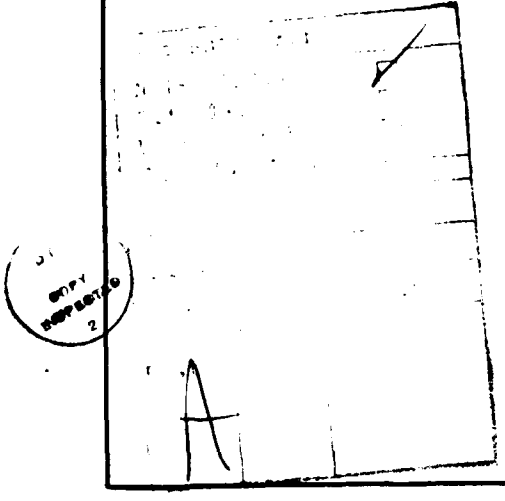

(DETACHABLE SUMMARY)

SSI 8142-6 Final Report
October 1982

THE ANALYSIS OF THE EFFECTS OF FRAME RESPONSE ON BASEMENT SHELTERS IN TALL BUILDINGS

by

B.L. Gabrielsen, G.J. Cuzner, J. Hendricks, and T.C. Zsutty

for

Federal Emergency Management Agency
Washington, D.C. 20472

Contract No. EMW-C-0570, Work Unit 1128E

Scientific Service, Inc.
517 East Bayshore, Redwood City, CA 94063

(DETACHABLE SUMMARY)

THE ANALYSIS OF THE EFFECTS OF FRAME RESPONSE ON BASEMENT SHELTERS IN TALL BUILDINGS

This report presents the results of a program to develop a theoretical analysis of the effects of frame response on basement shelters in tall buildings. The objective was to determine the effect on a upgraded basement key worker shelter of the aboveground portion of the structure being subjected to a blast wave (30 to 50 psi) that would destroy the building.

This program investigated both steel and reinforced concrete frame structures with the most emphasis on poured-in-place reinforced concrete beam, slab, and girder type framing and the poured-in-place flat-slab and flat-plate type of construction. These types are very common in the National Shelter Survey inventory of upgradable structures.

A prediction technique was developed using both hand and computer analysis. This technique was tested using a previously explosively demolished 15-story cast-in-place reinforced structure, the Continental Life Building in Atlanta, Georgia. The results of this analysis indicated that the upgraded basement would have survived even though the aboveground portion of the structure was exposed to 50 psi.

Large portions of the debris landed on the shelter roof so that serious questions remain as to the advisability of using such structures as shelters because of the possible problems of entrapment of the shelterees. Other problems that need to be addressed are the large amounts of dust created in the collapse process and the possibility of fire in the debris pile.

It also should be noted that the primary work in this program was on reinforced concrete structures, where the punching effects of falling columns do not appear to be a problem. Based on the experiences of an explosive demolition contractor, Controlled Demolition, Inc., this appears to be a serious problem in steel framed structures. It is recommended that future work in this area thoroughly investigate the collapse of steel frames both theoretically and in conjunction with building demolitions. Also, as was noted in Section 4, very little information is available on the load imparted to a frame by failing walls at pressures above 15 psi. Tests at the higher pressures of interest (30 to 50 psi) need to be conducted.

SSI 8142-6 Final Report
October 1982

THE ANALYSIS OF THE EFFECTS OF FRAME RESPONSE ON BASEMENT SHELTERS IN TALL BUILDINGS

by

B.L. Gabrielsen, G.J. Cuzner, J. Hendricks, and T.C. Zsutty

for

Federal Emergency Management Agency
Washington, D.C. 20472

Contract No. EMW-C-0570, Work Unit 1128E

FEMA REVIEW NOTICE:

This report has been reviewed in the Federal Emergency Management Agency and approved for publication. Approval does not signify that the contents necessarily reflect the views and policies of the Federal Emergency Management Agency.

Scientific Service, Inc.
517 East Bayshore, Redwood City, CA 94063

ACKNOWLEDGEMENTS

The authors wish to take this opportunity to thank all those involved in this project, particularly Dr. Michael A. Pachuta of the Federal Emergency Management Agency for his contributions to overall project direction and his thorough and helpful review. We would also like to acknowledge the assistance given by the staff of Controlled Demolition, Inc., both for allowing us access to their files and for sharing their insight into building collapse mechanisms.

Particular thanks for contributions to this project are due to our colleagues on the SSI technical staff: R. S. Tansley, R. E. Lindskog, R. DeMoraes and A. B. Willoughby. The excellent work by members of the SSI support staff, Larue Wilton, Evelyn Kaplan, Maureen Ineich and Michele Boyes in the preparation and reproduction of the report is also gratefully acknowledged.

TABLE OF CONTENTS

LIST OF TABLES

LIST OF FIGURES

Section 1

INTRODUCTION

Civil Defense planning in the United States is currently based on a policy termed "Crisis Relocation". This policy presumes that a period of crisis buildup in the world -- similar to the 1961 Cuban and the more recent Middle East crises -- will precede any future war. This period of crisis would allow time (a few days or weeks) to conduct a number of activities to protect the civilian population and industry from possible attack. These activities include: evacuation of the major portion of the population to low-risk areas where only fallout and possibly low level blast protection would be required; the hardening and protection of critical industries and facilities; and the provision of shelters for a small contingent of key workers (who will remain behind to maintain vital services - communications, fire protection, military production, etc.).

This project was concerned with the last of these activities, the provision of shelters for key workers. As stated in the RFP, the objective of this program was to "Develop a theoretical analysis of the damage to key worker basement shelters that may result when the buildings in which they are located are subjected to a nuclear weapons blast (peak overpressure 30 - 50 psi) so that the buildings are destroyed and the integrity of the shelters may be threatened. The response of the building frame as it relates to the integrity of the shelter and the survival of those in the shelter should be explored in detail."

Various key worker shelter concepts have been explored, including the upgrading of basements in existing structures (for example, Refs. 1 through 6.) Work has also been done on: predicting the collapse levels of floors over basements (for example, Refs. 2 and 7 through 10); failure predictions and full-scale tests of walls (for example, Refs. 11 and 12); the flow of blast waves through openings (for example, Refs. 13 through 21); and the effects of fire on basement shelters (for example, Refs. 22 through 24).

Until now, however, very little work has been done on the combined problem; i.e., what is the effect of the building collapse on the survivability of an upgraded shelter located in the basement? There are several concerns. For example, the blast wave might not shear off a building just above the basement, but might cause localized basement wall failures or upgraded basement roof slab failures, because of either the frame response or the impact of debris. Moreover, at pressure levels of 30 to 50 psi most structures will collapse, and much of the structure may land on the floor over the basement. The buildings considered in this study (4 to 6 story and 10 to 12 story) are expected to provide the greatest opportunity for massive superstructure collapse onto the floors over basement space. In addition, structures of these story heights often appear in groups; thus, if debris from a structure falls clear of its basement, surrounding structures would be likely to supply an equivalent mass of debris.

Relevant past research is best represented by the SRI reports by Wiehle, Refs. 9 and 10, and its limitations are best illustrated by the following statements extracted from these reports. From Ref. 9,

> "The strength of the exterior walls is important in calculating the collapse of the frame, since, for a given overpressure level, the blast loading on the total wall area can be much more severe than the blast loading on the frame alone plus an impulse loading from a frangible-type wall.
>
> To investigate the relative strength of the exterior walls and frame of a building would require a comprehensive computer program that includes inelastic response under dynamic loading as well as realistic frame collapse mechanisms. Since such a program was not available, a computer program for analyzing the elastic and inelastic dynamic response of two-dimensional structural frames was used . . . . Although the program does not include frame collapse mechanisms, it was felt that the results would provide a basis for estimating the possible collapse strength of a building frame relative to the strength of the exterior walls."

and from Ref. 10,

> "The collapse of the floor slab over basement areas is an important consideration in determining the survivors in nuclear blast environments. However, collapse predictions for the floors in the Greensboro-High Point buildings could not be included in this effort because the procedures are currently being developed. The analysis of floor slabs will be included in the building collapse predictions when the procedures become available."

In summary, previous efforts have consisted of investigations to establish exterior wall failure overpressures and approximate analyses of frame response in a corresponding range of overpressures, but excepting the SSI work on the key worker manual and the companion technical manual (Refs. 1 and 2), the failure analysis and theoretical efforts have been performed on "as is" structures. Such analyses fall short of present needs because, as discussed in Section 4, the failure modes are significantly different when a structure is upgraded. Another unfortunate circumstance with earlier work is that little of the existing test data on wall/frame interaction has been made directly available. In the early days of the shock tunnel test program (Ref. 11), measurements were made via load cells installed on all walls tested, to enable this interaction to be investigated. However, objectives at that time precluded the expenditure to reduce the unreported data for current application, so that only reported early data have been utilized.

Recognizing the limitations in the past research and the need to apply the wall/frame interaction data in the light of knowledge of basement upgrading schemes, the research described in this report was performed to answer the following questions: Given a time-varying blast load on a frame building structure, see Figure 1-1,

- What are the various conceivable collapse mechanisms (e.g., "falling tree", "soft story" and fractured members)?

- What combinations and sequences of these occur and which are the most prevalent?

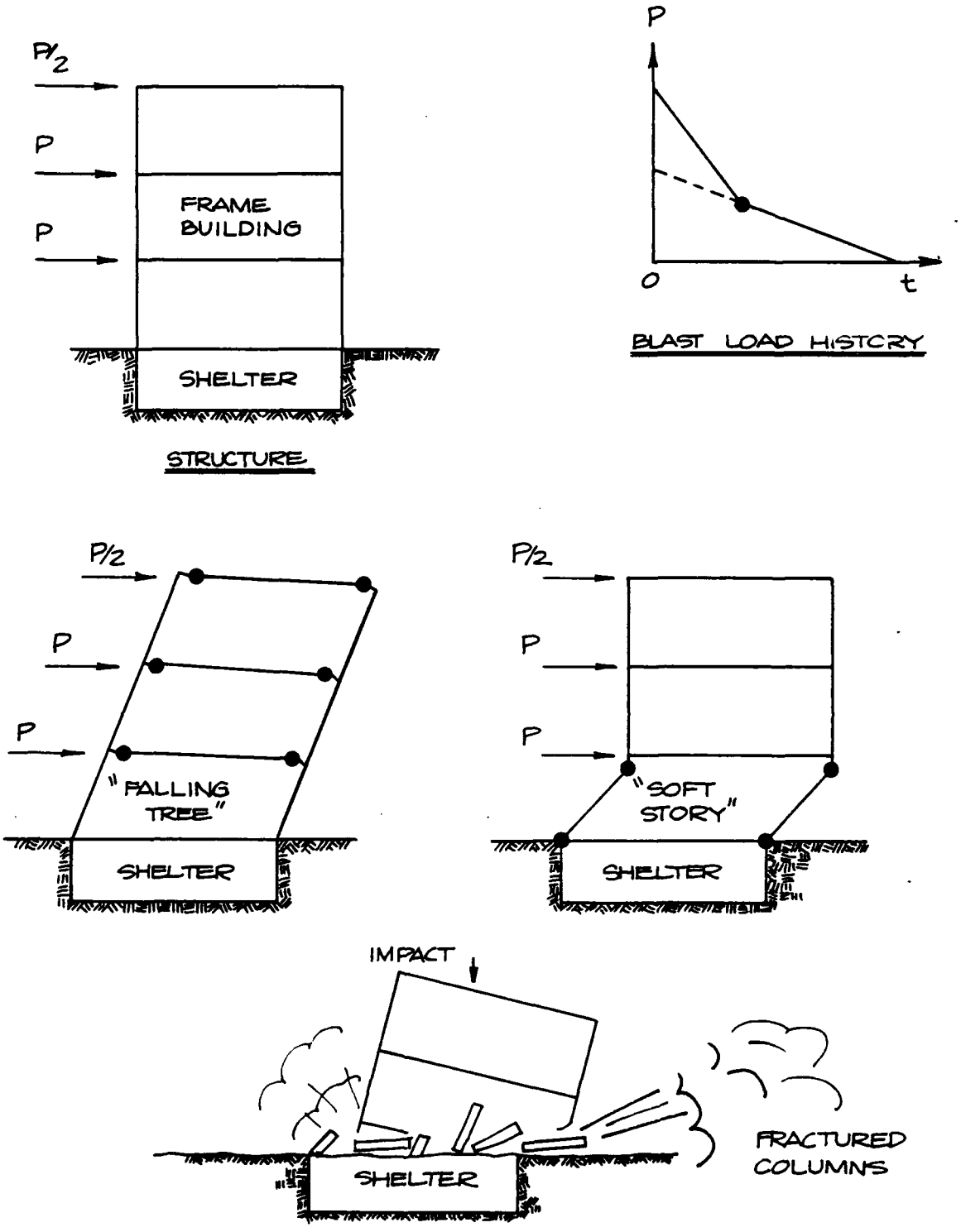

Fig. 1-1. Collapse Mechanisms.

- Given the prevailing collapse mode sequence, what effects do the collapse mechanism and debris impact have on the upgraded shelter space?

The technical approach taken to answer these questions consisted of four tasks:

Task 1 - Building Selection

Representative medium-rise and high-rise frame buildings with basement shelter space were reviewed for an example to demonstrate the analysis.

Task 2 - Development of Upgrading Plans

Previous SSI shelter work was used to prepare shelter area upgrading plans to apply in the structure selected for the example. The upgrading was for combined blast and radiation effects.

Task 3 - Theoretical Analysis

This was divided into three subtasks:

3A - Development of blast-generated loading criteria.

3B - Development of joint resistance functions. Ultimate strength capacities for both steel and reinforced concrete were adopted for the frame mechanism joint resistance functions.

3C - Theoretical analysis of the damaging effects of frame response. The theory of plastic analysis was used to predict the frame failure modes, and the resulting force and distortion information was used to evaluate effects on the shelter cover slab.

Task 4 - Computer Model Development and Analysis

The dynamic analysis portion of the program used the static and dynamic features of the Georgia Tech Integrated Civil Engineering System Structural Design Language, GTSTRUDL (Ref. 25), combined with a progressive collapse mechanism model to predict the time history of the frame response and mode of failure. The results were then evaluated with respect to the effect on the shelter cover slab.

The remainder of this report is organized as follows: Section 2 discusses building selection (Task 1); Section 3 deals with the development of upgrading plans (Task 2); Section 4 presents the theoretical analysis (Task 3 and its associated subtasks); Section 5 discusses the computer model development, analysis and results (Task 4); and Section 6 presents the summary and conclusions. Applicable concepts of plastic analysis are discussed in Appendix A, computer analysis fundamentals are presented in Appendix B, and a discussion of loading functions is to be found in Appendix C.

Section 2

TASK 1 - BUILDING SELECTION

INTRODUCTION

The selection of a building structure for analysis required that each candidate structure be evaluated using criteria that would assure that the final selection was representative, compatible with all of the tasks required in the program, and ultimately, would lend itself to a definitive assessment of the computer model. The following parameters were judged to be the most important, and were included in the selection process:

I. The structure should be either a high-rise (10 to 12 stories) or a medium-rise (4 to 6 stories).

II. The basement should be large enough to provide shelter space for 50 people when it was upgraded in accordance with Ref. 1 to survive 30 to 50 psi — before giving consideration to collapsing stories above the floor over the basement.

III. Sufficient data on the building should be available in the form of structural as-built drawings in order that the theoretical analysis could be performed.

IV. The structural building frame should not just "blow away", but be of a type that offers reasonable lateral resistance so as to develop representative results (e.g., a prybar effect on the below-grade structure). The frame columns should extend through the ground floor to the basement foundation, in order to determine the failure effects of the columns on the ground floor slab.

V. The building should be representative of those in use today, and not be a unique structure, such as possibly a very old building that was designed and constructed using methods and materials no longer in common use.

Two concrete structural types that fit these criteria are shown in Figure 2-1.

CANDIDATE BUILDINGS

Candidate buildings were obtained from three sources and a preliminary list of structures compiled for comparison with the above criteria (items I - V) in order to select one for complete analysis. The three pools of buildings were: (1) structures from the National Shelter Survey, (2) structures scheduled to be demolished, and (3) structures recently demolished. How this preliminary list was evaluated is discussed below.

National Shelter Survey

It was believed that the National Shelter Survey would be a viable source for candidates for analysis because of the large number of buildings and the various types of construction that were included, and the documentation of each that had previously been accomplished. The following six buildings (see Ref. 26) from the National Shelter Survey were selected for the preliminary list; the prints and data were provided by James E. Beck & Associates.

1. Henry R. Landis State Hospital, Philadelphia, PA (NSS No. 110) — Constructed in 1960, the complex consists of five attached structures, three seven stories in height, one three stories high, and one two stories high. The basic construction is a reinforced concrete frame with floors and/or roofs consisting of several types of reinforced concrete construction, including one- and two-way slab and beam, one-way pan and joist, waffle slab, and open-web steel joists with metal deck and concrete topping. The walls are of masonry construction, generally concrete block with brick veneer. One of the seven-story buildings contains a partial basement.

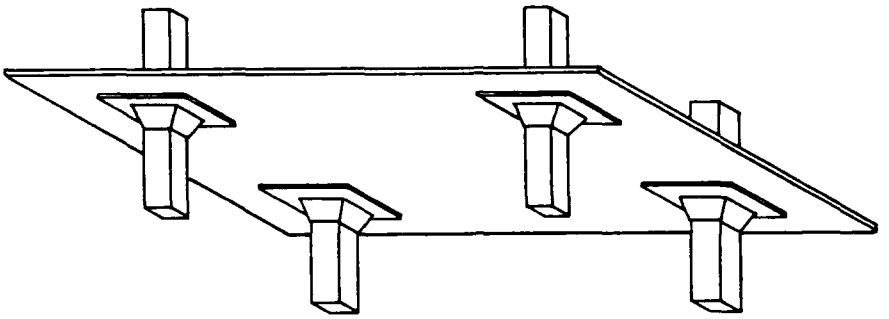

A. The Flat Slab

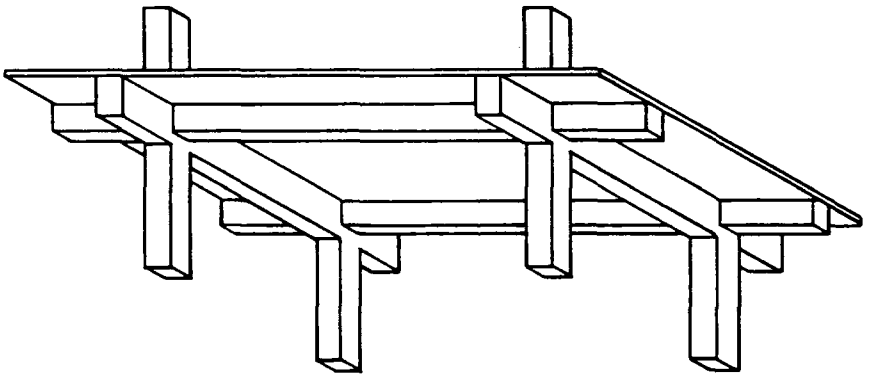

B. The Two-Way Slab

Fig. 2-1. Examples of Slab Systems.

These structures were judged to be unsuitable for this program because of the lack of size (item II).

2. Library Building, University of Illinois, Chicago, IL (NSS No. 149) — This building is a four-story structure with a full basement, and is constructed of reinforced concrete columns and girders supporting precast concrete beams and 5-in. thick slabs concrete topped with 3-in. of concrete. The walls are of infill masonry construction. The building was constructed in 1967.

The design of the building is rather unique and does not meet the criteria of what might be considered "typical" construction (item V). The building frame offers very little resistance to lateral loads (item IV), and it was therefore judged that the analytical results would not prove satisfactory.

3. City Hall, Houston, TX (NSS No. 196) — An eleven-story steel frame structure with a full basement constructed in three stages in 1937, 1939, and 1953. The photographs of the building and the NSS Data Collection Form indicated that the structure was a possible candidate for analysis; however, the drawings supplied were completely unreadable, and no usable data for analysis could be extracted (item III).

4. Fidelity Federal Plaza Office Building, Long Beach, CA (NSS No. 220) —This structure is an eleven-story reinforced concrete frame building with two full levels below grade. It was constructed in 1967. The structural floor system consists of reinforced concrete one-way slabs and beams, and the walls are 6-in. thick reinforced concrete. The building is very large and complex for the first efforts at collapse prediction. (This is not one of the criteria for rejection, but a somewhat simpler structure was sought.)

5. Eastland Shopping Center, West Covina, CA (NSS No. 227) — This shopping complex consists of five separate structures; i.e., one three-story department store and four one-story specialty shop buildings, all constructed in 1956.

The department store is of reinforced concrete frame construction and has a small partial basement. The first floor is of reinforced concrete flat slab and one

way pan and joist construction, and the second and third floors are all one-way pan and joist construction. The walls are a mixture of reinforced concrete and masonry.

The four specialty shop buildings are all of the same construction and are located over one full basement. The first floors are of reinforced concrete one-way pan and joist, one-way slab and beam, and precast prestressed concrete double-tee construction. The roof is entirely constructed of double-tees, and the walls are a combination of masonry and reinforced concrete.

The department store was judged to be unacceptable because of the absence of a suitable basement area (item II), and although the specialty stores had suitable basements, the building did not have sufficient height (item I).

6. Lincoln 1st Federal Savings Office Building, Spokane, WA (NSS No. 248) -- This structure is an eight-story building constructed in 1963. The first two levels are reinforced concrete one-way slab and beam construction, and the remaining floors are steel frame with steel beams and purlins supporting metal deck, topped with concrete. The walls are of metal studs, insulation, and various interior finishes, and the exterior is faced with marble. The building has two full levels below grade.

This building was rejected for analysis because of incomplete drawings - only the architectural drawings were furnished (item III).

Buildings Scheduled for Demolition

Another source for selecting candidate buildings was obtained through our work in connection with FEMA Contract EMW-C-0582, Building Demolition. It was anticipated that a minimum of eight to ten buildings would be explosively demolished during the contract period.

The use of these structures would have several advantages. They are more likely to be completely documented structurally, as the demolition contractor is required to make a thorough investigation in order to determine the optimum location

for placement of explosive charges (e.g., test shots are normally conducted to determine the strength of component parts) and they are usually vacant — thus accessible for surveys. Moreover, the post-demolition data would be valuable as input and as a check on the theoretical analysis. As there were no NSS buildings suitable from the plans at hand, we added a criterion; i.e., item VI - demolition data should be available to compare with analysis.

The six candidate structures that would possibly be available included the following:

1. **Brewery Building, NJ** — A six-story reinforced concrete structure. This building would be interesting from the standpoint of an experiment in that the planning was to demolish only the top floors and leave the lower two floors intact for future use as a shopping mall.

2. **Medical School Dormitory, Minneapolis, MN** — A seven-story building with floors of reinforced concrete pan and joist construction and hollow tile walls. The building was constructed in the early 1930's.

3. **Bank Building, Jacksonville, FL** -- A fifteen-story building constructed of a steel frame encased in tile.

4. **Office Buildings, Buffalo, NY** — Two fifteen-story buildings constructed of structural steel.

5. **Cornhusker Hotel, Lincoln, NB** — A ten-story hotel constructed in 1927 of reinforced concrete one-way slab, beam and girder construction. The infill walls were hollow clay tile covered with brick veneer, and the building had a partial basement.

6. **Olympic National Life Building, Seattle, WA** — A twelve-story reinforced concrete slab, beam, girder and column building constructed in 1906. The walls were reinforced concrete clad with sandstone veneer. The building had a full basement.

Because of the economic climate, during the past year only Nos. 5 and 6, the Cornhusker Hotel in Lincoln and the Olympic National Life Building in Seattle, have been demolished this year. Both of these structures were very old, not typical of contemporary construction, and it was therefore felt that they would not produce data consistent with the intent of the contract. Buildings Nos. 1 through 4 were rejected because of item VI — there would be no demolition data.

Buildings Previously Demolished

Further sources for candidate buildings in Contract EMW-C-0582 included previously demolished buildings. A data search of files on these buildings was performed to determine if any buildings previously demolished could be used. Four candidate structures were selected for analysis from the files of Controlled Demolition, Inc. (CDI).

1. **American Industrial Building, Hartford, CT** -- A 16-story box column steel-gusseted structure. This was an interesting structure from an analysis standpoint; however, no plans were available showing the structural details (item III).

2. **Abe Lincoln Hotel, Springfield, IL** -- A 14-story structure, cast-in-place concrete, with a large lobby area. Massive concrete beams spanned the lobby, and this would have provided an excellent example of the "soft-story" collapse mechanism; however, again no detailed plans were available (item III).

3. **Tutwiler Hotel, Birmingham, AL** -- A 14-story, steel framed structure. This building was built using steel produced in a local steel mill, and was designed with the exterior columns being approximately three times as stiff as the interior columns. Thus, this building was eliminated because the exterior frame was not typical of most buildings (item V).

4. **Continental Life Building, Atlanta, GA** — A 15-story, cast-in-place reinforced concrete structure. Constructed about 1950, the building covered and area 90 feet by 150 feet. The structure had a full basement 11 feet high, a first floor 16 feet high, with the remaining stories being 10 feet high (see Figures 2-2 and 2-3).

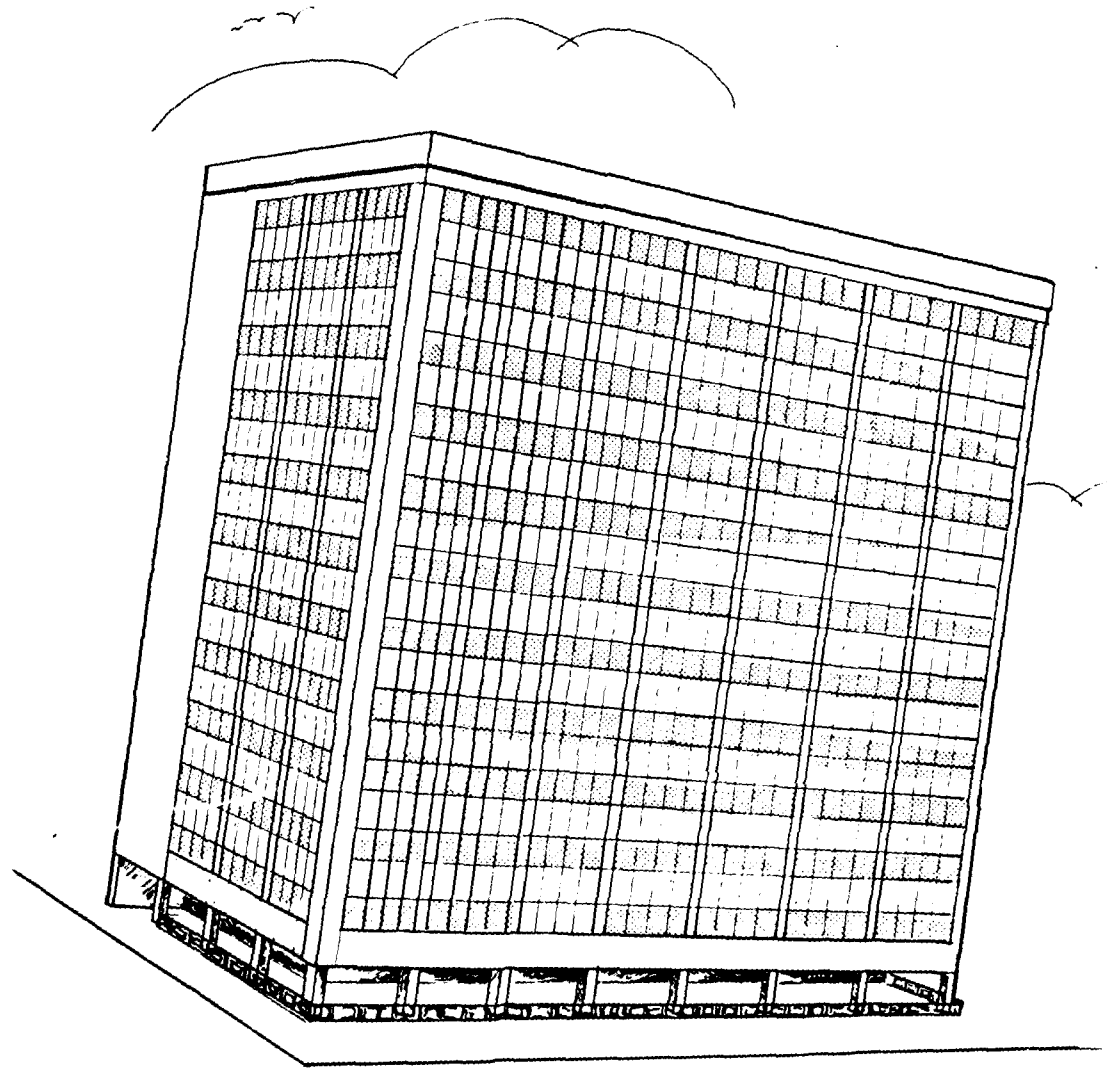

Fig. 2-2. Sketch of Continental Life Building, Atlanta, Georgia.

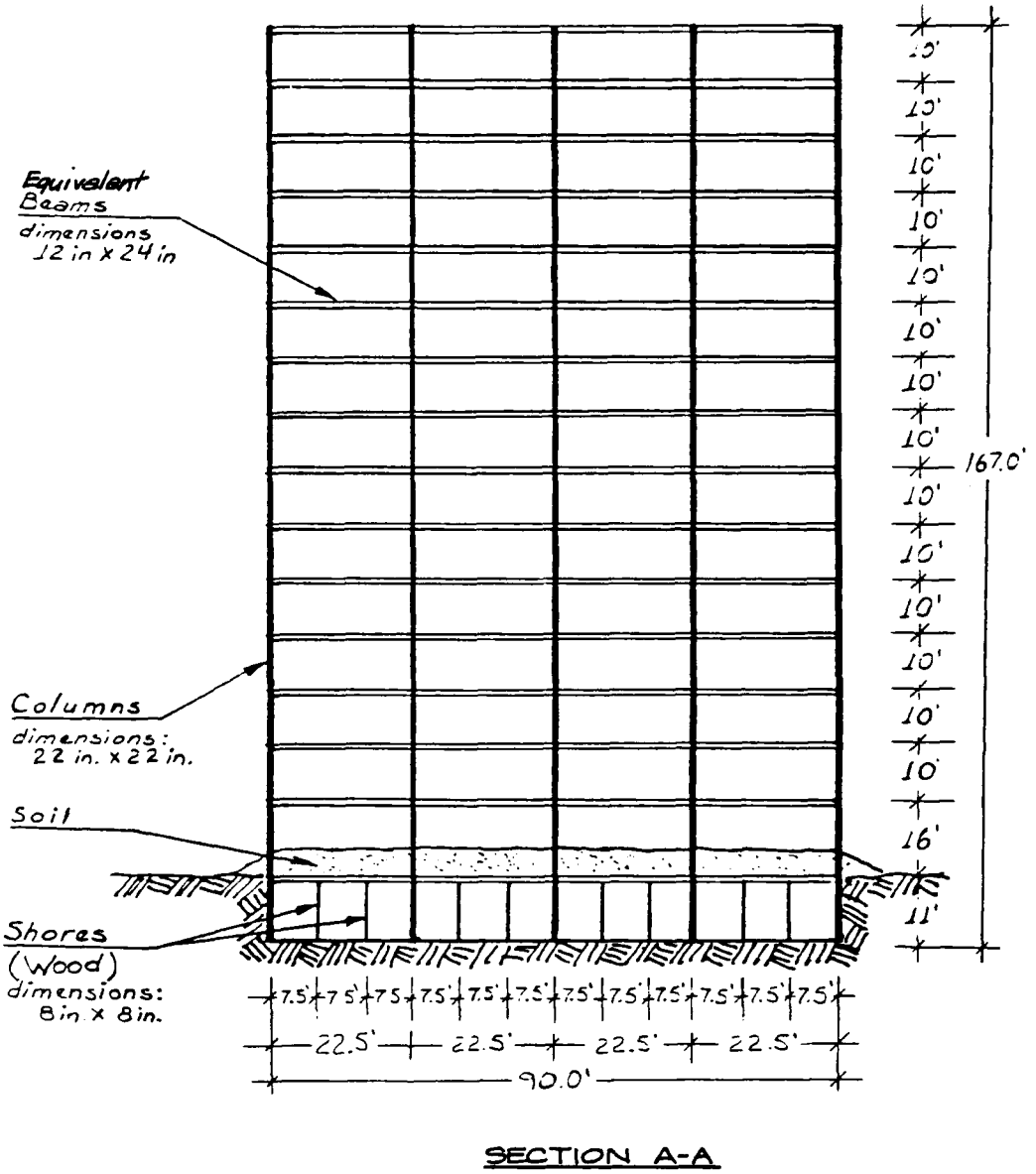

Fig. 2-3. Elevation View of Continental Life Building, Atlanta, Georgia.

On three sides the wall panels were of masonry and glass, while the fourth side (on the north) was constructed with a 5-story high reinforced concrete shear panel with block masonry the remainder of its height.

Supporting columns were 22 in. square, with three interior rows the length of the building supporting one-way pan joist beam and girder construction. Pans were 12 in. by 20 in. with a beam length of 22 ft 6 in. and a 12 in. by 24 in. structural section. Girders spanned 21 ft 6 in. with a 14 in. by 28 in. structural section. Column reinforcement was spiral wrapped.

BUILDING SELECTION

This last building, the Continental Life Building (or "Peachtree", after its street address) in Atlanta, met nearly all of the criteria, and was selected for the "program tuning" structure under this contract. The required data on the as-built structure itself, as well as information on its demolition, were readily available from the files of CDI, the demolition contractor. The fact that this building was a reinforced concrete structure, and thereby focused the investigation on this type of structures, does not in any way restrict the generality of the theoretical analysis or of the computer modeling, but only limits the breadth of the verification.

Section 3

TASK 2 - UPGRADING PLANS

BASEMENT UPGRADING PLANS

Using the guidance developed in previous SSI reports (Refs. 1 and 2), and augmented with other reports, upgrading plans were developed for the structure selected. Upgrading plan details include:

1. Layout of the basic upgrading system.

2. Selection of type, size, and location of the particular structural members used in the upgrading. Consideration was given to how the material would be brought into the structure and installed.

3. Design of closures to seal openings.

4. Special upgrading for unusual areas in or near the designated shelter space, including closures.

5. Specification of initial radiation and fallout protection.

6. Design of emergency access and egress structures.

Experience in the recent MILL RACE test event (Ref. 27) was used to supplement items 1 through 4 in the upgrading scheme.

The basement area for upgrading is shown in plan view on Figure 3-1a, and the structural details of the first floor slab are given in Figures 3-1b and 3-1c. Structural upgrading of the first floor is necessary to enable both the placement of soil to provide the necessary protection against radiation and to provide support to

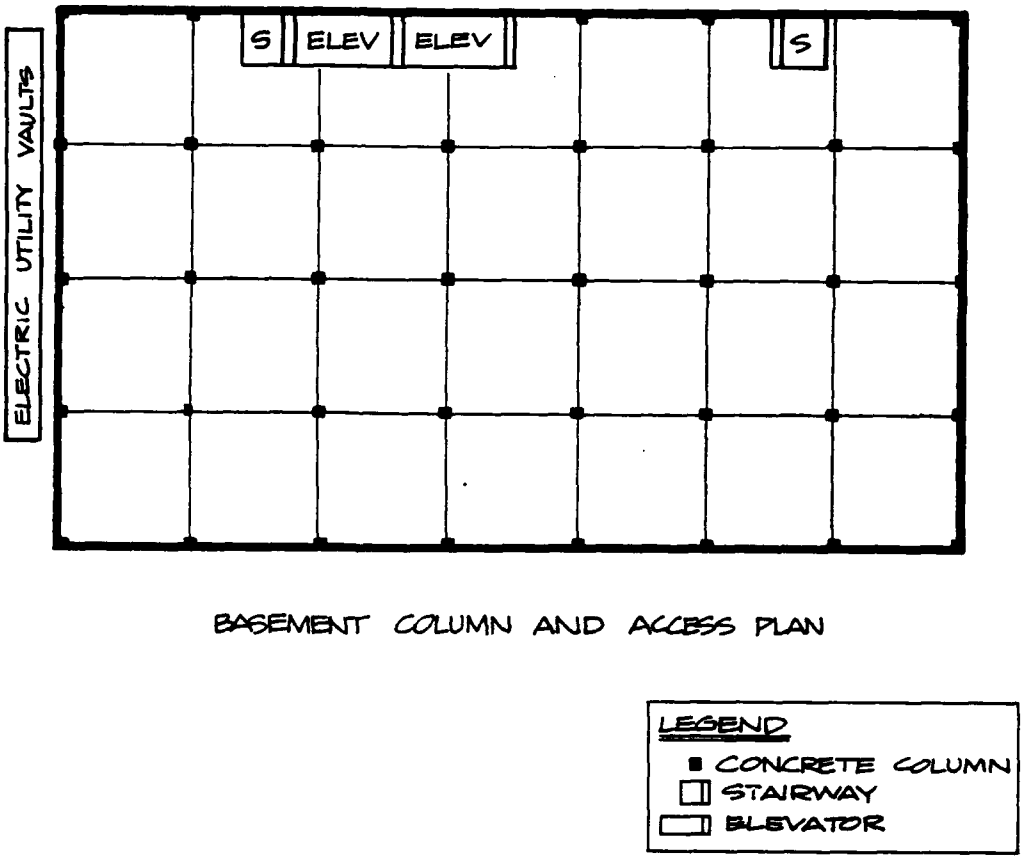

Fig. 3-1a. Plan of Basement Showing Column, Elevator, Stairway, and Utility Vault Locations.

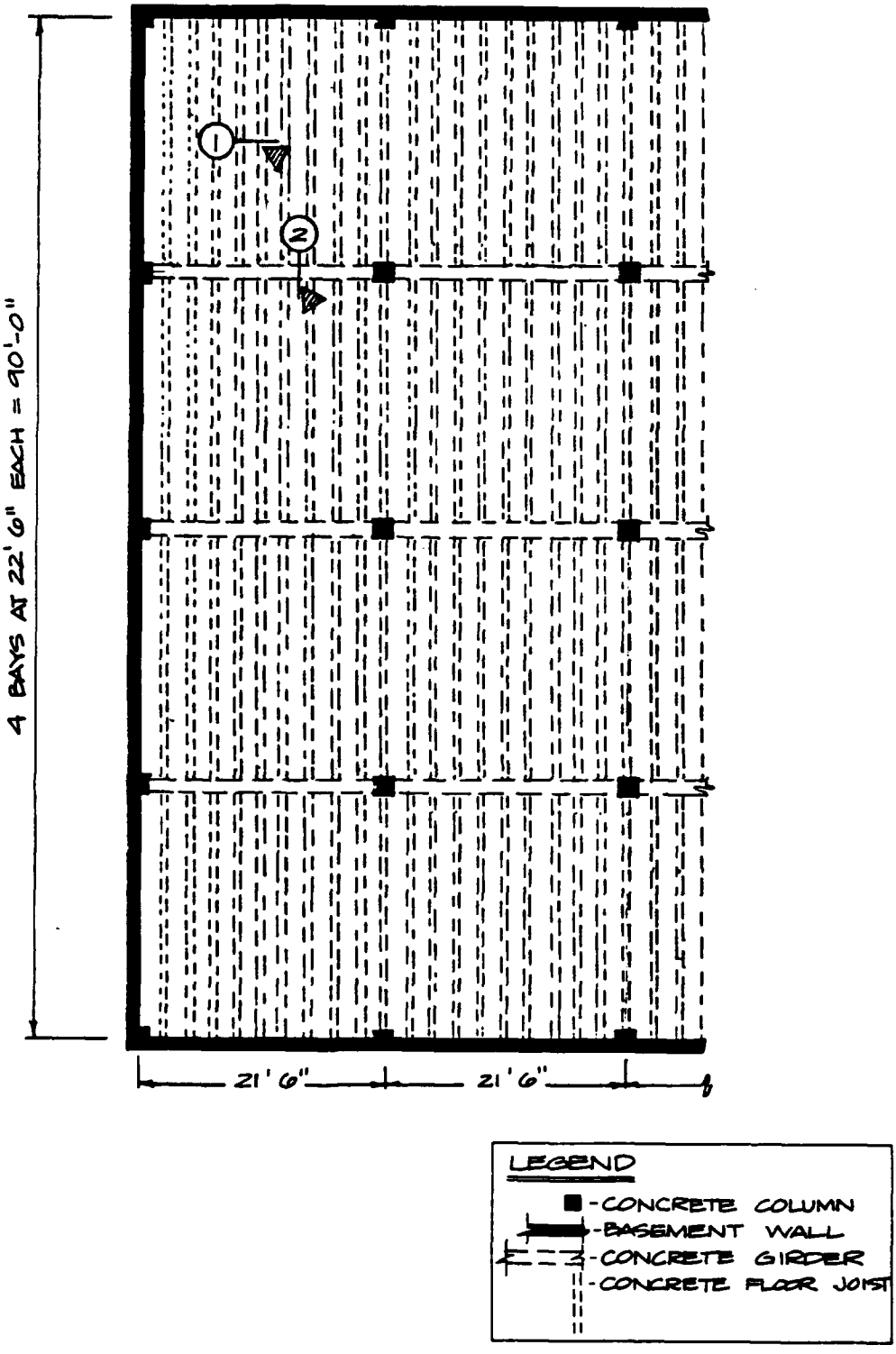

Fig. 3-1b. Section of First Floor Showing the Framing Plan.

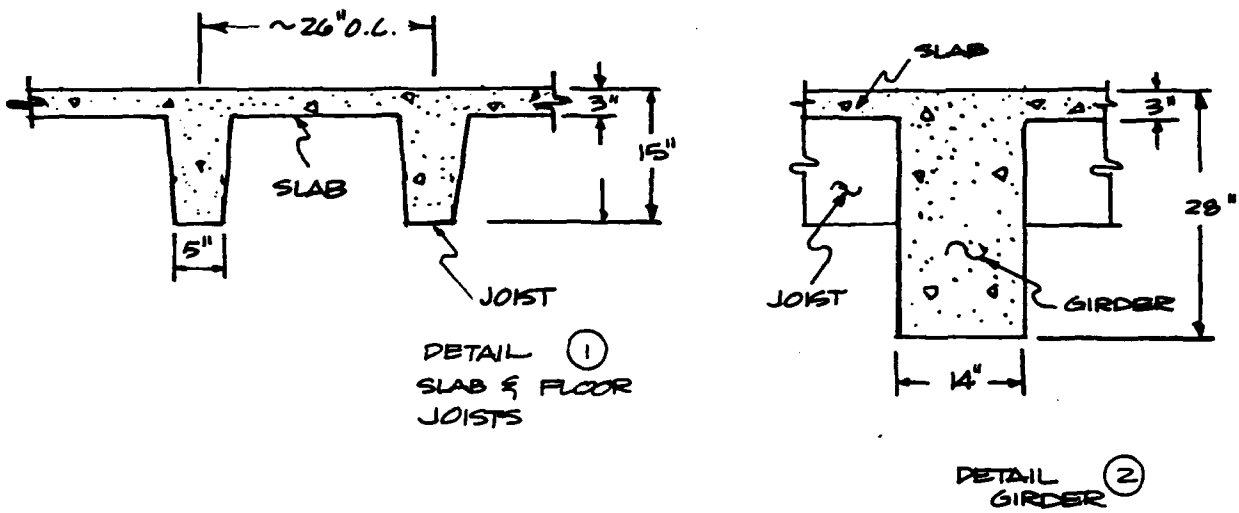

Fig. 3-1c. Details of Framing Plan in Figure 3-1b.

the floor for blast overpressures on the order of 30 to 50 psi. The upgrading plans, which follow, are designed for a protection factor (Pf) of 1,000 against fallout radiation.

Radiation Protection

The overhead mass required for radiation protection in this basement shelter is 300 psf to achieve the Pf of 1,000. The first floor slab is 3 inches thick and provides only 13% of the required overhead mass. Soil, having a density of 100 lb per cubic foot, and placed to a depth of 32 inches over the entire first floor, is the most expedient solution and will be used for this structural upgrading. The basement area 90 feet wide by 150 feet long with 32 inches of soil will require 1,330 cubic yards of soil to be hauled to the site and placed on the floor.

Blast Protection

The first floor must be upgraded to withstand from 30 to 50 psi blast overpressure in addition to the weight of the 32 inches of soil, which is required for radiation protection. The recommended method (Ref. 1) for a floor system of this type is to use post and beam shoring beneath the joists and post shoring beneath the girders. The shoring can be placed no farther apart than the quarter span distance for the members being shored. Figures 3-2a and 3-2b show the post and beam shoring that is required beneath the joists, and Figure 3-3 shows the post shoring that is used beneath the girders.

Shoring

A plan of the post and beam shoring arrangement for the basement is shown in Figure 3-4. It should be noted that the posts and beams weigh 150 lb and 350 lb, respectively; the timber posts and beams can be hauled via standard elevators into the basement. While two men can handle and erect the post shoring, the post and beam shoring will require mechanical assistance. Post and beam shoring can be placed by two men with the aid of either a sheetrock jack or a forklift, both of which are available at most equipment rental shops. Actual field testing has been conducted using this type of shoring showing its feasibility (see Ref. 27). In order to achieve lateral stability of the entire shoring system, it is recommended that the bracing shown in Figure 3-5 be installed.

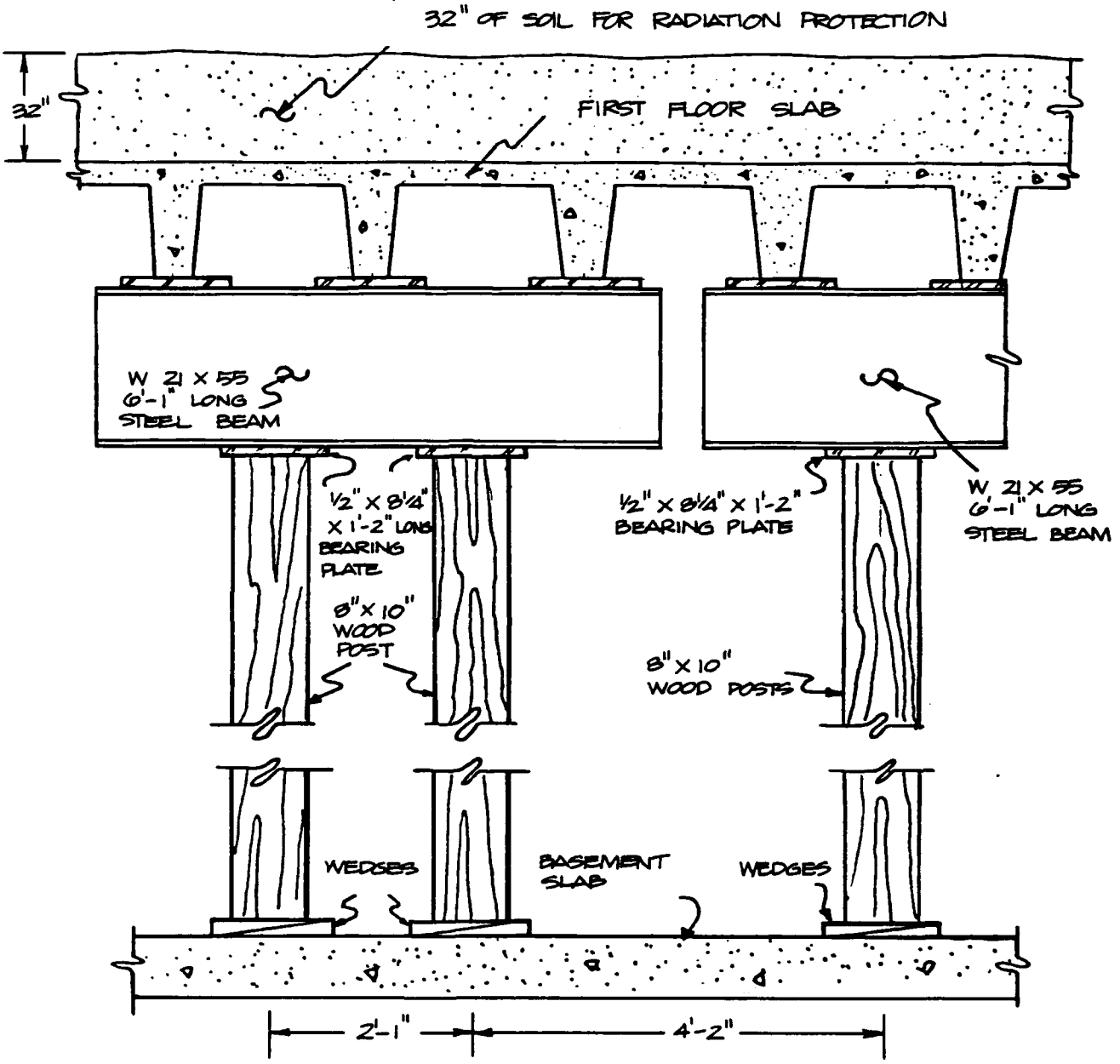

Fig. 3-2a. Post and Beam Shoring of Concrete Joist.

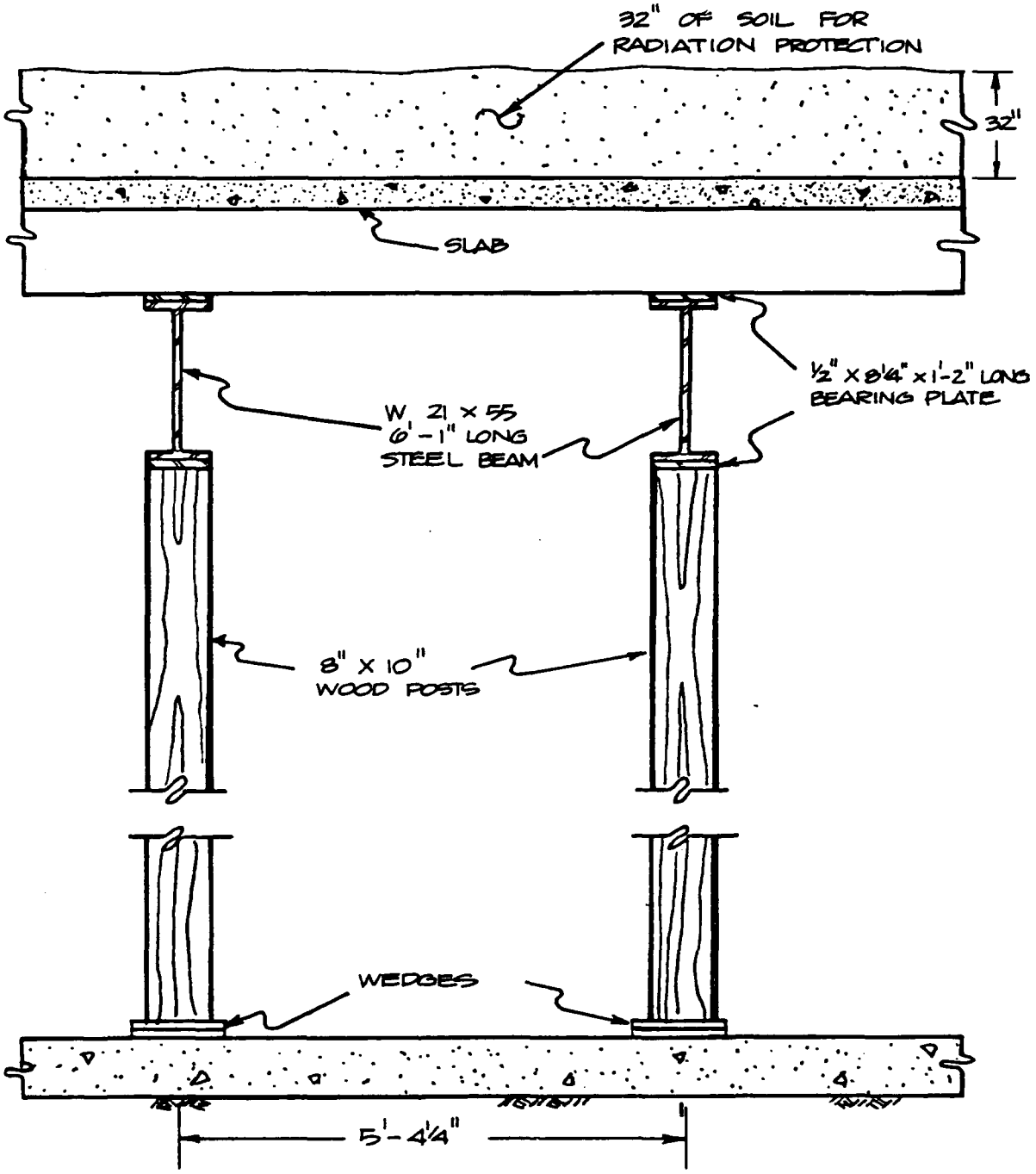

Fig. 3-2b. Post and Beam Shoring.

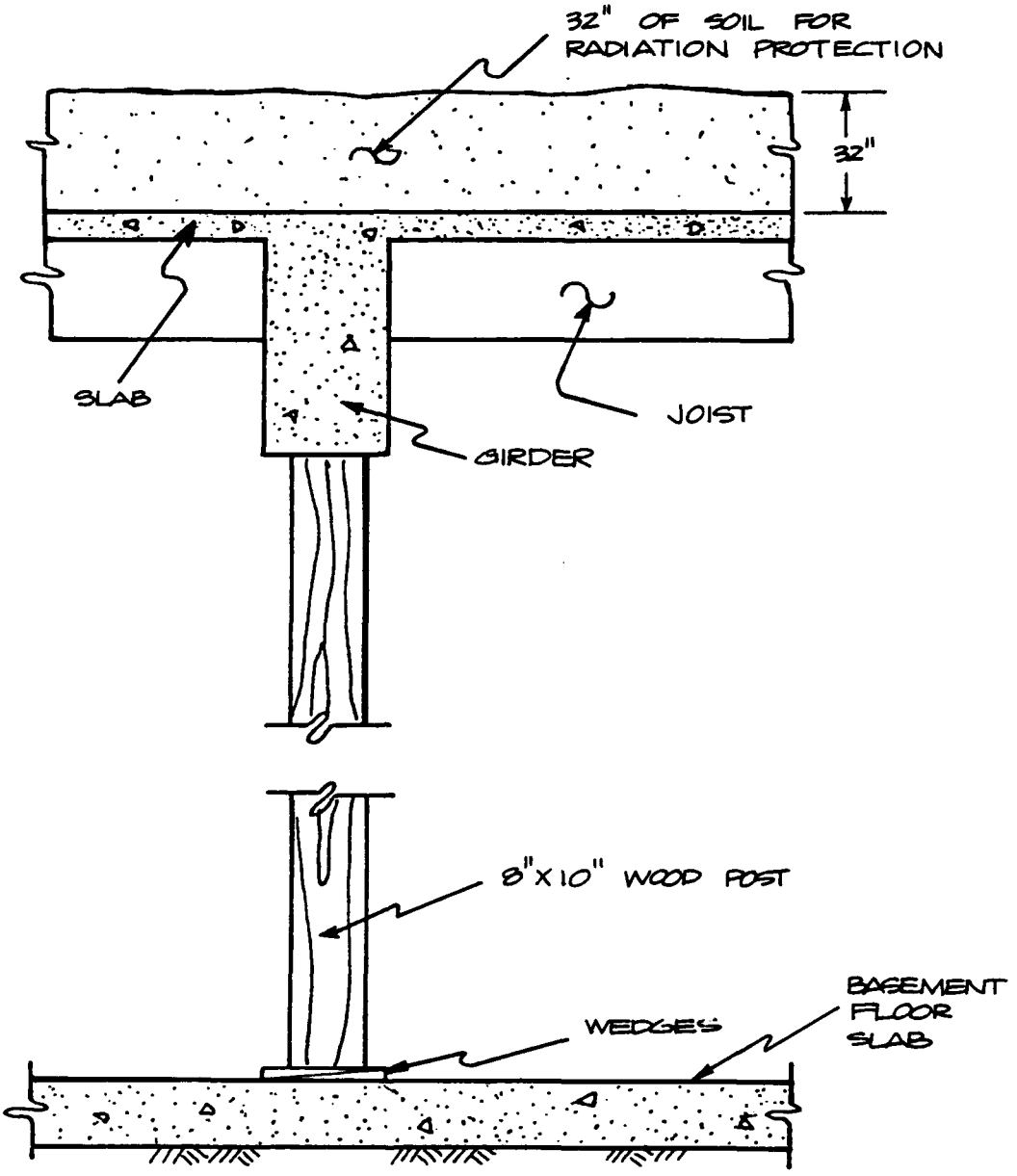

Fig. 3-3. Post Shoring Detail of Concrete Girder.

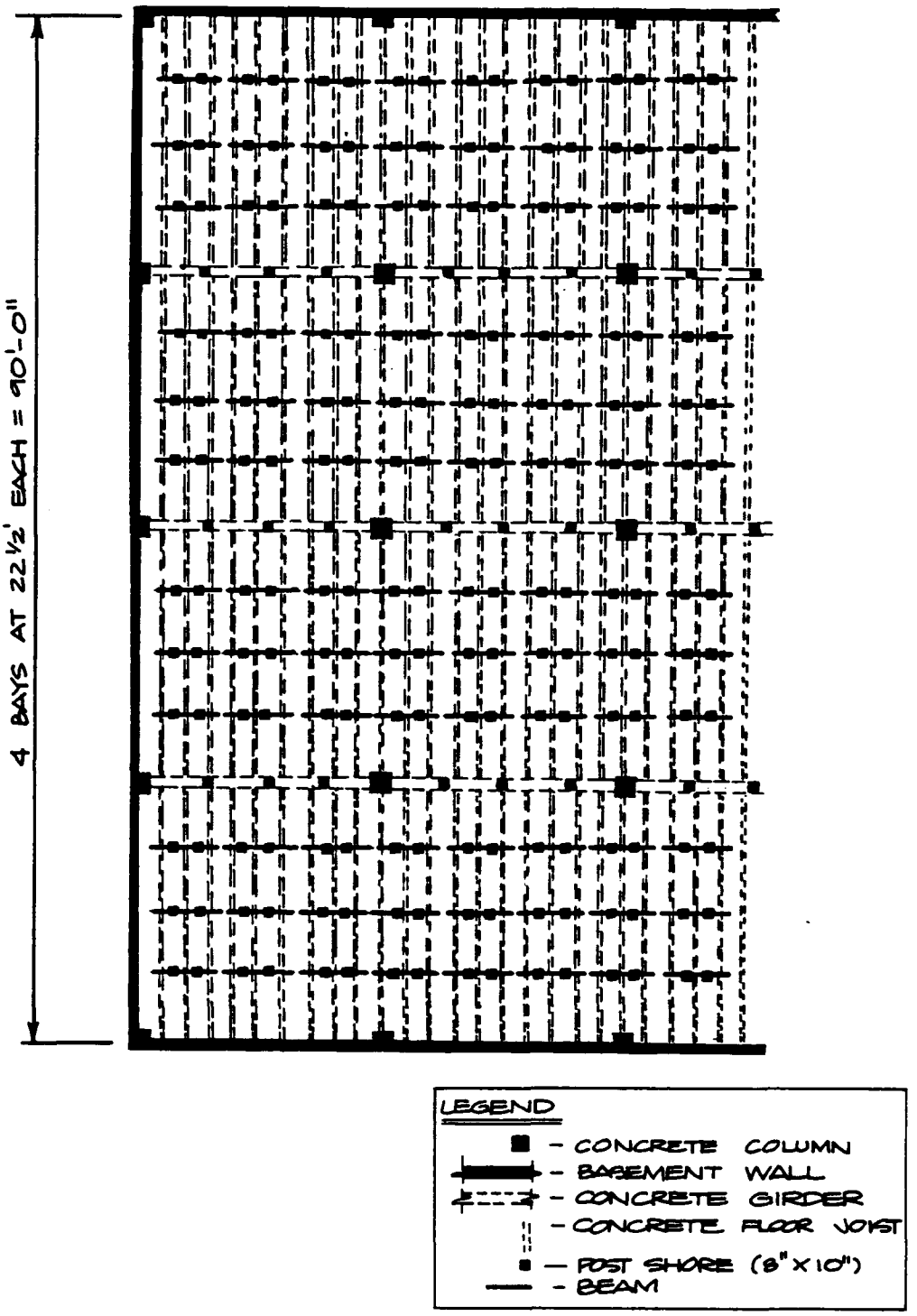

Fig. 3-4. Post and Beam Shoring for a Portion of the Basement Shelter.

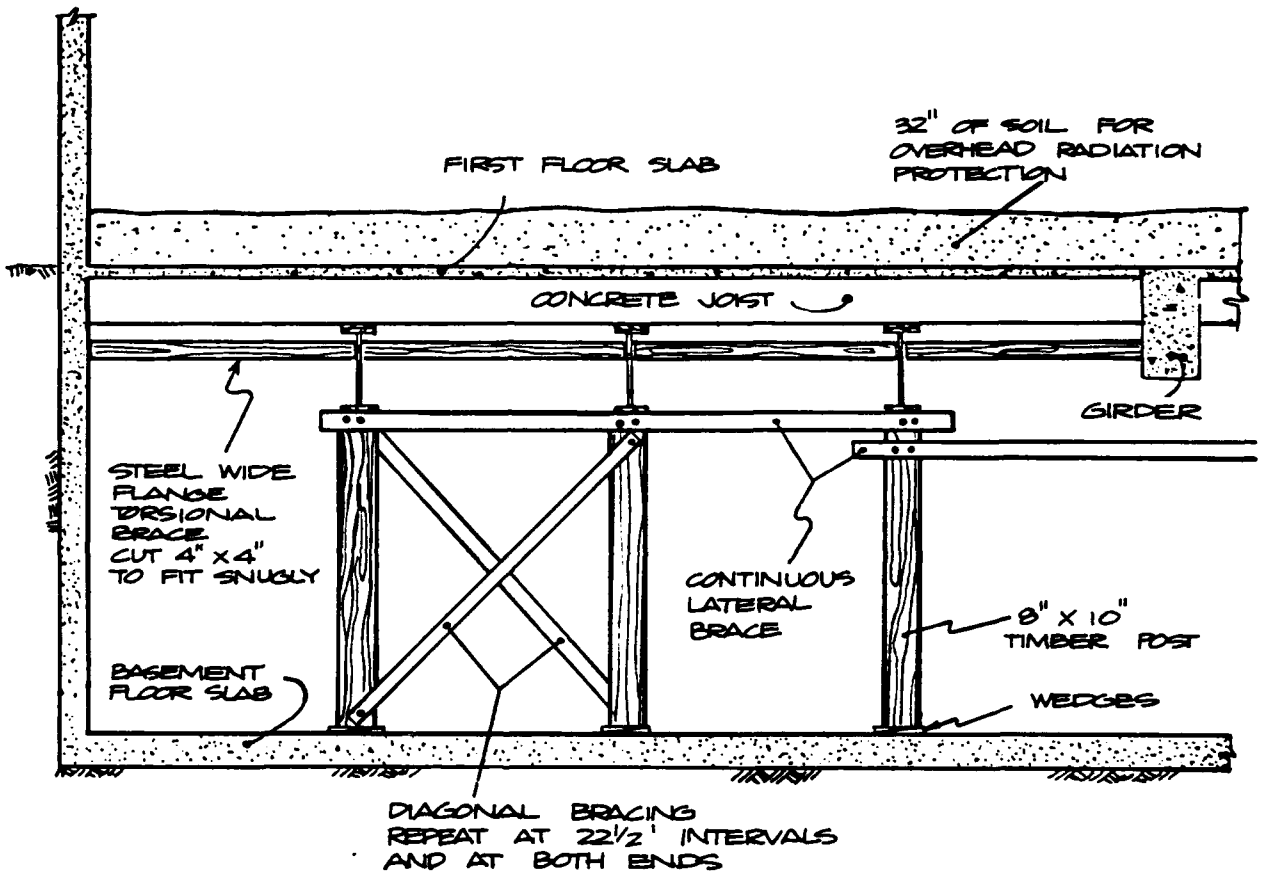

Fig. 3-5. Lateral Bracing Details for Post and Beam Shoring.

CLOSURE DESIGN

Two different closures will be required for the basement: the first involves the sealing off of the two stairways leading into the basement, and the second requires the sealing off of the two elevator shafts. The stairs can be sealed off by shoring the first floor landing and stairs leading into the basement and then placing soil to a depth of 36 inches above the first floor level. Figure 3-6 shows a detail of the stairway, shored and with soil placed for radiation protection. The two elevator shafts prior to upgrading should have the elevators run up to about mid building height so that both the elevator cars, counterweight, and associated connecting cables are well clear of the basement shelter area. Upgrading of the elevator shaft consists of placing soil to a depth of 36 inches above the first floor slab (see Figure 3-7).

Access and Ventilation

Large diameter culvert pipes or precast concrete manholes could be placed in the stairway or elevator shafts prior to their being sealed off, and having soil placed in them for radiation protection. The culvert pipes or manholes could serve the dual purpose of providing both access and ventilation for the shelter. Additional ventilation would probably be obtainable by disconnecting conduits and pipes that connect the utility vault along the east wall of the basement.

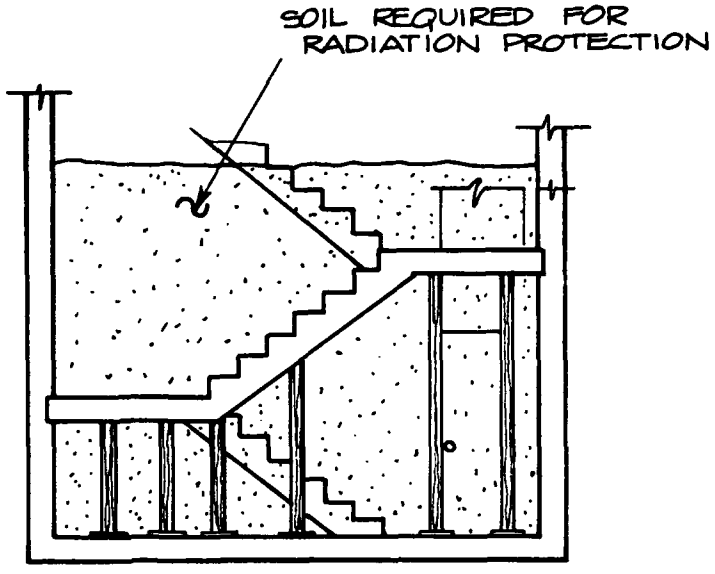

SECTION

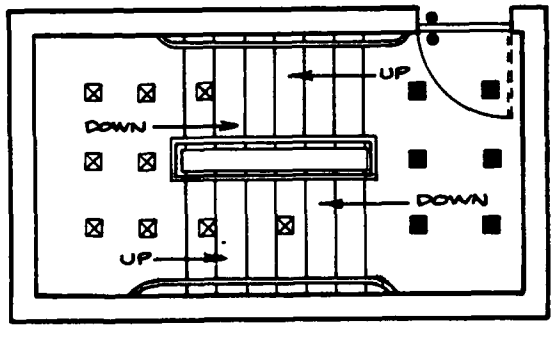

PLAN

Fig. 3-6. Upgraded Stairway Leading Into Basement Shelter.

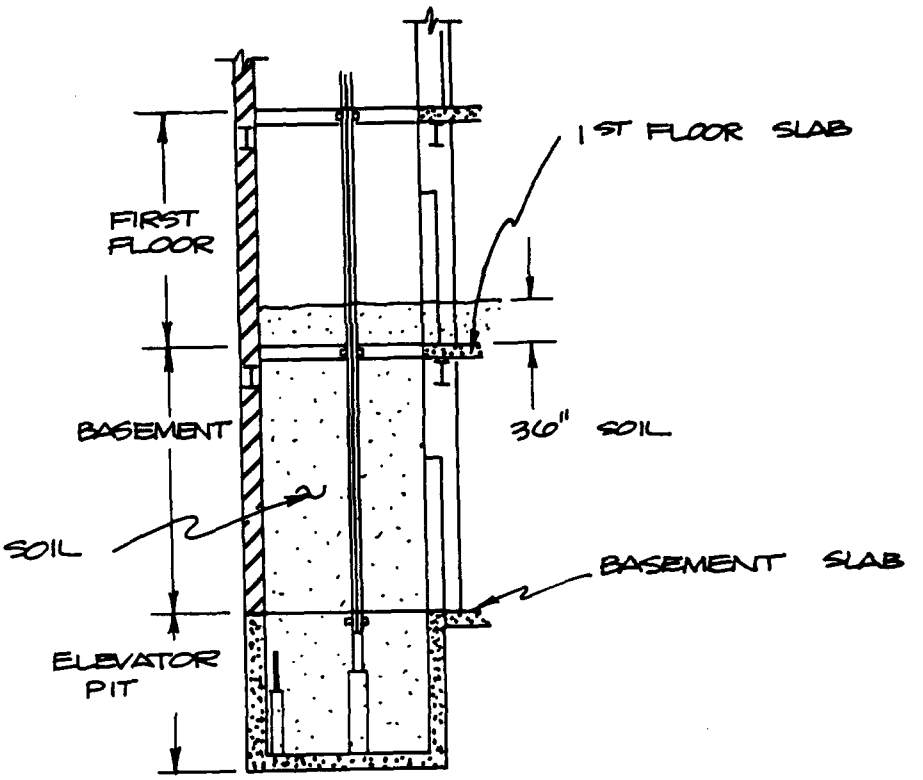

NOTE:

A CONCRETE MANHOLE OR CONCRETE CULVERT PIPE CAN BE PLACED IN THIS SHAFT PRIOR TO BACK FILLING AND CAN BE USED FOR BOTH VENTILATION AND ACCESS.

Fig. 3-7. Upgraded Elevator Shaft.

Section 4

TASK 3 - THEORETICAL ANALYSIS

INTRODUCTION

This task is the heart of the contract work and treats some shelter upgrading problems for the first time. Some work has been performed on the analysis of frame response to blast and earthquake forces and the failure analysis of the various components such as columns, beams, and floor slabs that make up a basement shelter (see Ref. 28); but little, other than the recent SSI work to develop a key worker shelter manual (Refs. 1 and 2), has been done with regard to the analysis of frame response on an upgraded shelter. Recent full-scale tests of a number of upgraded reinforced concrete floor systems and steel frame with concrete steel deck floor systems indicate that the modes of failure for upgraded shelters may be significantly different from those for non-upgraded systems.

It was found that the classical analysis of these floor systems, based on simple or continuous span ultimate strength design, is no longer a valid approach in failure prediction when considering a shored system. As an example of the different failure modes, Fig. 4-1A shows a prestressed precast concrete slab, simply supported at the ends, which was tested without shores. The mode of failure was by flexure, as predicted. The slab developed positive moment tension cracks under the load points early in the test, and failure occurred in flexure at these locations. This type of failure was predicted by conventional design methodology. Fig. 4-1B shows one end of a similar slab that was shored at midspan and loaded to failure. The failure shown in the figure occurred as a result of bond failure of the prestressing strands, causing a sudden shear/flexure near the end support. This type of failure was not predicted prior to the test. As a result of an extensive test program and companion analytical work, SSI has developed a prediction methodology (Refs. 5 and 6) by which modes of failure can be predicted in terms of the locations of the shores and the shear and moment stresses developed.

A

B

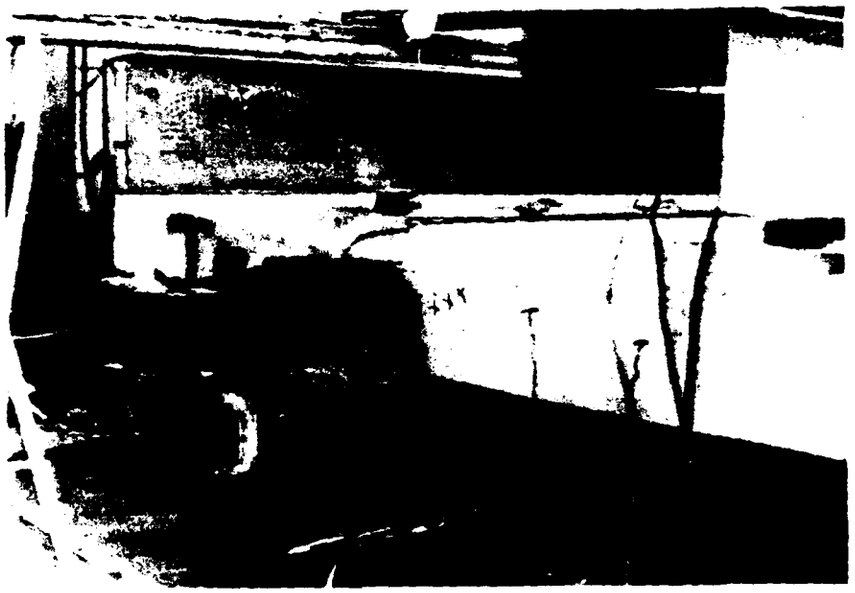

Fig. 4-1. Photographs of Failure Modes for Concrete Slabs.

The other major area not adequately covered by past research is the representation of the complete time history of frame collapse behavior under blast loading; this includes: the elastic phase, the elasto-plastic formation of joint yield hinges, the collapse mechanism, and finally the fracture of elements due to excess distortion. The dynamic analysis portions of the STRUDL program and the concepts of plastic analysis are used to fulfill this research need.

The complete theoretical effort in Task 3 was divided into three subtasks:

3A - Development of loading criteria

3B - Development of joint resistance functions

3C - Development of failure modes

SUBTASK 3A: LOADING FUNCTIONS

Introduction

The blast loading on a structure is a complex function of the incident blast wave (described mainly by its peak overpressure and dynamic pressure wave forms) interacting with structural parameters of size, shape, orientation, and response. To reduce the complexity of the analysis of the interaction process, the common approach has been to consider a structure to be in one of two possible categories, that is, either as a diffraction-type structure or a drag-type structure. In the former, the critical response is to the peak blast wave overpressure while in the latter the response is to the entire dynamic pressure pulse. The diffraction-type structure of principal interest here is a large building with strong exterior walls, typically a multistory reinforced concrete building with small window area, while typical drag-type structures are electrical, radio and television transmission towers, and truss bridges.

It should be noted, however, that few, if any, true diffraction-type high or medium rise structures exist. Research in Refs. 9, 10, and 11 on failure overpressures for various wall types shows that most nonreinforced walls fail at very low overpressures, less than 5 psi. Even arched nonreinforced (not normally found in high-rise structures) and reinforced concrete walls fail at overpressures less than 10

to 12 psi. Thus, large buildings with these types of walls, or with large window areas, have been commonly considered drag structures based on the rationale that brittle wall structures can resist the overpressure for only a fraction of the duration of the blast wave, leaving only the exposed frame to bear the load. While it is true some buildings will respond mostly as drag-type and others as diffraction-type structures, oversimplification of this approach ignores the real situation for a large number of buildings wherein frangible walls can survive long enough to impart very high loads into supporting frame members before being swept out. In other words, real buildings will experience both types of loading with the relative importance and contribution of each type in causing damage depending upon wall construction and blast wave characteristics.

An indication of the magnitude of the load that can be imparted to the frame by frangible portions of a structure was obtained from some shock tunnel tests on a wall having an opening both with and without glass window panes. Data from two pairs of these tests are shown in Figure 4-2. It will be noted that for the tests at incident pressure of p = 3 psi, the load on the frame with an open window was approximately 50 kips, but with window glass it was approximately 130 kips. Corresponding differences, 140 kips vs 250 kips, were noted for the p = 5.5 psi tests.

Figure 4-3 is a plot of the impulse transmitted to the frame by an unfailing wall with and without glass in a 27% open section. The net difference due to glass is (0.175 - 0.095) lb-sec/in.^{2}, or 0.080 lb-sec/in.^{2}. The data available in reduced form are limited because the some 300 tests done in the shock tunnel have never been analyzed for impulse (however, some data were presented in Ref. 29, and these are shown in Figures 4-2 and 4-3); there was no interest, until now, and all of the shock tunnel data are at much lower overpressures than are of interest in this program. Therefore, until these data are analyzed and some higher overpressure tests conducted in a field test (or, perhaps, scaled in a small-scale shock tube) it remains necessary at present to make a best estimate of loads and durations of the wall/frame interactions for the analytical purposes of this program. A discussion of debris and loading implications is presented in Appendix C.

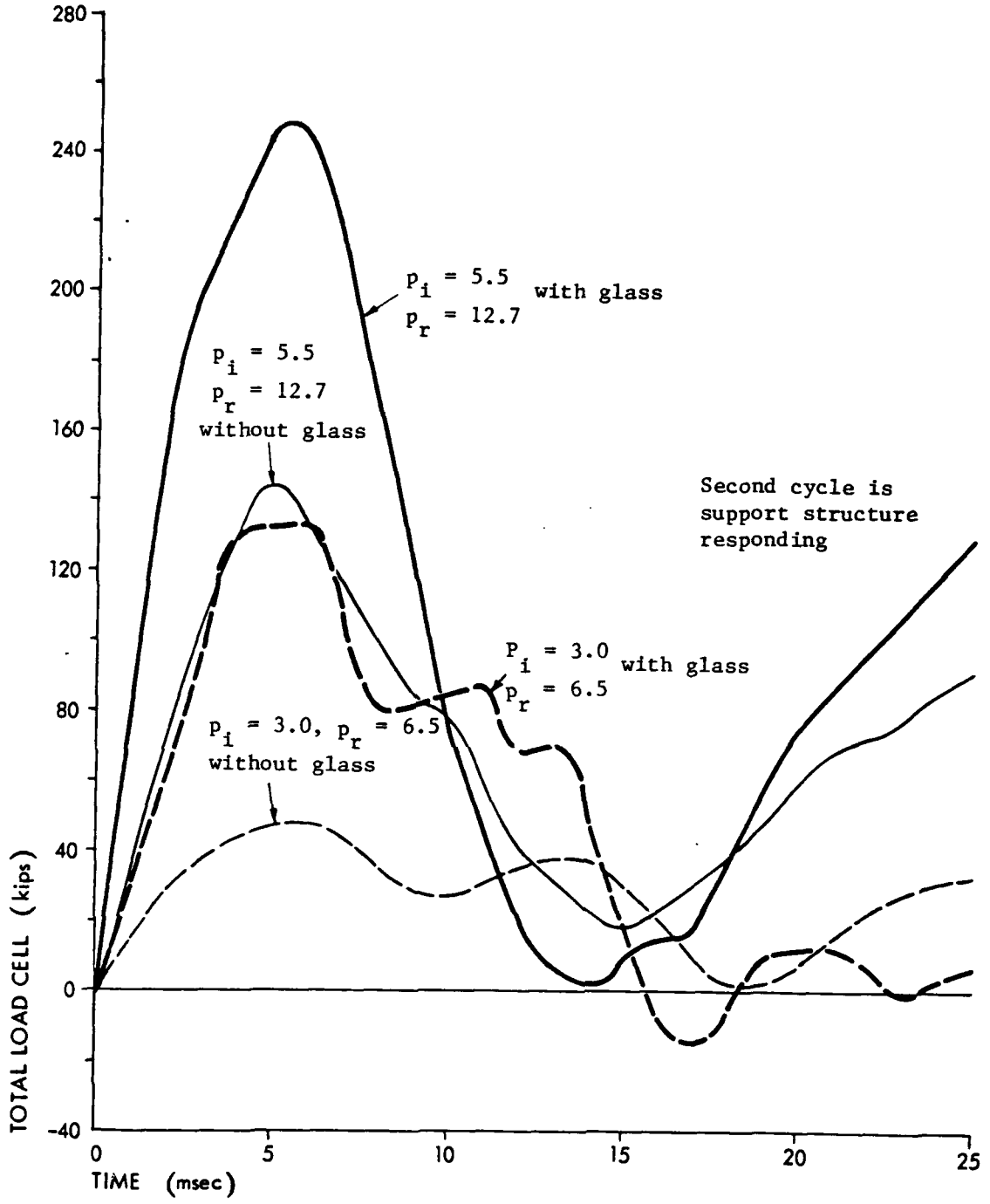

Fig. 4-2. Load Data from Tests With and Without Glass (27% window area).

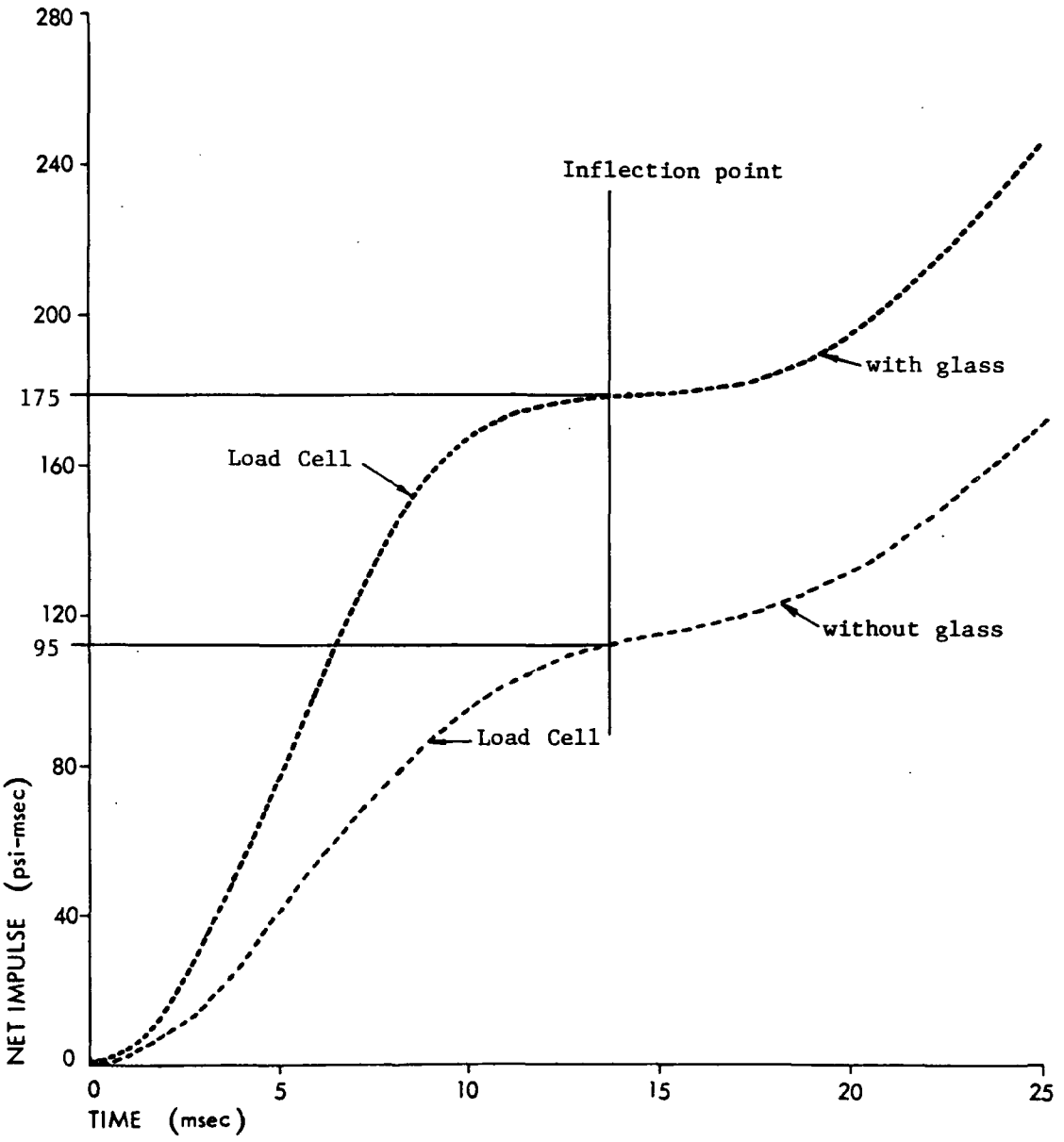

Fig. 4-3. Net Impulse Data at P_I = 12.7 psi (P = 5.5 psi) with and Without Glass (27% window area).

Development of Loading Function

The technical details of the blast loading of structures are taken basically from the Effects of Nuclear Weapons (Ref. 30). The loading condition of interest is that from a Mt weapon at 40 psi.

For a closed structure the front face loading is as shown below where:

p = peak overpressure

$p(t)$ = time variation of overpressure

q = peak dynamic pressure

$q(t)$ = time variation of dynamic pressure

p_r = reflected overpressure

t^+ = duration of positive phase of the blast wave

p_s = stagnation pressure = $p(t) + q(t)$

t_s = clearing time

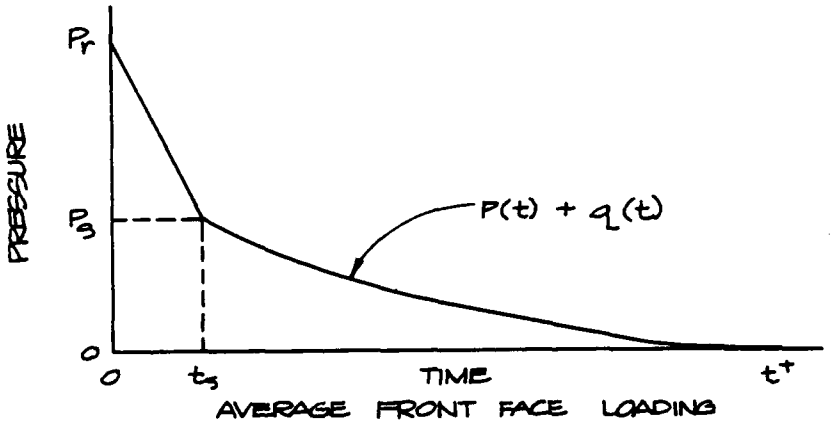

When the blast wave strikes a flat surface, such as the side of a building at 90 degrees (normal incidence), a reflected overpressure occurs which is more than twice the incident overpressure. As the wave front passes the front of the structure, rarefaction waves move from the edges across the front of the structure weakening the loading until at a time, t_s, the loading has been reduced to the stagnation value. The stagnation pressure then gradually reduces to zero at a time, t^+, as the incident loading pulse decreases. The time, t_s, is given by 3S/U where

S = the height or one-half width of the structure

U = the shock front velocity.

Values of p_r, q, and U as a function of p are given in Figure 4-4 (Ref. 30).

Once the shock wave has engulfed the entire structure,the back face will also be loaded as illustrated in the following sketch. This assumes that the pulse duration is very long compared with the travel time down the structure and the clearing times.

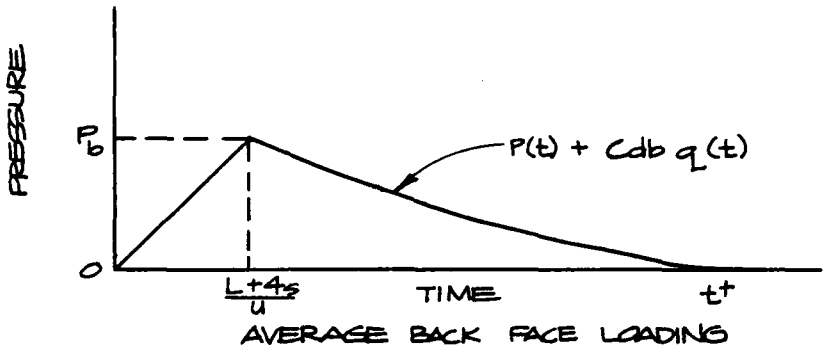

AVERAGE BACK FACE LOADING

The net horizontal loading is that given by subtracting the back face loading from the front face loading. The loading pulse shown below was selected as a first approximation to this rather complicated pattern.

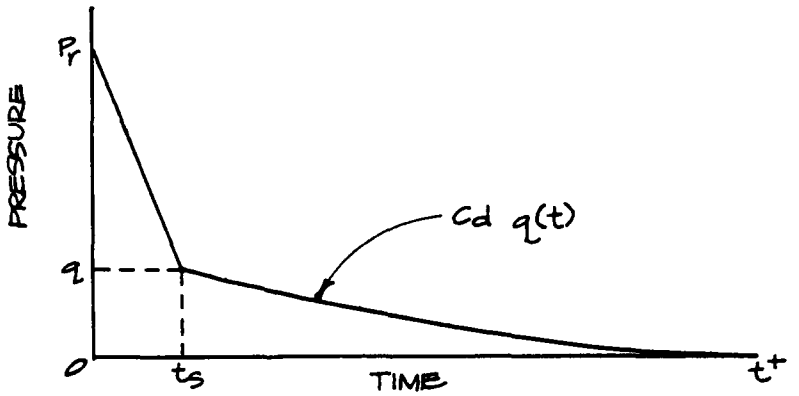

ASSUMED NET LOADING

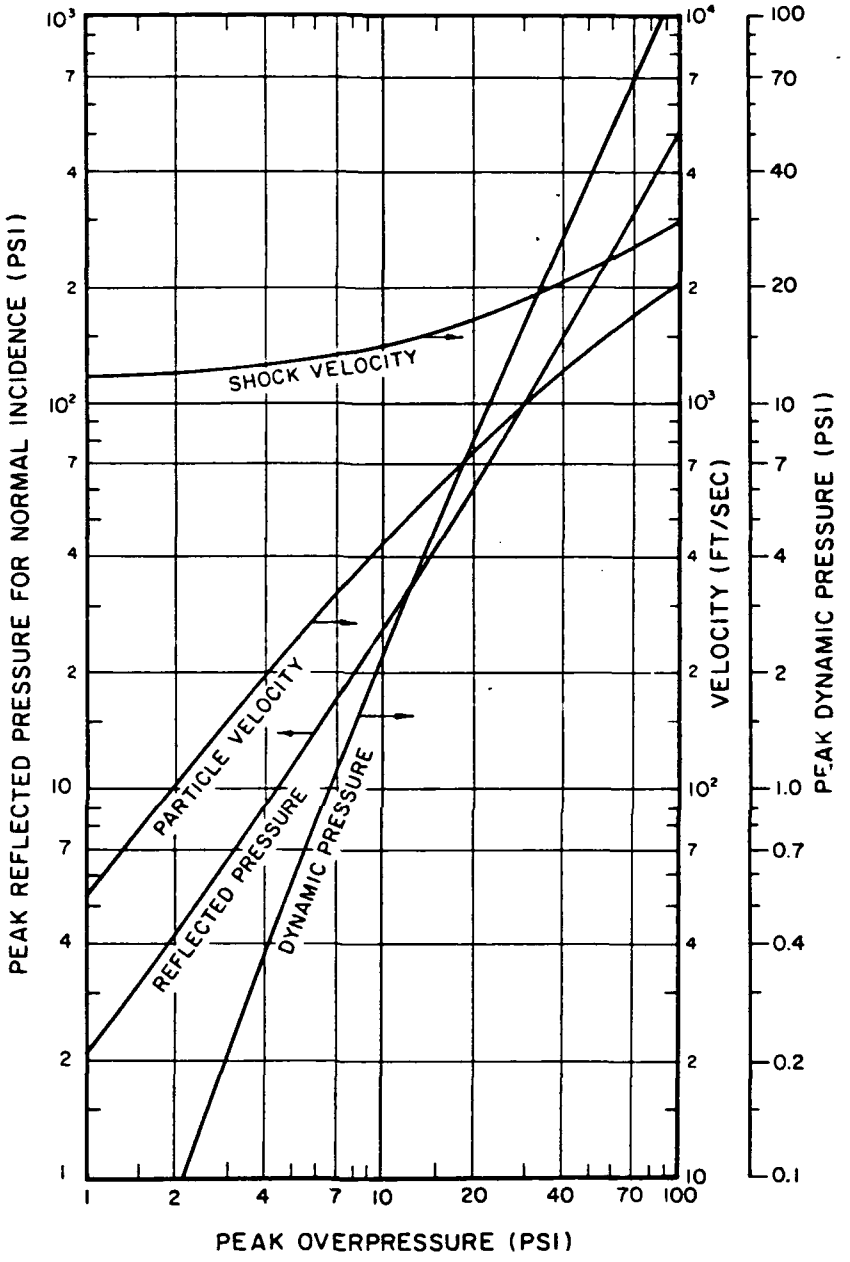

Fig. 4-4. Relation of Ideal Blast Wave Characteristics at the Shock Front to Peak Overpressure.

Source: Effects of Nuclear Weapons, Ref. 30.

For a structure with a large percent of its surface in glass, such as is of concern here, Ref. 30 suggests computing the loading on the individual structural elements treating them as closed structures and then summing them. This does not change the peak loading, which is still the peak reflected overpressure, but it greatly shortens the duration of the diffraction spike, since the half-width of the structural members is used for S in place of the half-width of the entire structure.

From the sketch of a typical panel of the structure shown below, the average S value is 1.1 ft, so that t_s is 1.6 msec.

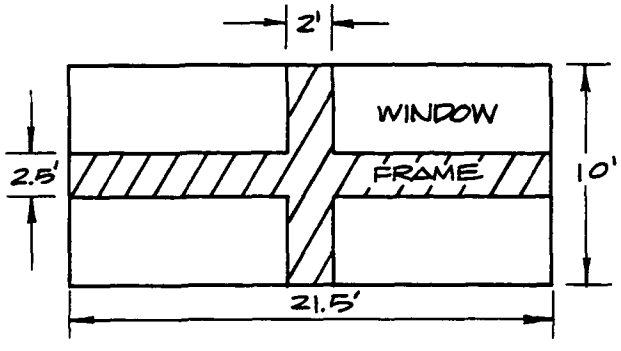

Total Area per panel 215 ft^2

Frame Area 69 ft^2

32% closed (steel)

68% open (glass)

This time, however, completely neglects the effects of the windows, which as pointed out earlier is not correct. From the window data it is possible to calculate an effective clearing time as follows: the impulse transmitted to the frame from the window with 27% glass was 0.08 psi-sec; extrapolating this to the 68% glass case of the structure of concern gives

$$I = 0.08 \times 68/27 = 0.20 \text{ psi-sec}$$

Distributing this impulse into a triangular loading spike of peak value equal to the peak reflected pressure of 147 psi gives an effective clearing time of:

$$t_w = 21/p - (2 \times 0.2)/147 - 0.0027 \text{ sec}$$

Adding this to the frame clearing time of 1.6 msec gives a total of 4.3 msec, which was rounded off to 4 msec for the computer calculations.

For the drag portion of the loading the following equation was used for the change of dynamic pressure with time:

$$q(t) = q(1 - t/t^+)^2 e^{-2(t/t^+)}$$

where t^+ is the positive phase duration of overpressure. For the time range of interest ($\leq$ 200 msec) the difference in impulse between this equation and that given by the data in Figure 4-5 (Ref. 30) is less than 5%.

A drag coefficient of 2.0 was used in calculating the loading during the drag phase. Ref. 30 suggests a value of 1 with the loading from the structural elements of both the front and back faces included. In the present calculation only the front face is considered so that a large drag coefficient is appropriate.

The loading characteristics used in the computer calculations are summarized below and illustrated in Figure 4-6.

Summary of Loading Conditions

Peak overpressure	40 psi
Weapon yield	Mt
Positive phase duration of overpressure*	2 sec
Peak reflect overpressure	147 psi
Peak shock front velocity	2000 ft/sec
Peak dynamic pressure	28 psi
Total clearing time	4 msec
Total area of panel	215 ft^2
Frame area of panel	69 ft^2
Drag coefficient	2

* at 40 psi

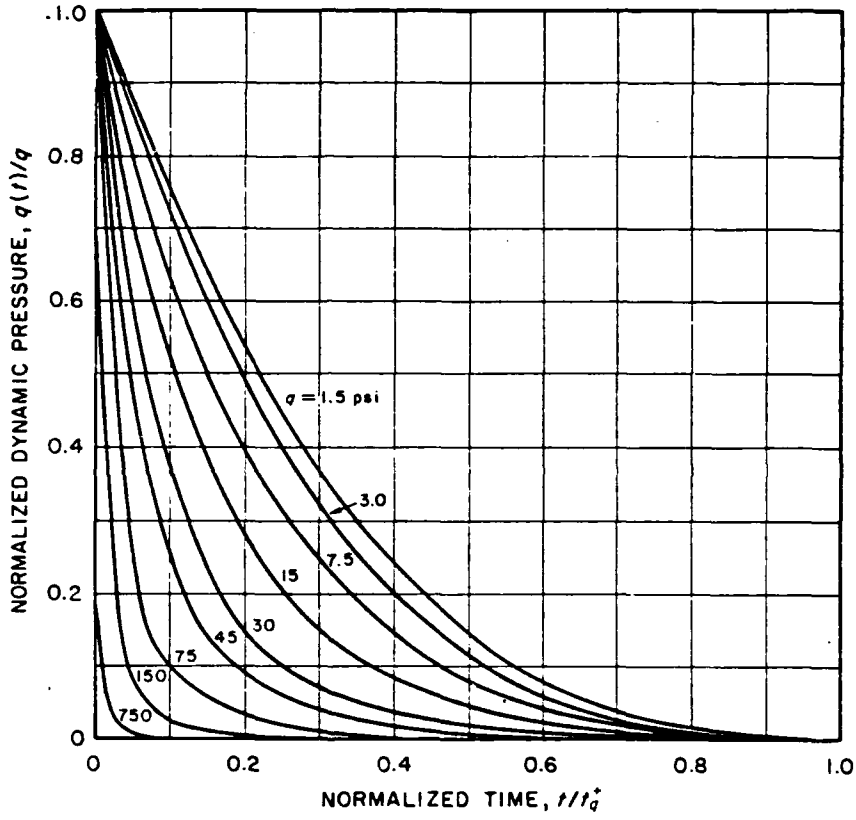

Fig. 4-5. Rate of Decay of Dynamic Pressure With Time for Several Values of the Dynamic Pressure.

Source: Effects of Nuclear Weapons, Ref. 30.

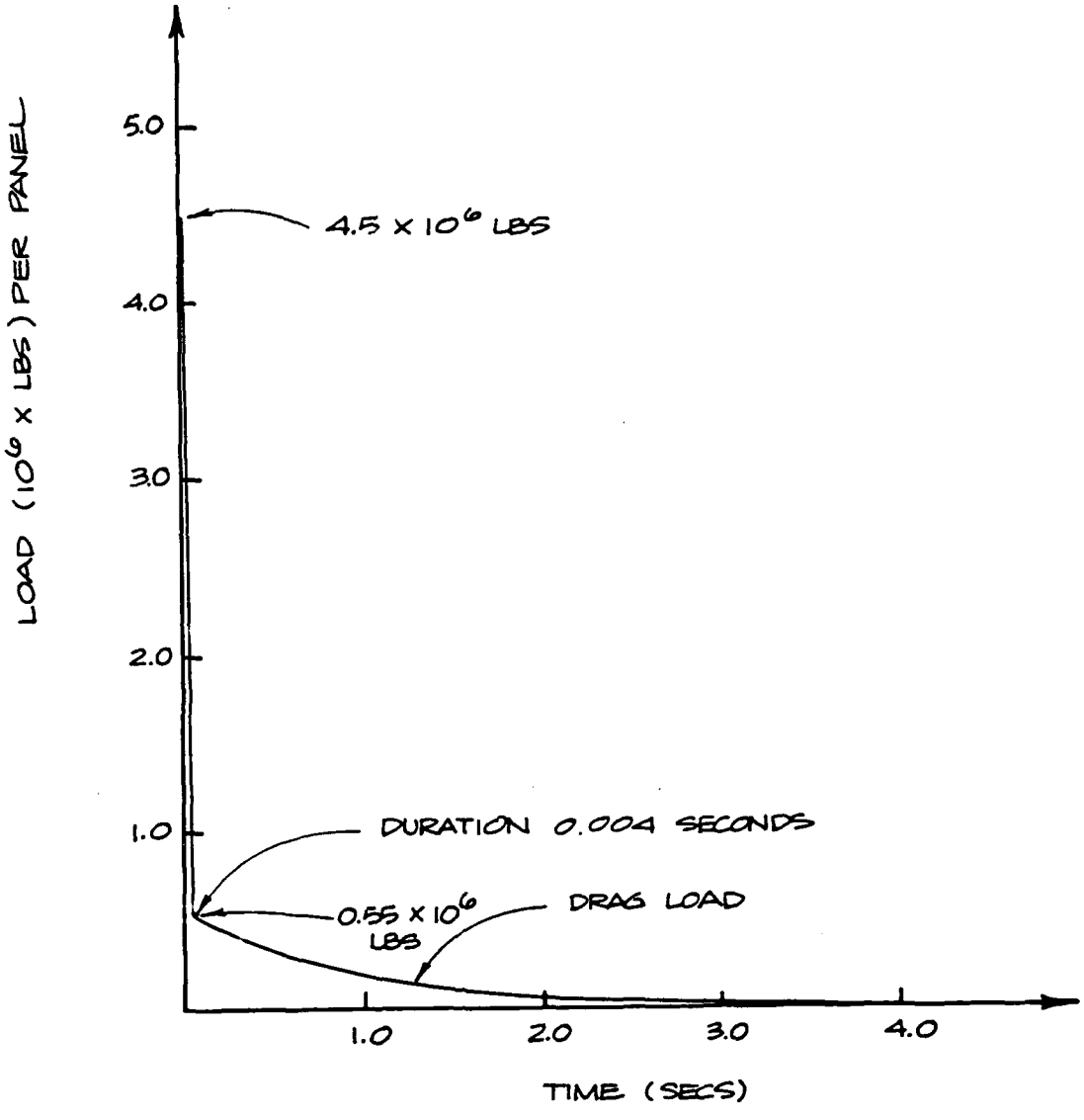

Fig. 4-6. Load Function Used for Computer Analysis.

It should be noted that the actual shape of the diffraction loading spike as well as the early time drag loading is not critical since the response of the structure to this loading is governed by the total impulse delivered. This is because the natural period of the structure (5 sec) is several orders of magnitude larger than the loading duration. Several computer analyses were performed to confirm that the diffraction loading is indeed an impulse. Figure 4-7 is a plot of mid-height velocity and displacement resulting from the 4 msec diffraction loading. This impulse alone is probably sufficient to collapse the structure, as the displacement at 0.5 sec is sufficient to yield the lower beams, and the velocity greater than over 12 in. per second.

SUBTASK 3B: JOINT RESISTANCE FUNCTIONS

Introduction

The analysis of building structures under blast loading requires a knowledge of the effective elastic limit capacity, M_p, for the beam and column joints. This section provides methods of evaluating these capacities for the structural elements in both steel and reinforced concrete frame buildings. The developments are limited to the beam and column elements of frames, since the common brittle exterior and interior wall construction will be removed by the peak overpressure of the 30 to 50 psi incident blast wave. Further, one principal objective of the analysis is to determine the effect of the frame column failure on the ground floor (shelter ceiling) slab. The presence of structural walls would complicate any findings concerning the integrity or failure of this slab due to the continuous column interaction. Both the steel and the reinforced concrete member capacities will be evaluated at the strength (ultimate strength design) basis.

Structural Steel Construction

The AISC Manual (Ref. 31) provides strength information for beams, columns, welded and bolted connections, and splices. Part 2 of this manual gives the specific plastic design or strength values (See interaction diagram, Figure 4-8, and Table 4-1 for all definitions):

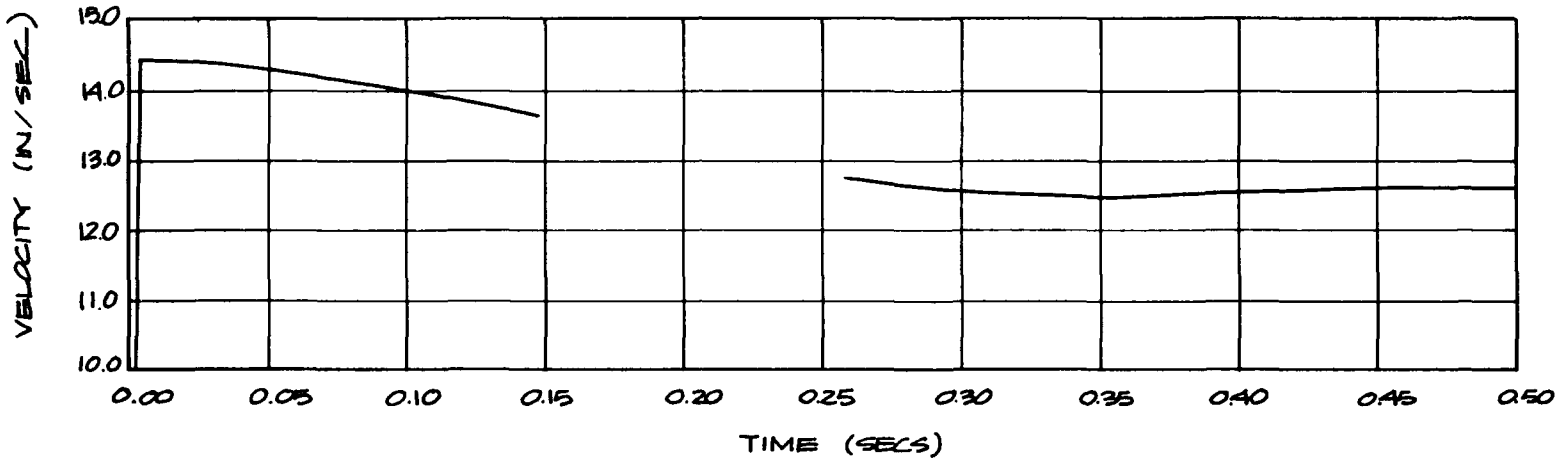

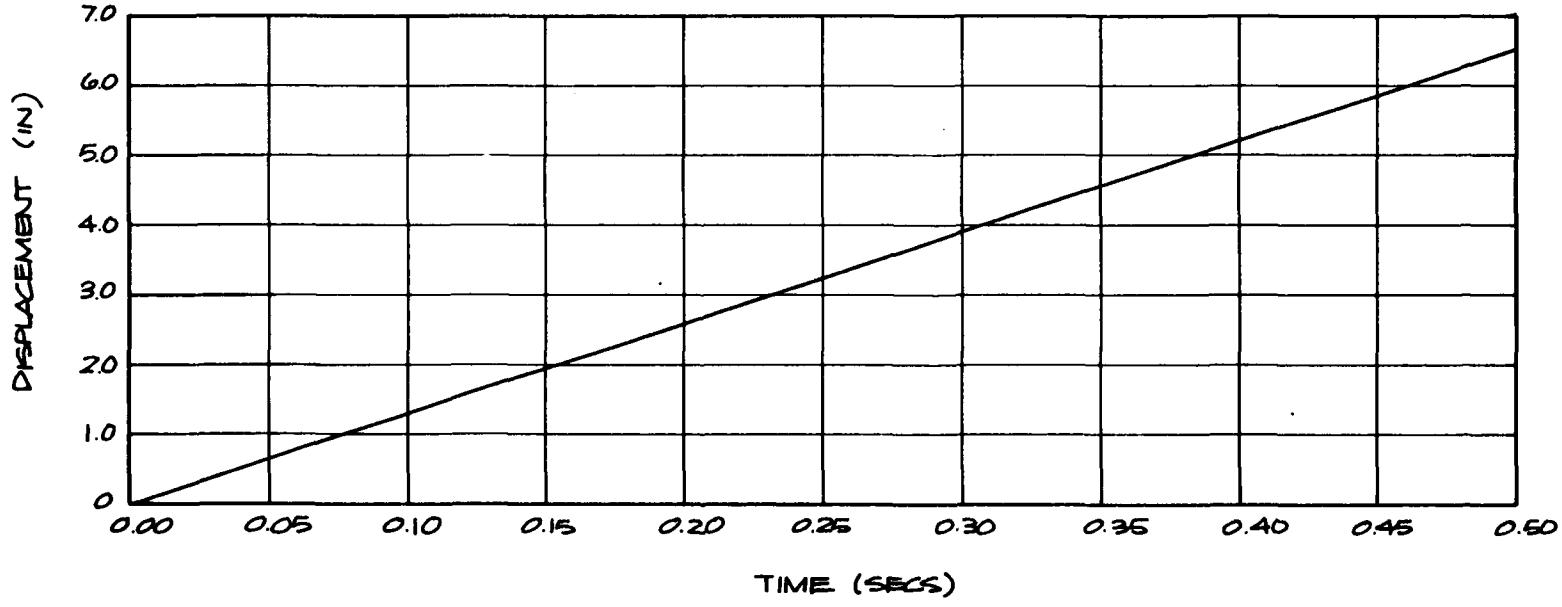

Fig. 4-7. Velocity and Displacement vs Time at Mid-Height of Building With Diffraction Loading Only.

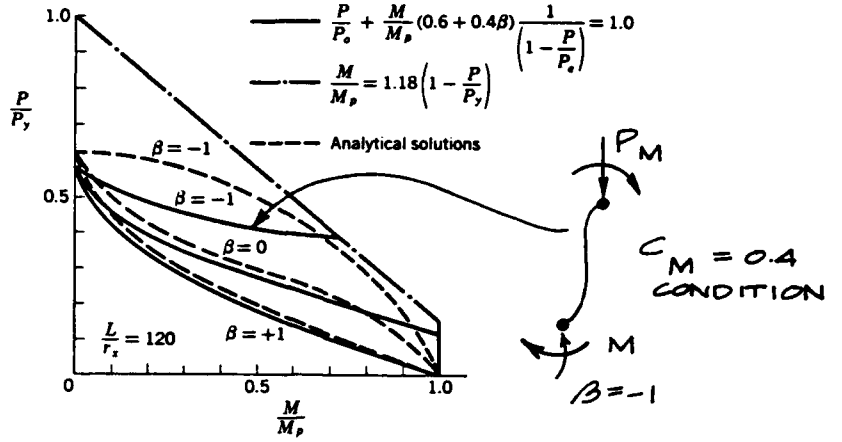

Fig. 4-8. Normalized Interaction Diagram.

TABLE 4-1: AISC MANUAL, PART 2 DEFINITIONS

A	Gross area of an axially loaded compression member
C_m	Coefficient applied to bending term in interaction formula for prismatic members and dependent upon column curvature caused by applied moments
F_a	Axial compressive stress permitted in a prismatic member in the absence of bending moment (kips per square inch)
F_y	Specified minimum yield stress of the type of steel being used (kips per square inch)
M	Factored bending moment (kip-feet)
M_m	Critical moment that can be resisted by a plastically designed member in the absence of axial load (kip-feet)
M_p	Plastic moment (kip-feet)
P	Factored axial load (kips)
P_e	Euler buckling load (kips)
P_{cr}	Maximum strength of an axially loaded compression member or beam (kips)
S	Section modulus
Z	Plastic section modulus

Beams,

$$M_p = ZF_y,$$

or $M_p = SF_y$ for older non-compact sections.

Columns,

$$P/P_{cr} + (C_m M)/\left[(1 - P/P_e)\, M_m\right] \leq 1$$

where $P_{cr} = 1.7\ AF_a$, $C_m = 0.4$ for reversed curvature, $M_m = M_p$. (Strengths for connections and splices are 1.7 times the corresponding AISC Manual Part 1 allowable stress values.)

With respect to beam flexural capacities, it is quite probable that older construction may have steel (builtup or rolled) sections that are non-compact, such that they would buckle before developing full plastic capacity. For these sections the M_p value should be taken as SF_y, for the tabulated or calculated section modulus, S.

In any given structure, and particularly in older structures, it may be possible that column splice details (such as shown in Figure 4-9) may constitute a weak link in column M_p values. If these splices are weak in flexural resistance and near the column base, then their estimated M_p capacity should be used at these locations. The transverse shear resistance of the splice may also be a weak link and should be investigated.

Also, particularly in older construction, the interior beam column connections may be simple web or flange clip angles with rather minimal M_p values (see Figure 4-10). This type of detail should be identified, and the appropriate estimated M_p value should be used in the analysis.

Recommended ductility ratios, $\mu = M_F/M_p$ are 8 to 10 for fully developed sections or rigid connections, where M_F is the failure moment. Other than for the case of weak splice details, the shear capacity of a steel section will not be less than the shear necessary to develop the M_p value.

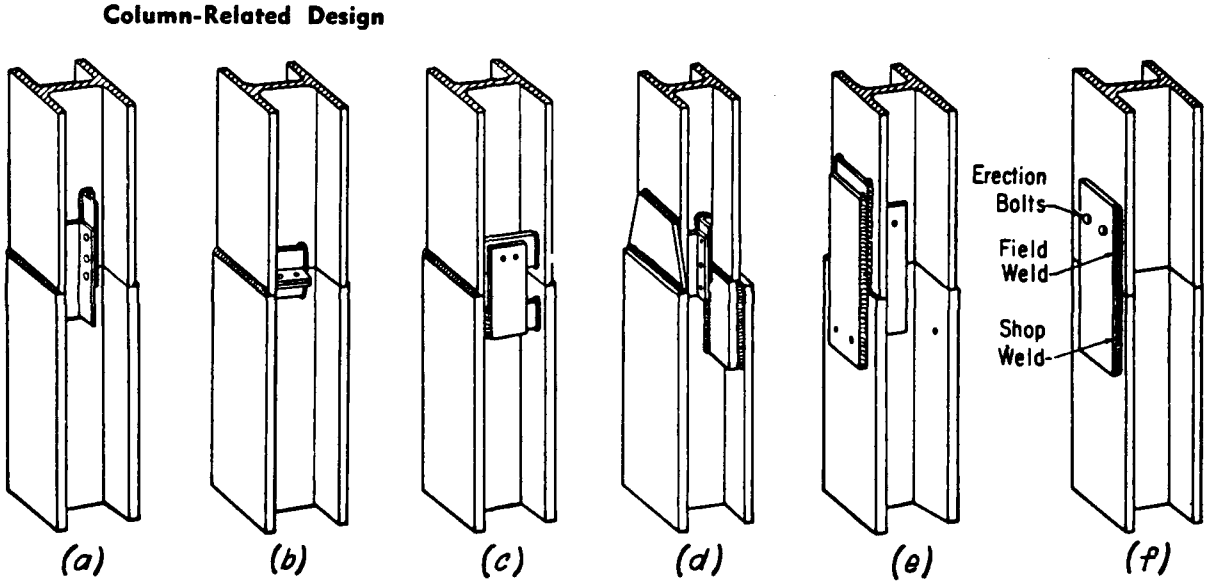

Fig. 4-9. Typical Steel Column Splices.

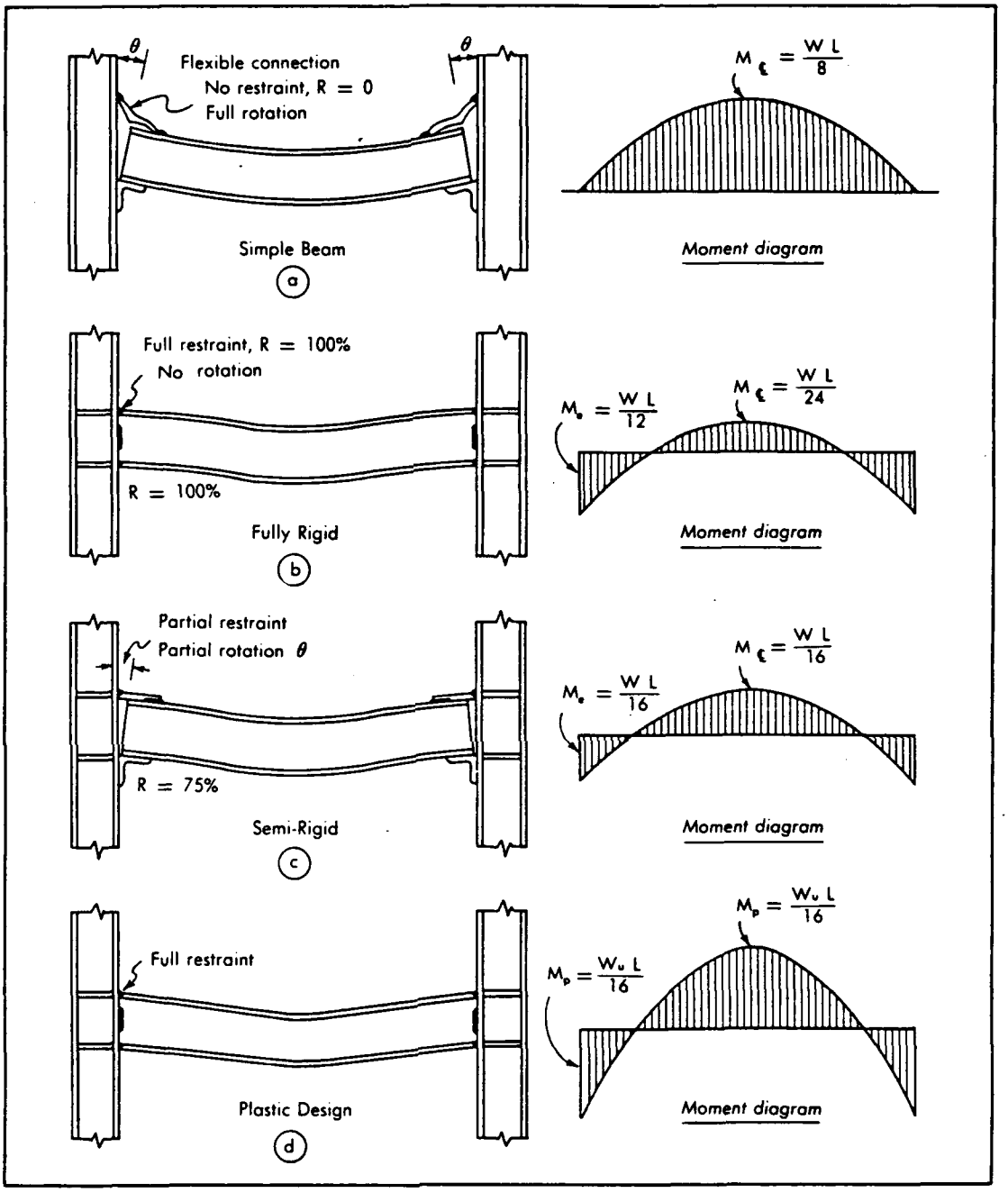

Fig. 4-10. Typical Steel Beam Connections.

Reinforced Concrete Frame Construction

By far the most prevalent forms of construction are the flat slab (or waffle slab) and the two-way slab systems, see Figure 4-11A and B. The CRSI Handbook (Ref. 32) provides most of the strength information required for these systems along with the beam and column section capacities for frame elements.

For the majority of slab system frame structures, the equivalent frame is defined by a frame strip along each column line, having a width equal to the bay width perpendicular to the column line. Figure 4-12 shows the general flexural section configurations. The flexural strength M_p of these beam sections can be taken from the CRSI Handbook using the assumption that strengths for F_y = 60 ksi steel with the ϕ factor are equal to strengths for F_y = 40 ksi without the ϕ factor. The most realistic estimate of M_p would be without the ϕ factor multiplier.

For a suitable approximate estimate of beam capacities, M_p, the following procedure can be applied to the construction elements in Figure 4-12.

- Assumption: Positive steel area equals one-third negative steel area at the column face

  Negative M_u = (Negative A_s)F_y(0.8h)

  Negative A_s = top steel

  Positive M_u = 1/3 Negative M_u

- Assumption: Negative dead load moment equals one-third Negative M_u (see Figure 4-13)

  Negative M_p = Negative M_u - M_{DL} = 2/3 M_u

  Positive M_p = 1/3 Negative M_u + M_{DL} = 2/3 M_u

  Therefore, Negative M_p = Positive M_p

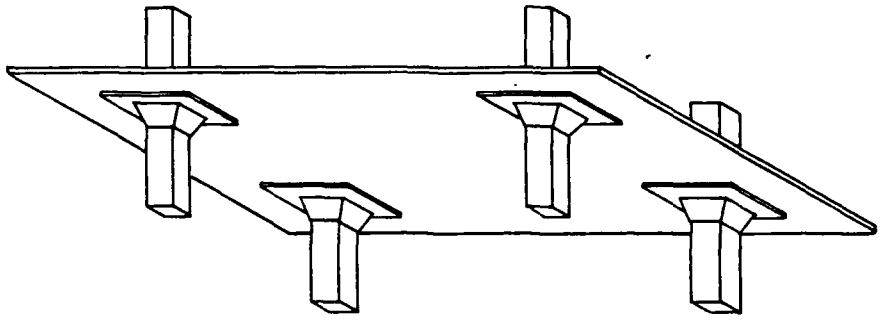

A. The Flat Slab

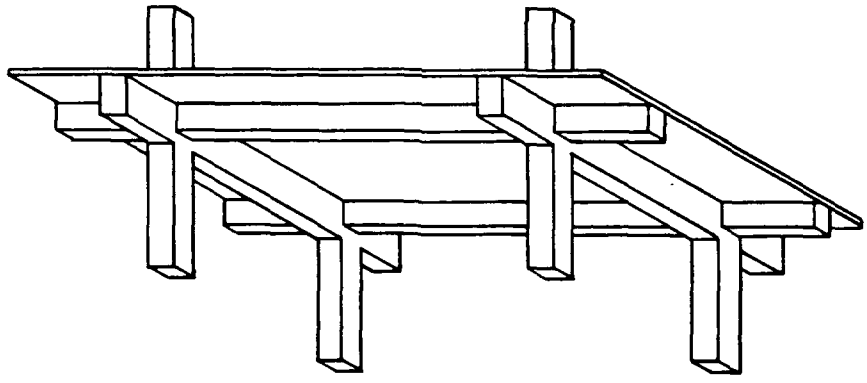

B. The Two-Way Slab

Fig. 4-11. Examples of Slab Systems.

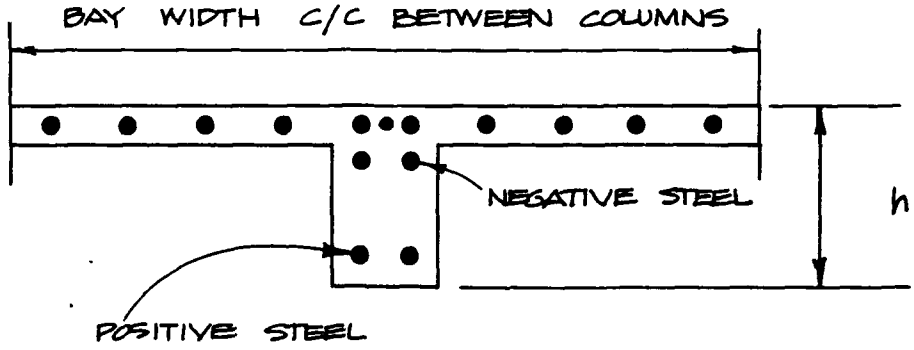

A) TWO-WAY SLAB

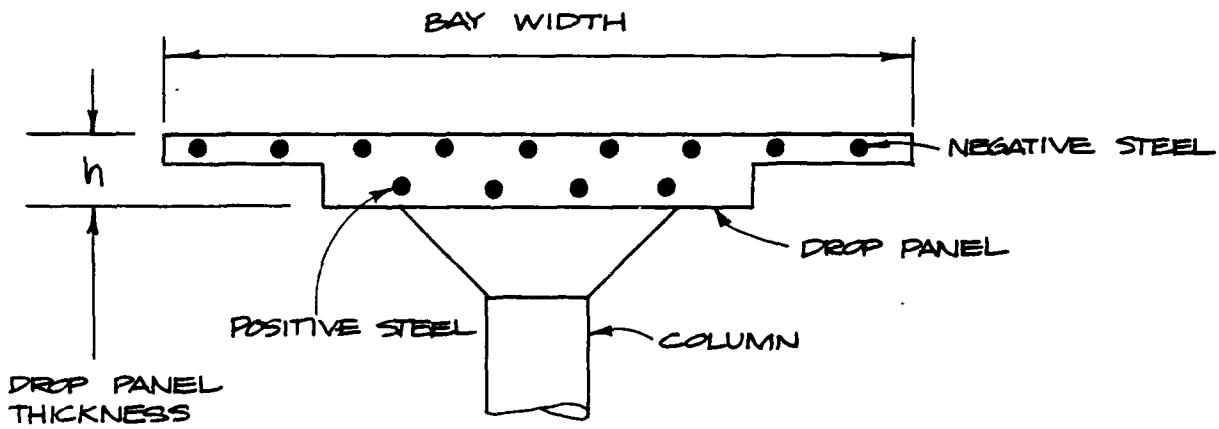

B) FLAT SLAB

Fig. 4-12. Slab System Beam Sections.

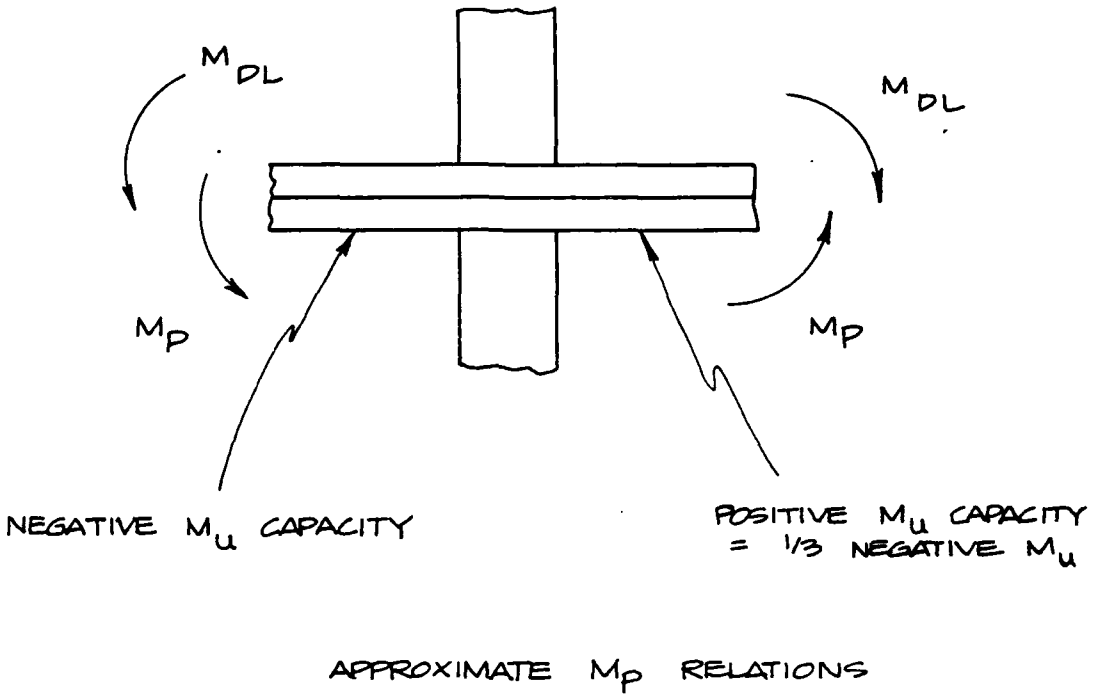

Fig. 4-13. Approximate M_p Relations.

For column M_p values, under the effects of axial and flexural load interaction, the interaction tables of the CRSI Handbook provide the $M_p = P_u$ times the eccentricity e. These values are for F_y = 60 ksi with the ϕ factor and can be assumed to be equal to the M_p for F_y = 40 ksi without the ϕ factor. Figure 4-14 shows an example interaction curve, and Figure 4-15 shows the CRSI table values for the Peachtree Building columns.

It is important to recognize that columns may fail in shear; this capacity can be estimated by

$$V_u = 4\sqrt{f'_c}\, A_c \qquad 250\, A_c \text{ lb}$$

where A_c is column section area in square inches.
The shear stress of $4\sqrt{f'_c}$ represents the presence of shear stirrup steel in the form of column ties.

Also, reinforcing steel splices may provide a weak link if the spliced bars are not staggered; one-half M_p might be used when this splice condition is present.

Recommended ductility ratio $\mu = M_F/M_p$ is 5 for fully developed sections or rigid frame joints.

Joints at the Ground Level Slab Intersection

Although the joints that exist at the ground level; i.e., at the superstructure of the basement, are similar to other joints in the structure, they behave much differently. The reason(s) for this behavioral difference is that the upgrading of the basement structure will greatly change the floor stiffness. The slab portion of the structure will be shored, which will increase its stiffness relative to the as-built, pre-upgrading stiffness. The dead load will also be increased two to three times owing to the depth of soil needed for radiation protection. In addition, the slab restricts lateral motion at the ground level if the basement is a satisfactory shelter space, i.e., the slab and basement walls must be poured integrally. Typical upgrading schemes that illustrate these differences are shown in Figure 4-16.

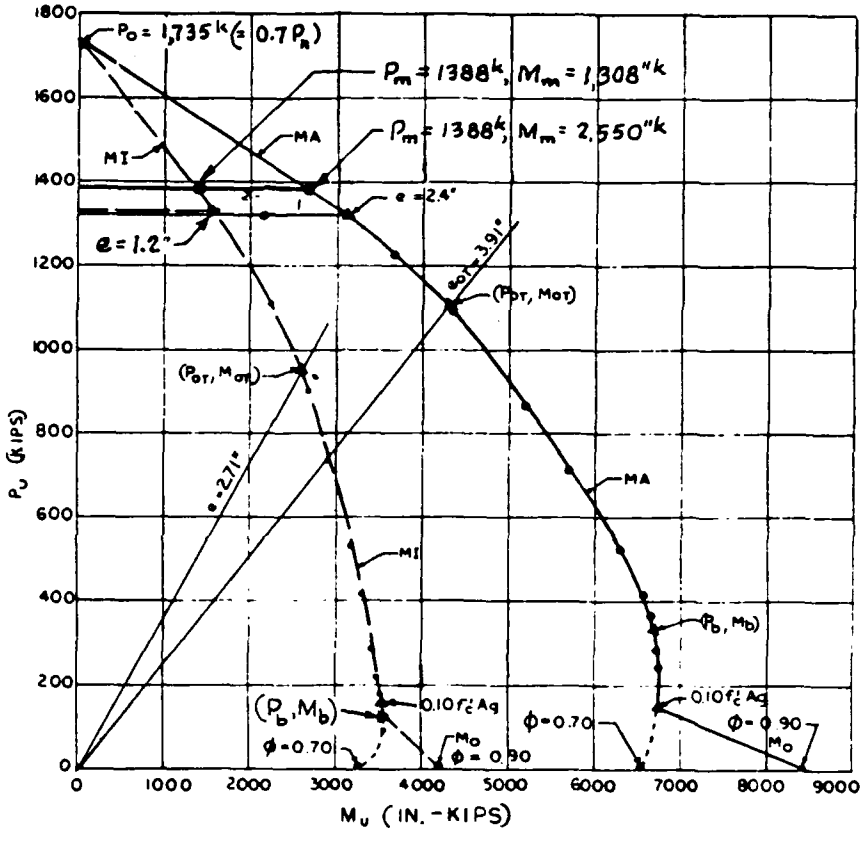

Fig. 4-14. Example Interaction Curve for Concrete Columns.

Bars Grade 60		SQUARE TIED COLUMNS 20″ × 20″ Short columns; no sidesway [1] Bars symmetrical in 4 faces												$0.10f'_cA_g$ = 160 kips [2] For P_u at [2]				
Concrete f'_c = 4,000 psi		P_u (kips)—Ultimate Usable Capacity												OT [3]	Balance		160 k [2]	O [2]
		M_u/P_u = e (in.) (ϕ = 0.70)																
Bars	p %	0	0.1h	2″	3″	4″	6″	8″	12″	16″	20″	24″	28″	e (in.)	e (in.)	P_u (k)	e (in.)	M_u (k-ft.)
4-#9	1.00	1110	891	891	793	703	551	442	260	160	0	0	0	3.04	8.61	416	16.02	150
4-#10	1.27	1153	925	925	825	733	581	471	302	192	0	0	0	3.17	9.44	413	18.02	187
4-#11	1.56	1199	960	960	857	763	608	496	338	221	0	0	0	3.34	10.32	407	19.92	223
4-#14	2.25	1308	1043	1043	935	836	674	557	411	289	213	166	0	3.61	12.40	400	24.73	310
4-#18	4.00	1586	1251	1251	1125	1011	827	693	521	417	331	264	218	4.11	17.73	383	36.39	517
8-#7	1.20	1142	905	905	800	704	544	433	263	179	0	0	0	2.84	8.23	422	17.29	179
8-#8	1.58	1202	949	949	841	742	580	467	302	210	0	0	0	2.96	9.09	420	19.95	231
8-#9	2.00	1269	998	998	885	783	617	501	341	241	184	0	0	3.07	10.04	418	22.55	286
8-#10	2.54	1354	1061	1061	942	834	662	541	387	279	214	173	0	3.20	11.26	415	25.80	355
8-#11	3.12	1446	1126	1126	999	885	704	578	423	313	241	195	164	3.34	12.58	407	28.72	421
8-#14	4.50	1665	1284	1284	1139	1011	810	670	497	392	308	251	211	3.56	15.73	399	36.19	571
8-#18	8.00	2220	1680	1680	1486	1320	1064	885	665	530	440	376	319	3.88	24.26	372	53.58	876
12-#10	3.81	1556	1209	1209	1072	950	758	624	457	349	276	228	193	3.33	13.67	411	33.23	491
12-#11	4.68	1694	1307	1307	1156	1024	819	675	497	390	310	256	217	3.46	15.61	400	37.38	574
12-#14	6.75	2022	1544	1544	1364	1209	971	804	596	473	392	327	279	3.66	20.34	387	47.74	780
16-#10	5.08	1757	1360	1360	1205	1069	856	707	523	414	330	274	234	3.46	16.02	413	40.21	628
16-#11	6.24	1941	1491	1491	1318	1168	935	773	573	455	372	309	265	3.58	18.56	401	45.72	728
SQUARE TIED COLUMNS 22″ × 22″														$0.10f'_cA_g$ = 193 kips				
4-#10	1.04	1353	1088	1088	1001	899	722	589	382	241	0	0	0	3.31	9.63	507	18.25	211
4-#11	1.28	1399	1123	1123	1034	930	752	617	423	275	194	0	0	3.49	10.45	501	20.07	253
4-#14	1.85	1508	1208	1208	1115	1007	823	685	506	357	259	200	0	3.77	12.38	494	24.62	353
4-#18	3.30	1786	1419	1419	1315	1193	989	835	632	507	402	319	262	4.31	17.25	478	35.70	592
8-#8	1.30	1402	1112	1112	1019	909	722	584	380	262	194	0	0	3.11	9.30	516	20.10	261
8-#9	1.65	1469	1161	1161	1065	952	762	621	424	299	226	0	0	3.23	10.16	514	22.78	324
8-#10	2.09	1554	1225	1225	1124	1007	811	666	477	342	262	211	0	3.36	11.28	511	25.93	403
8-#11	2.57	1646	1290	1290	1184	1061	857	708	520	381	294	238	199	3.52	12.48	504	28.82	481
8-#14	3.71	1865	1451	1451	1331	1195	972	809	604	474	372	304	255	3.76	15.32	496	35.99	668
8-#18	6.61	2420	1852	1852	1698	1526	1249	1048	789	636	530	450	383	4.16	22.73	476	52.97	1039
12-#10	3.14	1756	1374	1374	1261	1130	915	758	558	424	334	275	232	3.51	13.43	509	32.69	569
12-#11	3.86	1893	1472	1472	1350	1210	982	815	603	473	374	309	262	3.67	15.16	500	37.20	666
12-#14	5.57	2221	1714	1714	1569	1407	1146	958	716	570	471	391	334	3.91	19.31	488	47.48	905
16-#10	4.19	1957	1525	1525	1401	1257	1021	849	632	499	397	329	281	3.66	15.54	514	39.41	729
16-#11	5.15	2141	1658	1658	1520	1363	1108	924	690	549	447	371	317	3.81	17.77	503	44.90	852
20-#10	5.24	2158	1673	1673	1537	1384	1128	943	704	560	457	381	326	3.80	17.86	512	46.06	878

(1) See "Slender Columns, Capacity Reduction for", page 2-11.
(2) See "Control Points for Interaction Curves"; "Typical Interaction Curve", Fig. 3-11, page 3-18.
(3) "OT" is zero tension in bars on the tension side. Splices carry design compression only.

Fig. 4-15. Column Interaction Table for Peachtree Building.

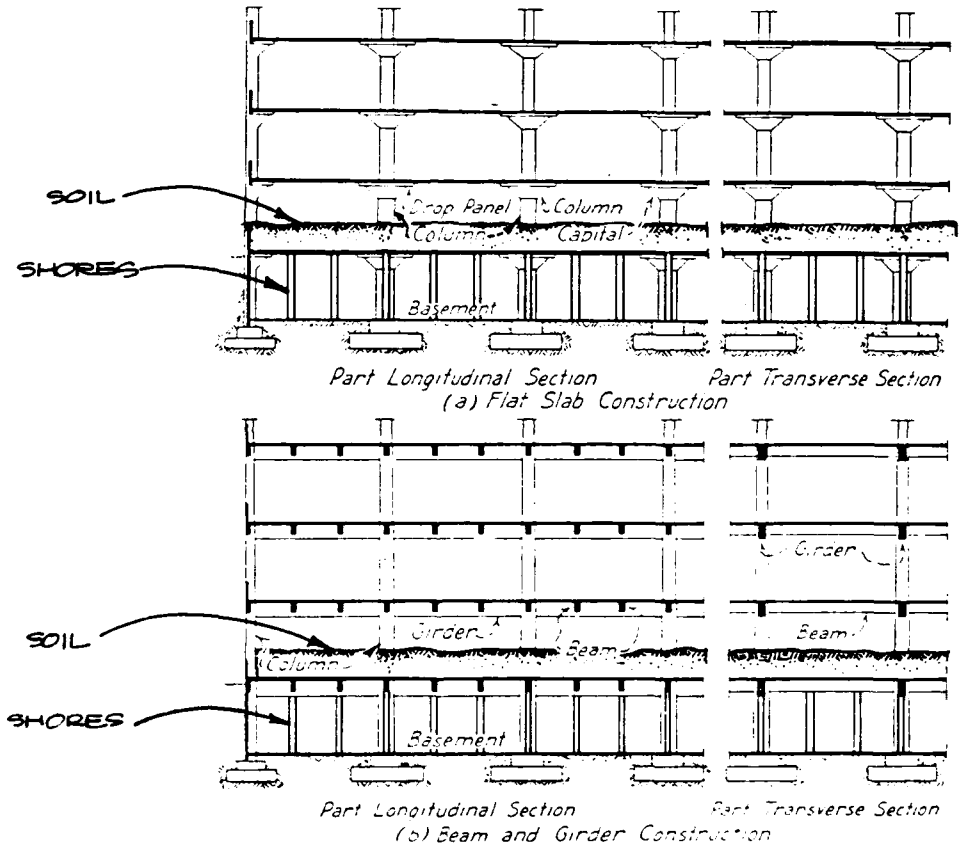

Fig. 4-16. Upgrading Schemes for Typical Concrete Framing Systems.

Close-in Shoring

For cases where there are high moments induced in the ground-level slab; either due to heavy-debris loads or due to the "crow-bar" prying action of strong steel frame columns, the shores may be placed "close-in" to the columns in order to assist the slab or a weak steel frame connection in resisting the imposed column movement, see Figure 4-17.

SUBTASK 3C: DEVELOPMENT OF FAILURE MODES

The Role of Plastic Analysis Techniques

In the introductory paragraph of this section, the comment about collapsing frames constituting a "new frontier" turned out to be truer than even the authors initially perceived. In the late 50's and early 60's, the plastic design of framed structures was a primary part of structural engineering. The concept of plastic design had the potential for economies in building design and construction and for the development of a more uniform factor of safety throughout the structure (i.e., a more uniform probability of collapse of the various components). However, the evolution of plastic design of framed structures has almost ceased since the recent advent of sophisticated computer programs. These computer programs permitted rapid economical linear elastic analysis of even the most complex frame structures, and hence, the simple "plastic mechanism" analysis advantage of plastic design has been outmoded. Also, the material economies of plastic design, inherent in member section capacities and in moment redistribution, have been incorporated into building code provisions. Hence, present design is performed by use of elastic analysis for stresses, and section design by approximations of plastic capacity.

For the purposes of the frame response history analysis, however, there was a specific need to identify the different mechanisms of frame collapse and the respective collapse loads. This "mechanism" analysis is based on the resistances of the beams and columns for a typical frame as determined by the methods in Subtask 3B and on the particular computer model. The form of analysis and prediction of failure modes in this section follows the classical plastic design techniques presented in Appendix A. By the use of the computer, the fundamental theories of limit design

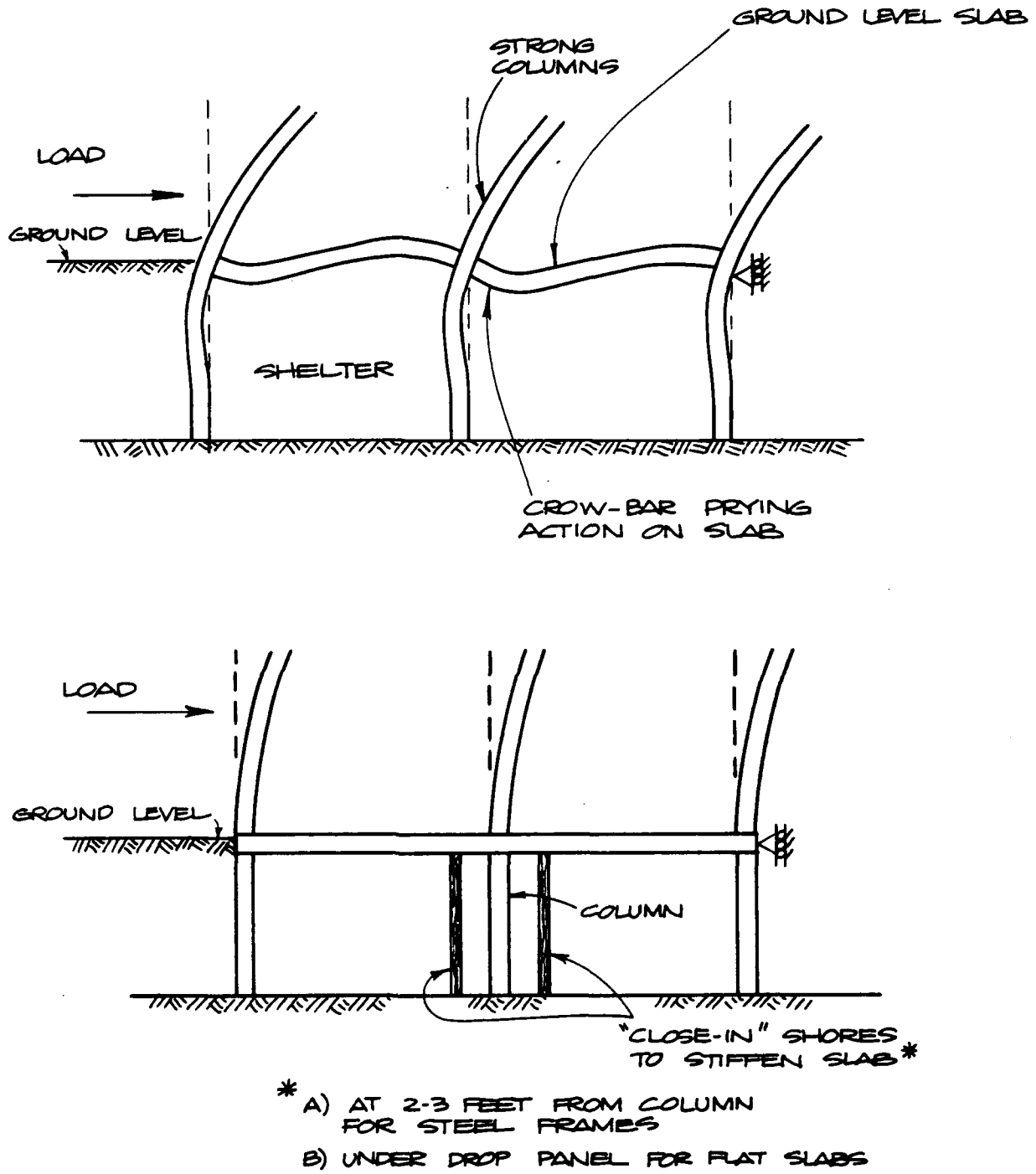

Fig. 4-17. Shoring Countermeasure Against High Induced Moments in Ground-Level Slab.

will predict the most probable failure modes for a building frame. The initial fully elastic response of the framed structure, however, may show some anomalies, in that higher moments may be achieved at levels other than those predicted by the limit design failure mode analysis. These moments will be elastic failures, however, and as successive trials approach the mechanism of collapse, classical plastic design will eventually dominate the failure mode. This will be demonstrated in Section 5, Computer Analysis.

Figure 4-18 shows a representation of a typical framed structure model. The hinge formation in this type of structure, if the basement is properly shored, will be forced in the column above the floor level. At the column-beam intersection at joint "A", in the corner at the first level, as long as the column is continuous through the joint and the beam has some moment reistance, there should be yield hinge development in the column. Because of the relative stiffness of the floor system, it is very possible that in the elastic analysis initial yielding may develop in the beam at M_b prior to complete hinge formation in the column labeled M_p. However, since side sway is prohibited at this ground level, a hinge will ultimately develop at M_p, and only small damage will occur in the M_b area. For the interior joint at "B", M_b occurs twice, M_c is on the basement side of the column, and M_p is on the column above the first story. Here again, if the column is continuous through the joint, and M_b has any value at all, the hinge will form at M_p. In concrete frames this would nearly always be the case, since the column steel is generally spliced above the floor level, thereby creating a zone of weakness.

As discussed in Subtask 3B, many steel frames have essentially pin connections or seated connections at the beam-to-column connection, and the column is indeed continuous through the joint. This results in a lack of moment capacity in the beam, but this deficiency may be overcome by locating shores near the columns. Placing of shores near a column generates significant moment resistance in a member, even if it is nominally pin connected. This resistance occurs because the shear capacity of the joint times the short lever arm distance to the shore generates sufficient moment to cause the hinge to occur above the floor level.

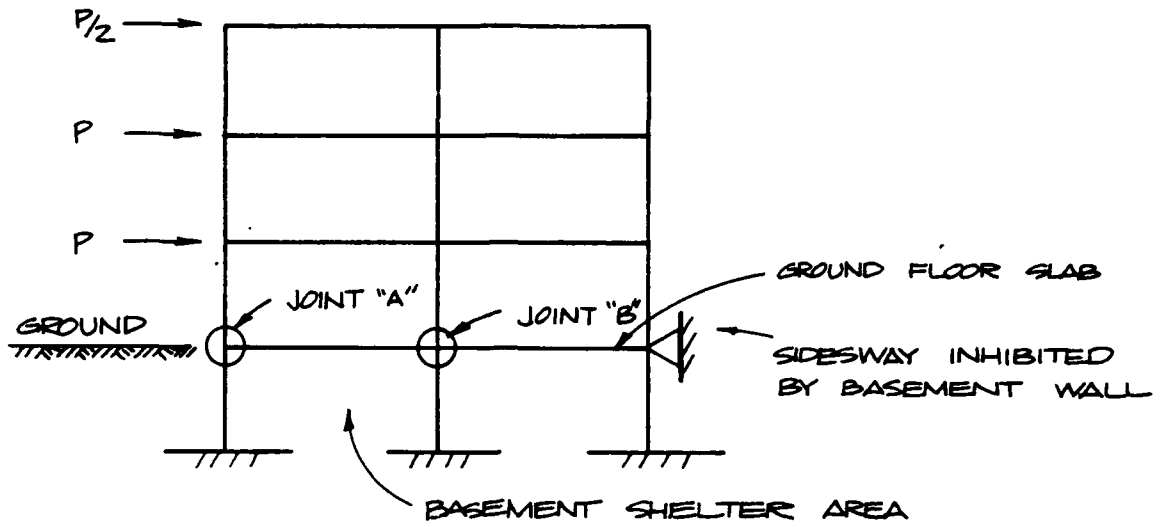

JOINT "A"

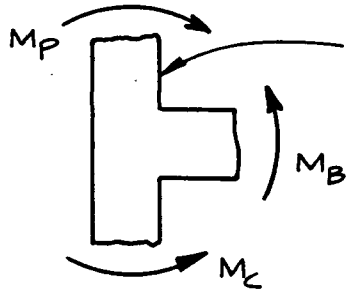

IF $M_B + M_C > M_p$
THEN COLUMN HINGES

JOINT "B"

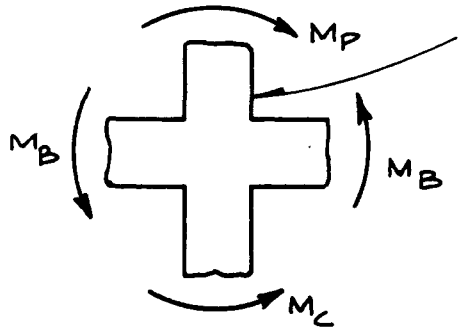

IF $2M_B + M_C > M_p$
THEN COLUMN HINGES

REVIEW OF CAPACITIES FROM TASK 3B

COLUMN M_p = 483 KIP-FEET

BEAM M_p = 200 KIP-FEET, USING M_u = 300 KIP-FEET

Fig. 4-18. Hinge Formation in Typical Structure.

For reasons discussed previously, the basement selected should include a reinforced concrete floor cast monolithically with the wall system in order to resist side sway at ground level.

Simplified Plastic Analysis of Peachtree Building

The particular frame used as our example, and which will be discussed below in more detail, is a small portion out of the larger Peachtree Building, the structure that is analyzed in Section 5. The moment capacities for the beams and columns in this frame are based on the calculations shown in Subtask 3B. The moment capacity of the beam, M_p, is approximately 200 kip-ft for both positive and negative moment directions, and the moment capacity of the columns in the lower story is approximately 483 kip-ft, or 2.41 M_p of the beams.

Figure 4-19 is a sketch of the basic frame used in this mechanism study. It is a three-story, two-bay frame with a basement structure restrained at the ground level. The frame consists of 15 joints, 10 reactions external, and 20 bars, and results in 15 independent mechanisms of collapse. One interesting observation is that all of the possible beam mechanisms (see Appendix A) are not developed as a result of side loading. This differs from what is usually presented in the typical plastic design text, where often gravity loads are the prime concern in building design. In this study, the blast load dominates, shown as P on this structure, and the gravity loads are merely the dead loads of the structure. Hence, in the limit analysis for these structures, only the lateral loads are considered; the dead load has been nominally taken care of in the adjustment of the moment capacities for the various beam and column components.

Another very interesting aspect of this particular problem is that of the 15 independent mechanisms, 12 are degenerate modes or joint rotation modes where external work is not done, and this leaves only three independent side-sway modes where external work is done. This implies that far more complex problems can be performed by hand analysis than was originally thought possible. In a sense, there are only three independent mechanisms, and these can be used to very closely approximate the true failure load.

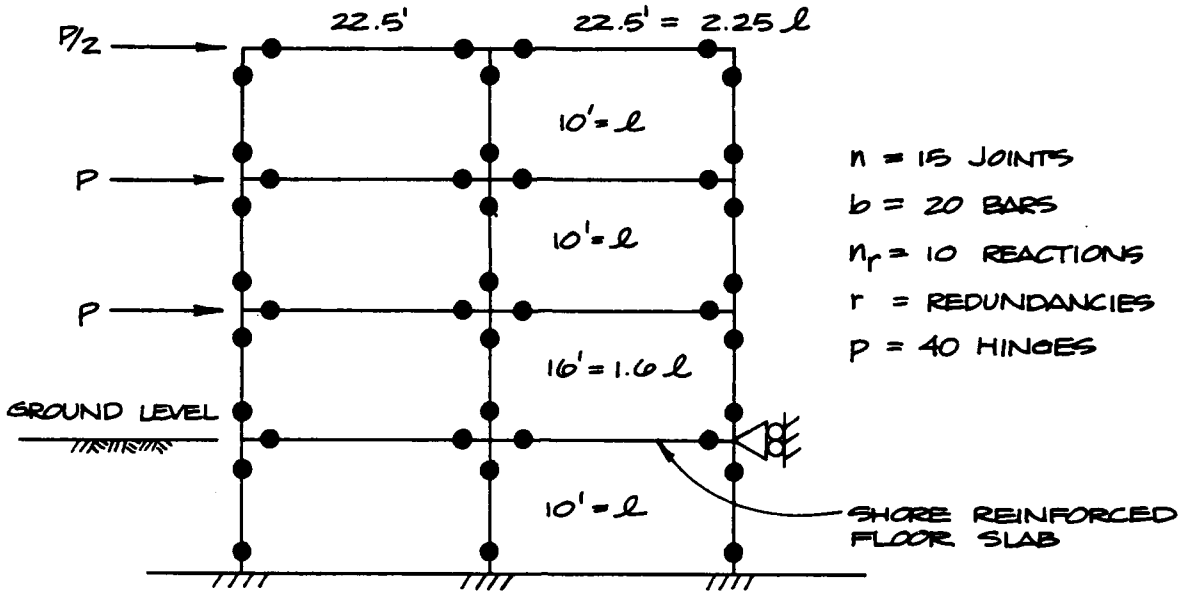

$r = |3n - 3b - n_r| = |45 - 60 - 10| = 25$ DEGREES INDETERMINATE

$10 - 3 = 7$ EXTERNAL INDETERMINATE DEGREES

18 = INTERNAL INDETERMINATE DEGREES

$m = p - r = 40 - 25 = 15$ INDEPENDENT MECHANISMS

OF THESE 15, 12 ARE JOINT ROTATIONS OR DEGENERATE MODES WITH NO ENERGY DISSIPATION.

THREE CASES OF MEMBER CAPACITIES TO BE INVESTIGATED:

- STRONG COLUMN CASE: COLUMN $M_p = 483\ K' = 2.41\ M_p$
  BEAM $M_p = 200\ K' = M_p$
- MEDIUM COLUMN CASE: COLUMN $M_p = 283\ K' = \sqrt{2}\ M_p$
  BEAM $M_p = 200\ K' = M_p$
- WEAK COLUMN CASE: COLUMN $M_p = 200\ K' = M_p$
  BEAM $M_p = \sqrt{2}\ M_p$

Fig. 4-19. Side-Sway, Hinge, and Combined Mode Assessment.

MEDIUM COLUMN CASE = COLUMN = $\sqrt{2}$ M_p

BEAM = M_p

INDEPENDENT MODE 1 (SIDE-SWAY)

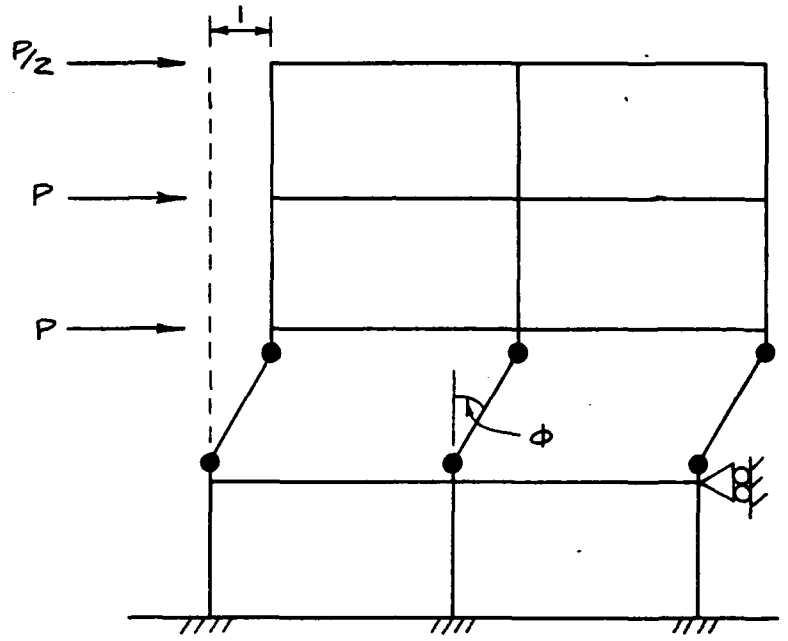

$\phi = 1/1.6\,\ell$

EXTERNAL WORK = INTERNAL WORK

$2.5P = 6\sqrt{2}\,M_p/1.6\,\ell$

$P = 2.12\,M_p/\ell$

* MINIMUM FOR MEDIUM CASE

Fig. 4-19. (contd)

INDEPENDENT MODE 2

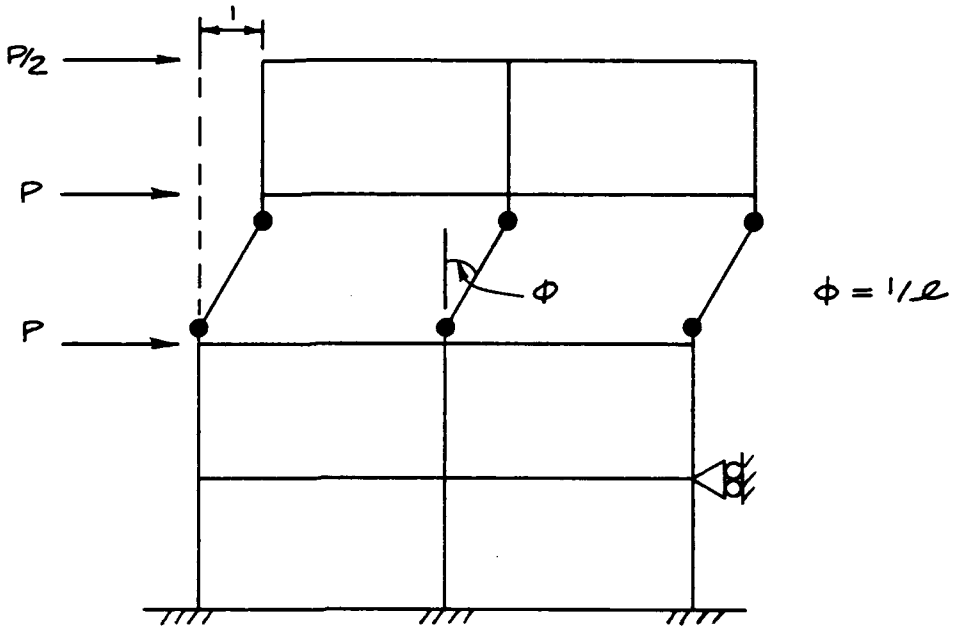

$1.5\ P = 6\sqrt{2}\ M_p/\ell$

$P = 5.66\ M_p/\ell$

INDEPENDENT MODE 3

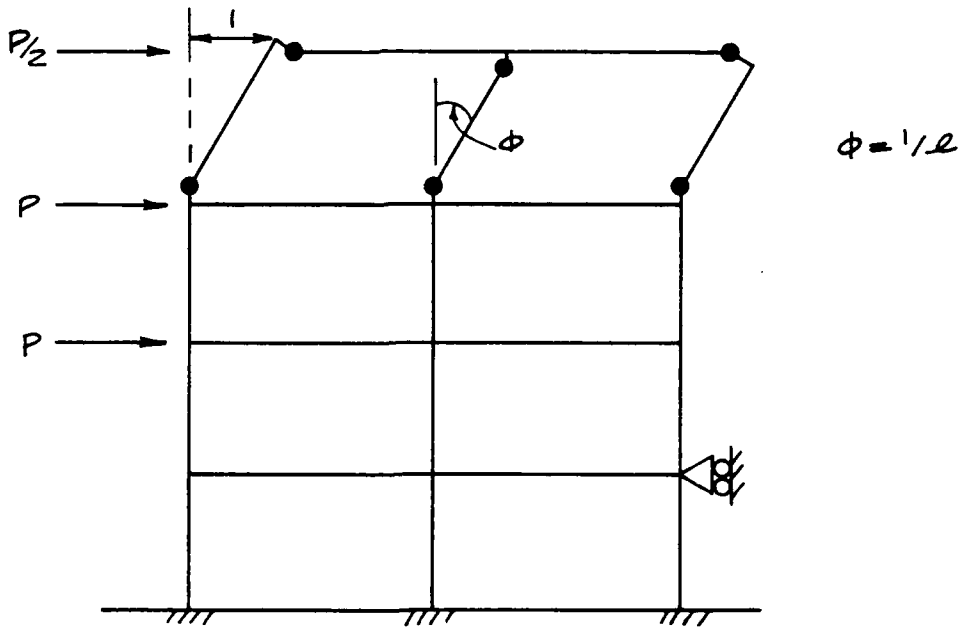

$P/2 = 4\sqrt{2}\ M_p/\ell + 2\ M_p/\ell$

$P = 15.30\ M_p/\ell$

Fig. 4-19. (contd)

COMBINED MODE 1

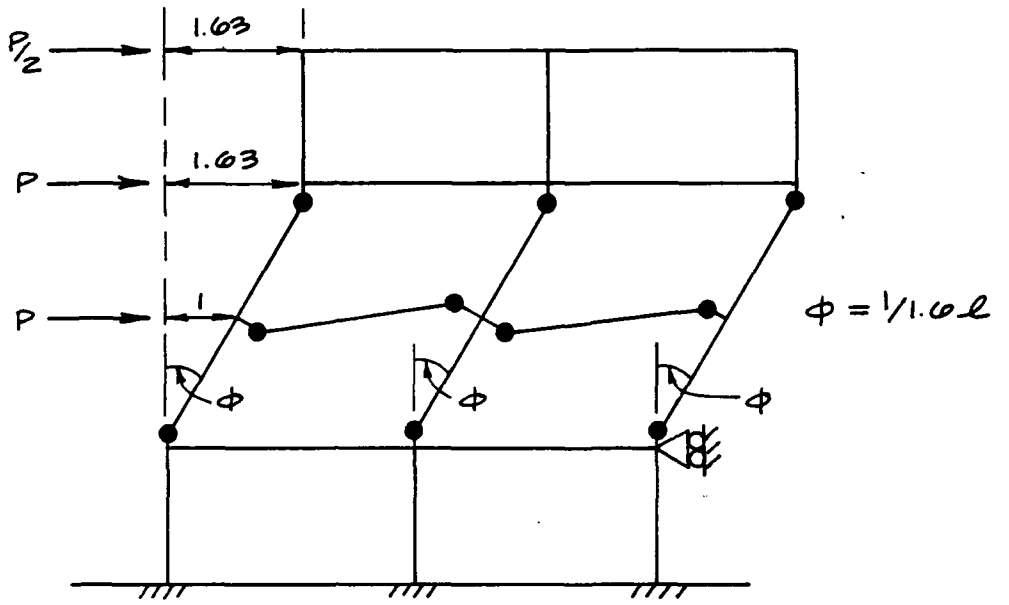

$$2.63\,P + P/2\,(1.63) = 4\,M_P/1.6\ell + 6\sqrt{2}\,M_P/1.6\ell$$

$$P = 2.26\,M_P/\ell$$

COMBINED MODE 2

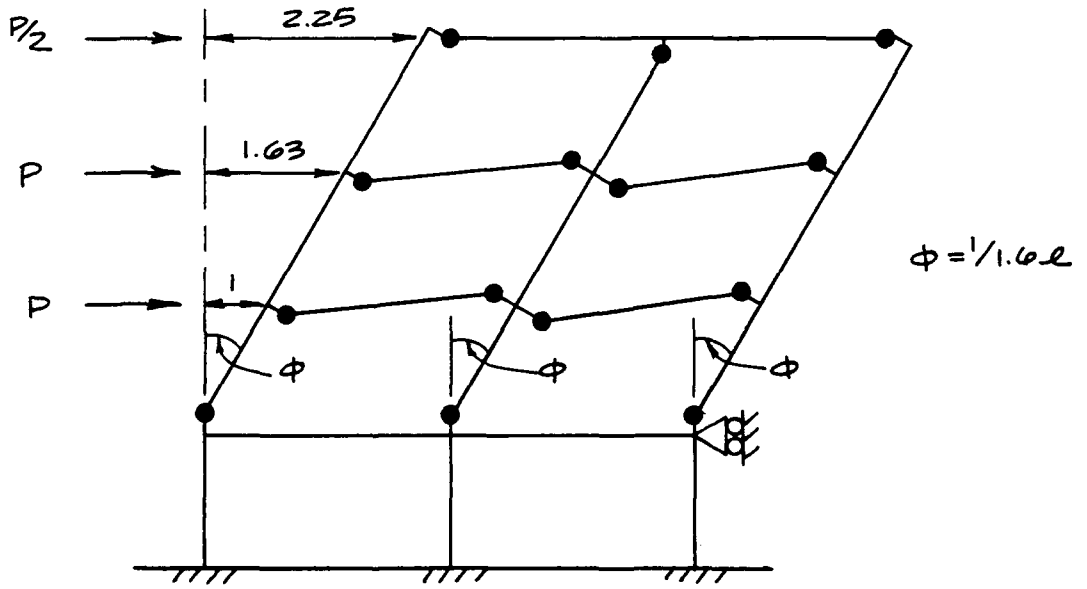

$$P(2.63) + P/2\,(2.25) = 10\,M_P/1.6\ell + 4\sqrt{2}\,M_P/1.6\ell$$

$$P = 2.61\,M_P/\ell$$

Fig. 4-19. (contd)

STRONG COLUMN CASE: COLUMN $M_p = 403\ K' = 2.41\ M_p$
BEAM $M_p = 200\ K' = M_p$

NOTE THAT THESE ARE THE MEMBER STRENGTHS USED FOR THE FULL PEACHTREE BUILDING ANALYSIS

INDEPENDENT MODE 1

$$2.5\ P = 6(2.41)\ M_p/1.6\ell$$

$$P = 3.62\ M_p/\ell$$

INDEPENDENT MODE 2

$$1.5\ P = 6(2.41)\ M_p/\ell$$

$$P = 9.04\ M_p/\ell$$

INDEPENDENT MODE 3

$$P/2\ (1) = 3(2.41)\ M_p/\ell + 4\ M_p/\ell$$

$$P = 22.5\ M_p/\ell$$

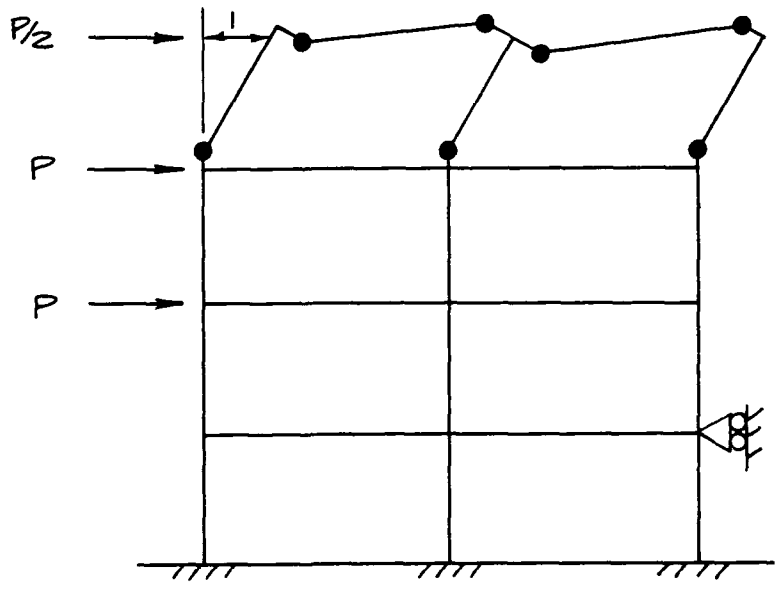

Fig. 4-19. (contd)

COMBINED MODE 1

$$2.63P + P/2\,(1.63) = 4(Mp)/1.6\ell + \frac{6(2.41)\,Mp}{1.6\ell}$$

$$P = 3.34\ Mp/\ell$$

COMBINED MODE 2

$$(1+1.63)P + P/2\,(2.25) = 10\ Mp/1.6\ell + 4(2.41)\ Mp/1.6\ell$$

$$3.76P = 12.4\ Mp/\ell$$

$$P = 3.30\ Mp/\ell$$

* MINIMUM FOR STRONG COLUMN CASE

Fig. 4-19. (contd)

WEAK COLUMN CASE: COLUMN $M_p = 200\ K' = M_p$

BEAM $M_p = \sqrt{2}\ M_p$

INDEPENDENT MODE 1

$$2.5\ P = 6M_p / 1.6\ell$$

$$P = 1.5\ M_p/\ell$$

* MINIMUM FOR WEAK COLUMN CASE

INDEPENDENT MODE 2

$$1.5\ P = 6M_p/\ell$$

$$P = 4\ M_p/\ell$$

INDEPENDENT MODE 3

$$P/2\ (1) = 6\ M_p/\ell$$

$$P = 12\ M_p/\ell$$

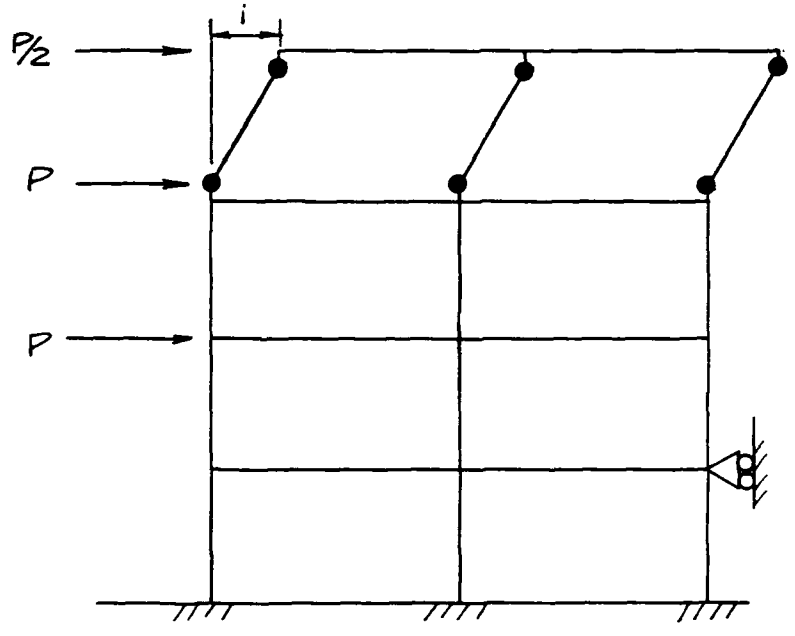

COMBINED MODE 1

$$2.63P + P/2\ (1.63) = \frac{6M_p}{1.6\ell} + 4\sqrt{2}\ M_p/1.6\ell$$

$$P = 2.11\ M_p/\ell$$

COMBINED MODE 2

$$P(2.63) + P/2\ (2.25) = 4M_p/1.6\ell + \frac{10\sqrt{2}\ M_p}{1.6\ell}$$

$$P = 3.02\ M_p/\ell$$

Fig. 4-19. (contd)

The three independent side-sway modes, as illustrated in Figure 4-19, are first level (1), second level (2), and third or top level (3), respectively. Combined Mode 1 is the combination of side-sway Mode 1, side-sway Mode 2, plus the appropriate independent hinge modes. Combined Mode 2 is a combination of all three side-sway modes, and again, the appropriate independent hinge modes. Although other possible modes of failure exist, it is felt that these are the dominant modes based on the simplicity of the blast loading system.

Table 4-2 is a summary of the analysis of the frame described above with beam strength to column strength ratios representing strong columns, medium columns, and weak columns. The first case, strong columns, could occur where design criteria require substantial resistance to lateral loads, such as in earthquake zones, and the third case, weak columns, is not uncommon when the span between the columns is fairly long compared with the story height, or the vertical loads are very heavy. The medium column case takes into account a structure lying between these two extremes.

TABLE 4-2: SUMMARY OF FRAME ANALYSIS

	M_{column}/M_{beam} Ratio		
	(1)	(2)	(3)
MODE	Strong Column $2.41\ M_p/M_p$	Medium Column $\sqrt{2}\ M_p/M_p$	Weak Column $M_p/\sqrt{2}\ M_p$
Independent 1	$3.62\ M_p/\ell$	$*2.12\ M_p/\ell$	$*1.50\ M_p/\ell$
Independent 2	$9.64\ M_p/\ell$	$5.66\ M_p/\ell$	$4.00\ M_p/\ell$
Independent 3	$22.5\ M_p/\ell$	$15.30\ M_p/\ell$	$12.00\ M_p/\ell$
Combined 1	$3.34\ M_p/\ell$	$2.26\ M_p/\ell$	$2.11\ M_p/\ell$
Combined 2	$*3.30\ M_p/\ell$	$2.61\ M_p/\ell$	$3.02\ M_p/\ell$

* indicates minimum or failure P.

As shown in Table 4-2, the Combined Mode 2 is the collapse, or failure, mode when columns are considerably stronger than the beams. In this case, the entire building leans over, and failures occur at the column bases, just above the floor grade, and then lateral movement of the upper stories occurs similar to a falling tree. In the case of columns that are only slightly stronger than beams, the shift is toward Independent Mode 1, where the upper stories remain intact, and the building moves sideways above the first level. It should be noted that the differences between loads for Independent Mode 1 and Combined Mode 2 are not great. Accordingly, where structures have a fairly equal beam/column resistance, the modes can be either "soft story" with the upper stories remaining rigid, or "falling tree".

In the third analysis, where the beam is stronger than the columns, there is a very large difference between the Independent Mode 1 and Combined Mode 2. As the structure fails in Mode 1, it moves laterally at the first story and basically remains a vertical and intact system above. This type of "soft story" is often noted in earthquake catastrophes, such as the failure of Olive View Hospital in San Fernando and several of the apartment buildings in Caracas, Venezuela. In these cases, the structures had been designed as rigid frames, but above the first story, masonry infill walls had actually formed a shear wall building such that the frame did not respond in a frame-like manner, but as a rigid box on a one-story frame. It is important to note that a similar phenomenon would occur in a true frame by simply changing the column-to-beam strength ratio.

Another observation that can be made from this analysis is that, in many steel frame buildings, the exterior frames are designed to carry all the lateral load, and the interior frames are "pinned" at the beam-to-column connection; i.e., the interior frames are actually in the so-called combination Mode 3 by design. Hence, one may expect these steel frames to be forced into Combined Mode 2 even though the moment-resisting frame in the building itself may not otherwise be governed by this mode. As an example, if the Peachtree Building had been a steel frame building, the interior five frames may have been framed in the manner of Combined Mode 2, with all the beams pinned to the columns, and the two end frames would have probably been designed as rigid frames with continuous beams and columns in order to be the moment resisting or lateral load resisting system of the whole structure. In modern

building construction, the floors are generally poured concrete on steel decking and act as a diaphragm to carry the load to the rigid frames. When there are several frames in the center of the building that are actually constructed in this manner, Combined failure Mode 2, there is a high probability that the moment resisting frames at the end would be forced into this mode shape, and the calculated lower bound failure mode may be exceeded.

A simplified analysis of the Peachtree Building is summarized in Figure 4-20. It examines the entire 15 stories and 4 bays in brief. Because it is known that in this particular structure, the column strength is much greater than the beam strength, one would expect the combined modes could be important. Figure 4-20 illustrates the various modes of failure and provides the corresponding value of the load, P, from the simplified analysis. It is apparent from the latter that the lower bound static failure mode is Combined Mode 5, where $P = 0.73\ M_p/\ell$ (a static load of 14.6 kips). This represents hinges in four floors of beams and hinges in the columns at the base and below the sixth floor. The static-elastic computer analysis predicts first hinges forming at P = 10 kips in the second story beams, and if beams did not fail, columns would fail at about P = 17 kips, which of course bounds our plastic lower bound of 14.6 kips.

It is interesting to note that the predictions for the various failure modes (represented by the P values in the figure) are relatively close; i.e., ±15% from the average modal value, which is really quite close, considering our knowledge of the blast phenomena and actual construction details as built. Further, one would expect the response under dynamic loads to migrate toward lower modes (perhaps as low as Mode 2 or Mode 3) once the contribution of the upper story interiors is taken into account. This added resistance to motion is due to inertial forces of the upper stories, which tend to make the upper stories lag (see Section 5, Figure 5-10).

Another consideration would be reduction of column strength, as one goes up in the building. The effect here is that, if the column bending strength is reduced as one moves to upper stories (because of the reduced vertical load requirements in the building), this would reduce the variation in P values above the fourth floor and hence, the collapse mode in one of the higher side-sway modes. Even so, it is

THE PEACHTREE BUILDING

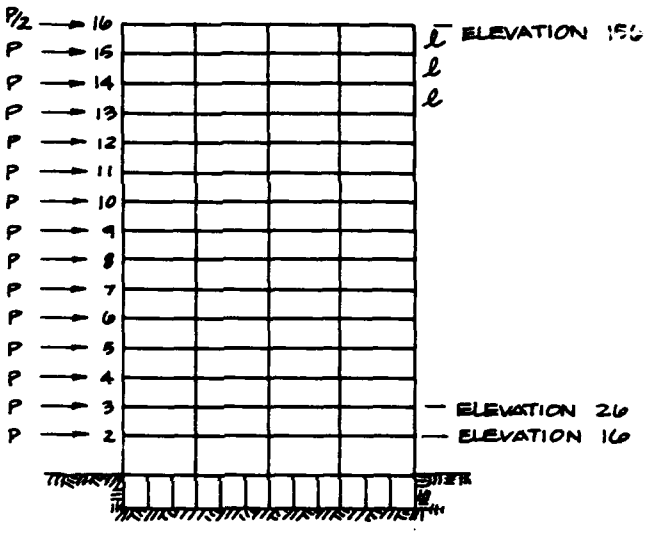

WHERE Mp FOR BEAM 2.41 Mp FOR COLUMN

SIDE - SWAY MODE 1

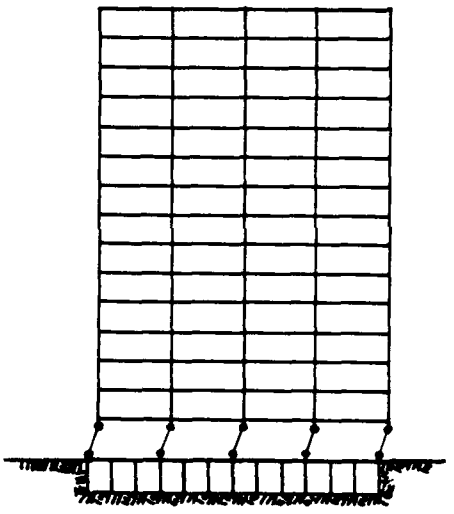

$$P = \frac{1.04\ M_p}{\ell}$$

Fig. 4-20. Modes of Failure for Peachtree Building.

COMBINED MODE 2

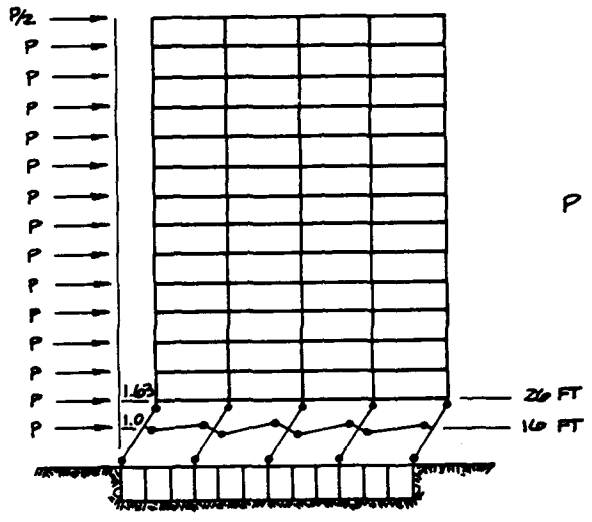

$$P = \frac{0.87\ Mp}{\ell}$$

COMBINED MODE 3

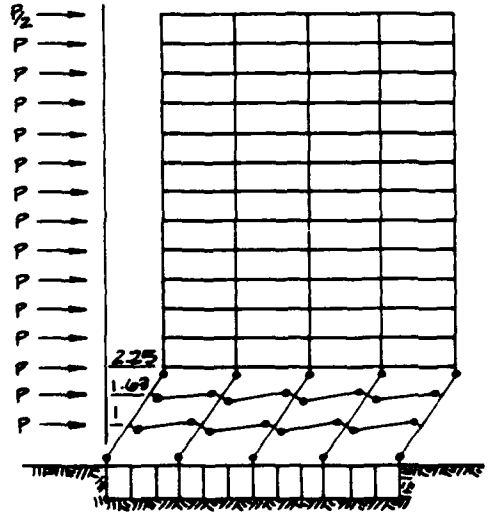

$$P = \frac{0.81\ Mp}{\ell}$$

Fig. 4-20. (contd)

COMBINED MODE 4

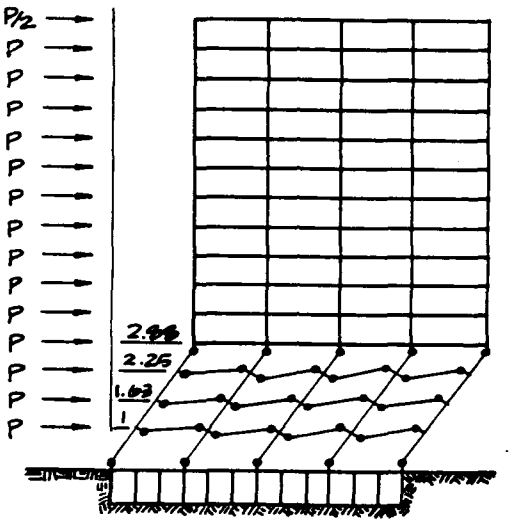

$$P = \frac{0.79\ M_p}{\ell}$$

COMBINED MODE 5

$$P = \frac{0.73\ M_p}{\ell}$$

COMBINED MODE 6

$$P = \frac{0.79\ M_p}{\ell}$$

COMBINED MODE 7

$$P = \frac{0.81\ M_p}{\ell}$$

Fig. 4-20. (contd)

COMBINED MODE 14

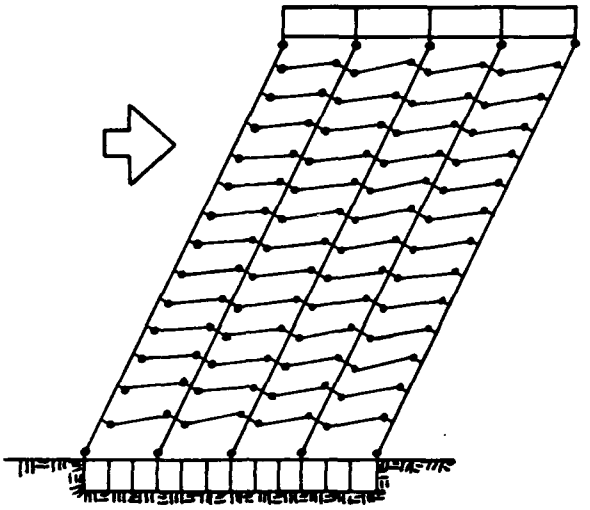

$P = \frac{0.96\ M_p}{\ell}$

COMBINED MODE 15

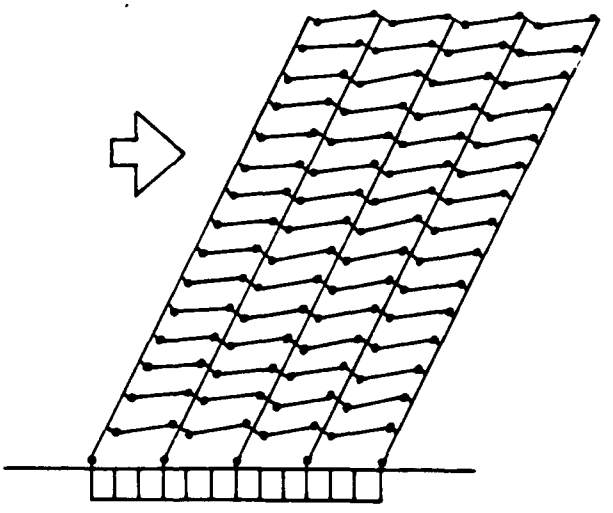

$P = \frac{1.09\ M_p}{\ell}$

Fig. 4-20. (contd)

unlikely that this effect could cause a collapse at a significantly lower load with typical building design.

For example, in the Peachtree Building it would be difficult to reduce the lateral resistance (or the bending resistance) of the columns below about 50% base column and maintain compliance with building code requirements. The beam strengths would be expected to remain constant throughout the structure, so that in the upper stories one could visualize a change in tendency toward a combined mode effect in the upper regions and the side-sway mode in the lower regions of the building. An assessment of the above conditions shows such a change would reduce Mode 14 from 0.96 M_p/ℓ to about 0.93 M_p/ℓ.

Variations such as these should be checked in future work, and some simple bounding rules need to be evolved for quick gross analyses of high-rise buildings. Another important observation is that, for this large scale building, the difference between the side-sway mode of the first story and the Combined Mode 2 is only 16%; although the columns are much stronger than the beams in this particular building, the condition for a column-induced failure and a beam-induced failure is relatively small. Hence, a possible approach to use in order to bound failure loads for the shelter space is to look at the two most divergent modes and assume:

(1) that the building collapse is in a mode like the side-sway (soft story) mode, with the first floor columns falling and the building moving as a rigid body laterally until the upper stories collapse on the basement somewhat as a unit;

(2) that the building collapse is in a combined mode, where the beams and columns fail and all or part of the building rotates like a falling tree.

Consequences and effects on the shelter space will be investigated for these two cases.

From the results of the simplified analyses (Figure 4-20) the constant or statically applied (not time varying) failure load P can be determined, or at least bracketed to an accuracy of about 25%. For the Peachtree Building this failure

blast load is $P = 0.87\ M_p/\ell$, or about 17.4 kips (vs 14.6 statically). This is the result of the blast pressure at each story level. When this static value of P is compared with the time-varying blast level used in the computer analysis of Section 5, it is quite obvious that failure will occur at a very early time.

Objectives of the Dynamic Analysis

Knowing that the "static" failure load, P, is on the order of 15 kips and comparing this with the very high blast load, P_t shown in Figure 4-21 (a straight-line approximation to Figure 4-6), it is quite obvious that frame failure will occur. Therefore, the main questions to be addressed are:

(1) What is the primary mode of failure, "soft story" or "falling tree"?

(2) Is the blast load intensity and duration sufficient to cause progressive mechanisms in the structure after the formation of the primary failure mode?

(3) Will the entire structure be virtually shattered before it drops to the ground, or will it remain intact and destroy itself by gravity action and impact on the shelter slab?

(4) Will the imparted velocity and residual blast force be sufficient to carry the failing structure beyond the shelter area, or will most of the structure come down on the shelter slab?

In Section 5, the complete successive elastic, elasto-plastic, plastic mechanism analysis is performed for the given blast loading of Subtask 3A and member strength properties of Subtask 3B.

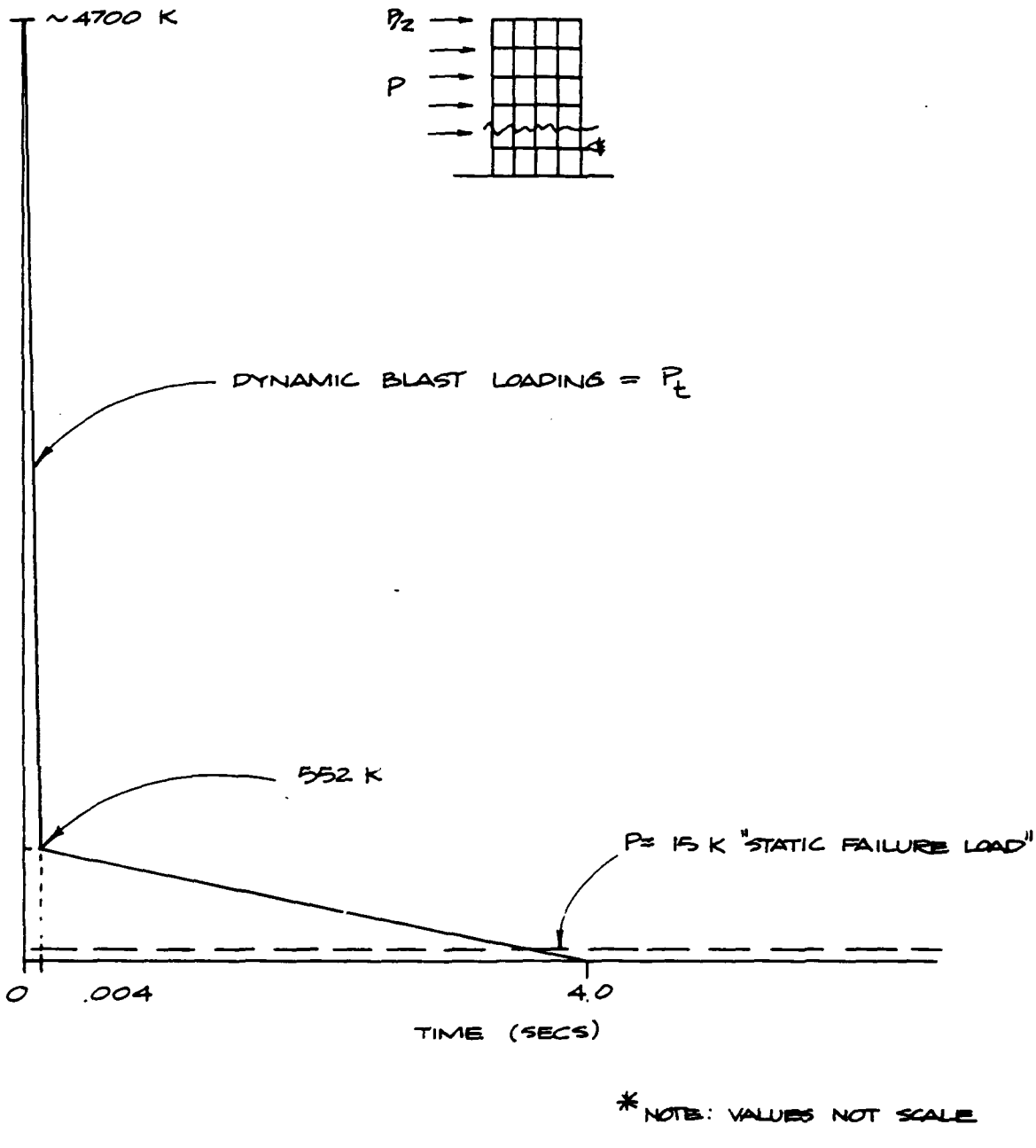

Fig. 4-21. Comparison of Dynamic Blast Load and "Static" Failure Load.

Section 5

COMPUTER MODEL DEVELOPMENT, ANALYSIS, AND RESULTS

INTRODUCTION

It has been common practice in civil engineering to represent time-varying dynamic loads as equivalent, pseudo-static loads for the analysis of structures. This applies to blast, wind and earthquake loading conditions. However, as more data are obtained regarding the nature and effects of transient dynamic loadings, structural engineers are becoming increasingly aware of the necessity to perform more realistic dynamic analysis in order to predict structural response.

Also, acceptable procedures for generating pseudo-static loadings have not been developed for many dynamic loading conditions. The requirement for dynamic analyses leads to a direct need by the engineer for a sophisticated general purpose computer software system. For the analysis in this report the static and dynamic features of the Georgia Tech Integrated Civil Engineering System Structural Design Language (GTSTRUDL) were selected.

Figure 5-1 shows the dynamic capabilities of the chosen computer software system. Several types of dynamic analysis are available. The program offers a choice of performing a shock analysis (response spectrum) to determine the maximum effect due to an input frequency spectrum, or the choice of a normal mode analysis, or a direct integration of the equations of motion to determine the transient response due to specified transient loads or support accelerations. A description of the fundamental computational methods in the dynamic analysis program is presented in Appendix B.

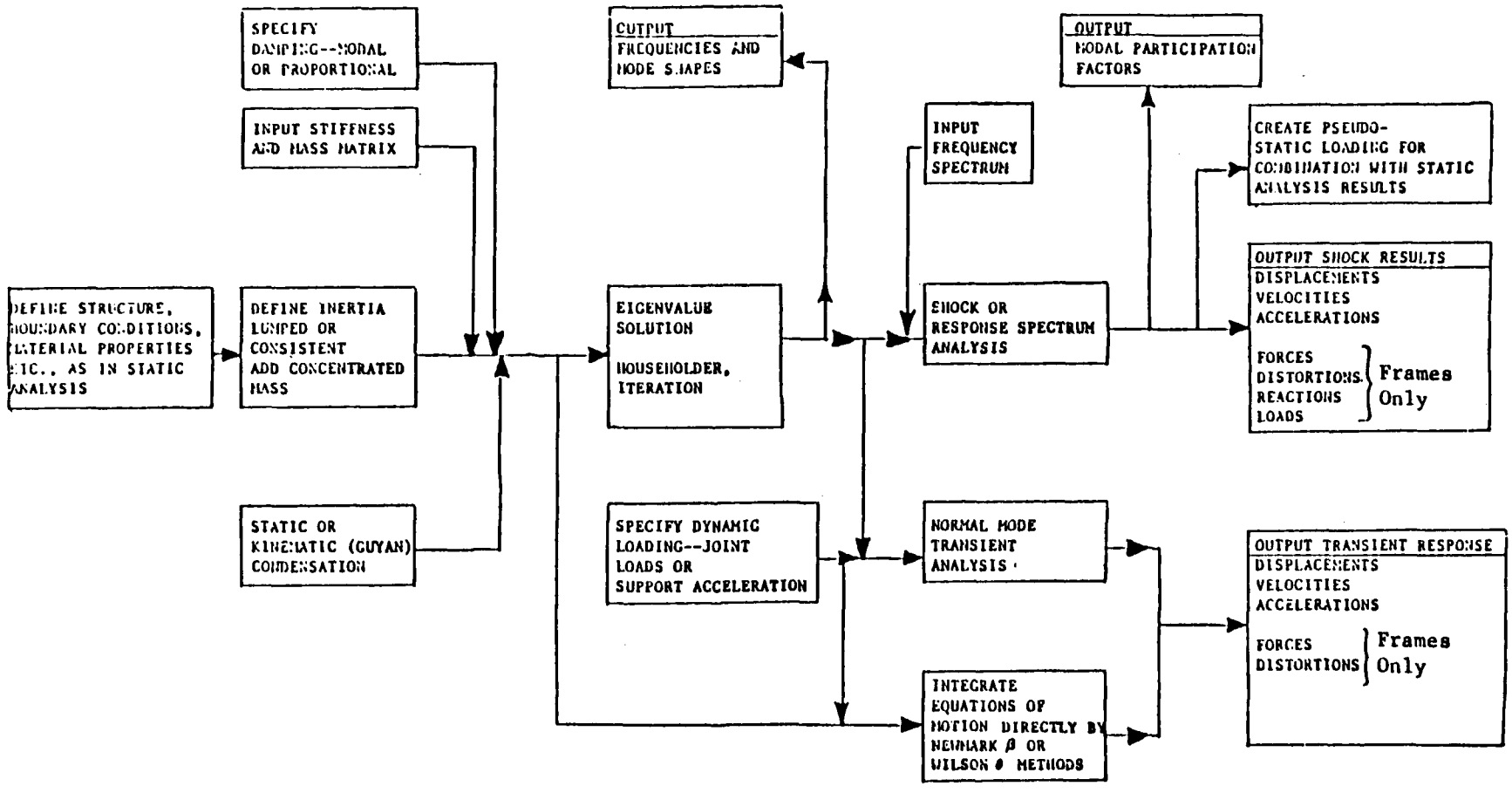

Fig. 5-1. GTSTRUDL Dynamics Overview.

DESCRIPTION OF BUILDING STRUCTURES FOR ANALYSES

Two separate structures were analyzed under both static and dynamic blast loading conditions. A three-story, two-bay structure was used to verify the method and accuracy of the analysis procedure. A fifteen-story, four-bay concrete structure with basement* was used as the representative structure to predict the collapse mechanism when subjected to a 30 to 50 psi blast pressure level. To facilitate the analysis and reduce the amount of data to be handled, only one representative cross section through the full width and height of the building was used. Verification of the chosen computer code consisted of modeling the three-story building using 15 nodes, 12 column elements, and 8 beam elements. Total degrees of freedom numbered 36, considering the structure as a planar-moment resisting frame ignoring the out-of-plane displacements and rotations. Boundary conditions consisted of the columns being fixed at ground level and the first floor being resisted from displacing horizontally.

Static analyses performed on the structure were verified using moment distribution techniques. Dynamic analyses were verified using approximations to fundamental frequencies and mode shapes. A single mass-spring system was used to verify time behavior of the structure. The computer code applied checked out well against the behavior predicted via the simplified analysis. However, to lend credence to the collapse predictions for the representative structure actual data are needed.

The representative structure was modeled for static analysis using 101 nodes, 80 column elements, 72 beam elements and 8 basement shoring elements. The column elements were 22 in. square reinforced concrete, beam elements were 12 in. x 24 in. reinforced concrete, and basement shoring elements were 8 in. x 8 in. wood posts. (See Figure 5-2 and 5-3 for elevation and floor plan.) All beam and column intersections were considered moment resisting, except that the wood shoring was considered pin connected to the basement floor and concrete first floor beams. In addition, for the dynamic analyses a lumped mass system was used using 88 masses with a total of 237 dynamic degrees of freedom.

---

* Peachtree Building, demolished by CDI in 1980, located in Atlanta, Georgia.

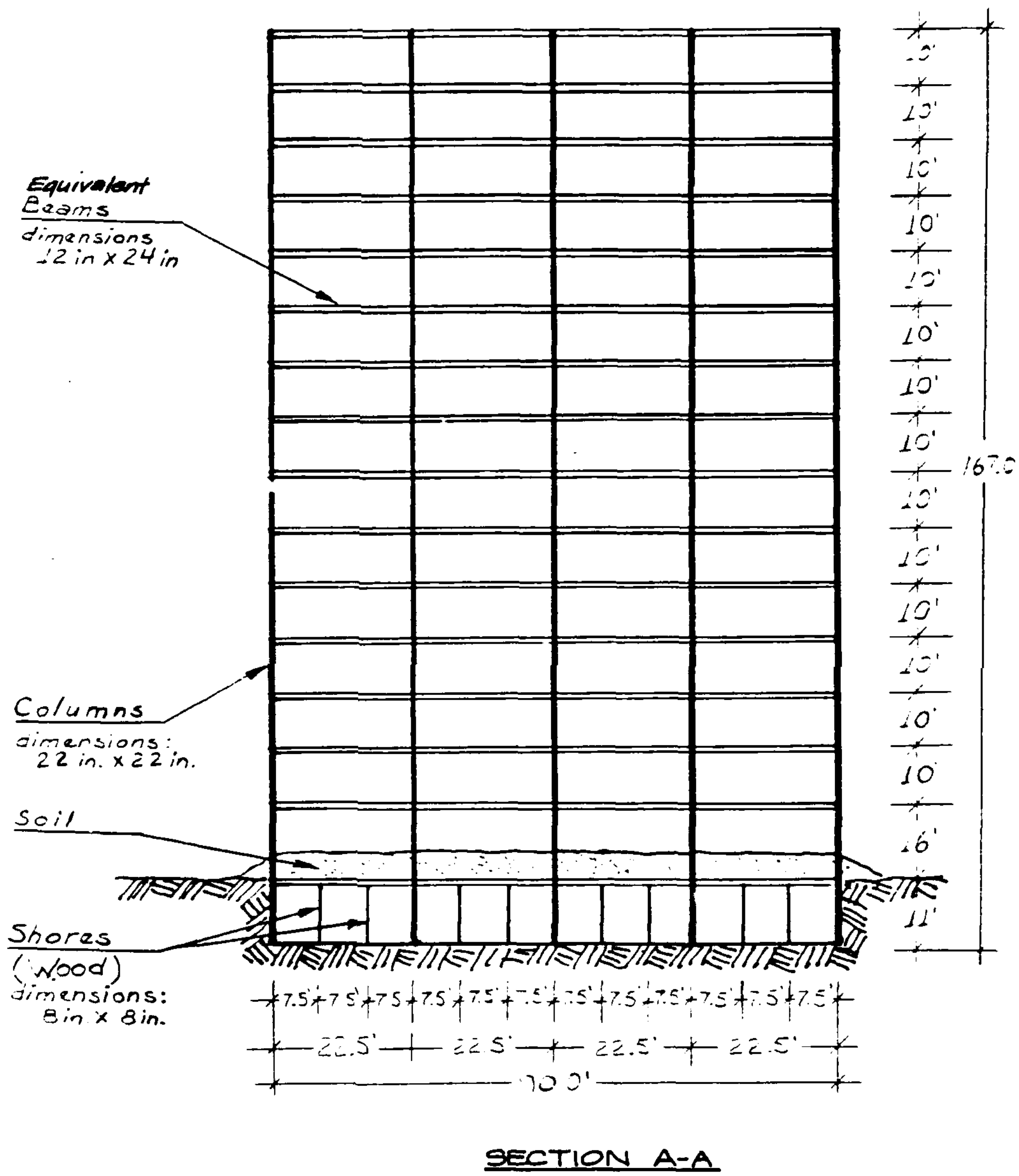

Fig. 5-2. Concrete Framed Structure.

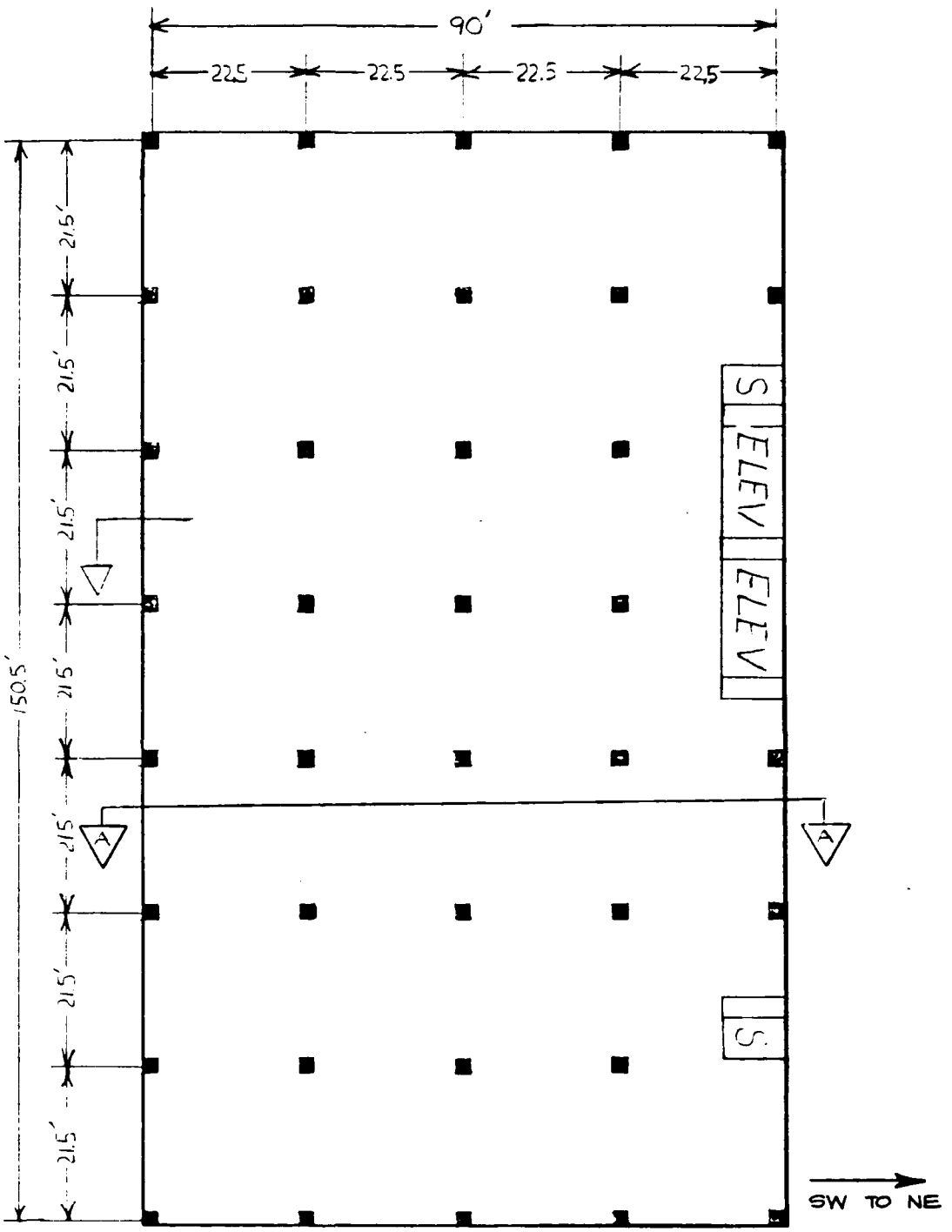

Fig. 5-3. Typical Floor Plan View.

For dynamic history analysis, a modal analysis method of solution was used, as described in the appendix under the heading of computer analysis fundamentals. Figures 5-4, 5-5, and 5-6 show the joint and member numbering scheme, member forces at any time instant, and the shape of the deformed structure under static load.

RESULTS OF ANALYSES OF PEACHTREE BUILDING

To determine the behavior of the structure when subjected to a blast, a conversion must be found to translate the blast into a force history as it impinges on the structure. Subtask 3A developed this conversion, and Figure 5-7 shows the resulting load function as it applies to the joints on the side of the building facing the blast. The application of the blast load in addition to the dead load of the building are shown pictorially in Figure 5-8. Joint resistances were developed in Subtask 3C, the column resistance is 480 kip-feet and the beam resistance 200 kip-feet to reach the yield limit of the concrete.

For the pseudo-plastic phase, the reduced stiffness $E_R I$ was taken as one-tenth of the initial elastic stiffness EI. The ductility factor for the ratio of failure (fracture) rotation $_F$ to elastic limit rotation $_P$ was taken as five. Ordinary reinforced concrete construction could have a range of equal to 3 to 6, and the selected value gives the model a chance to exhibit a reasonable amount of mechanism development before failure.

Initial failure due to yielding under blast load conditions occurs 60 milliseconds (0.06 seconds) after initial blast impingement, when a collapse mechnism as shown in Figure 5-9 has formed. Total collapse of the structure occurs when all the yield hinges have reached their ultimate moment carrying capacity. Failure of the collapse mechanism starts at 120 milliseconds and total failure is complete at 200 milliseconds after initial blast impingement.

The lower two floors have completely collapsed and are in the process of depositing rubble within a few feet of their original position. The rest of the structure is free from its foundation and is now a free falling object governed by its

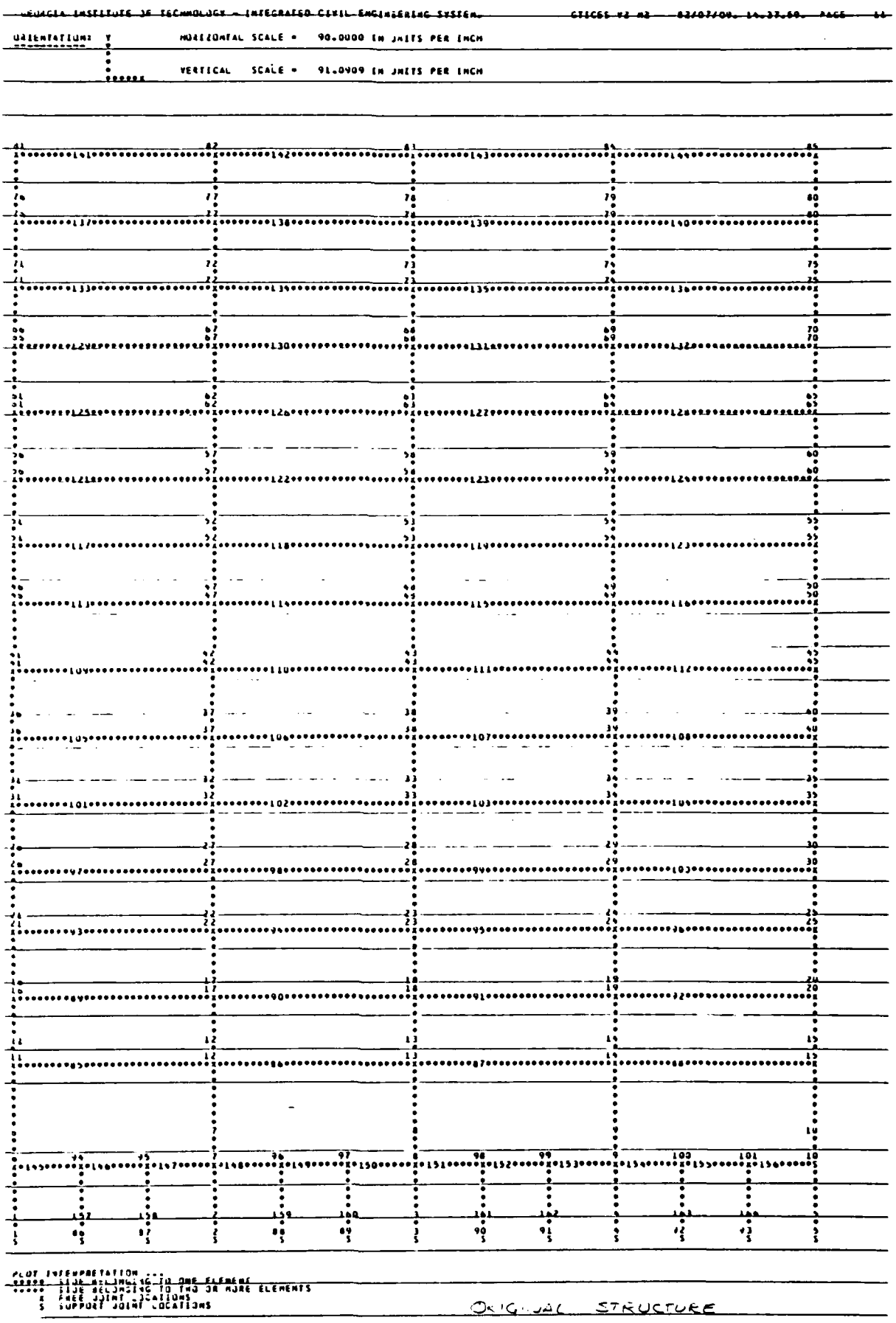

Fig. 5-4. Member and Joint Numbering Scheme.

RESULTS OF LATEST ANALYSES

PROBLEM - RCASDYN TITLE - DYNAMIC ANALYSIS OF BUILDING WITH SHORES AT THE BASEM

ACTIVE UNITS INCH LB CYC DEGF SEC

LOADING - 1 LATERAL BLAST LOAD PLUS DEAD LOAD

MEMBER FORCES

MEMBER	JOINT	TIME	FORCE AXIAL	FORCE SHEAR-Y	FORCE SHEAR-Z	MOMENT TORSIONAL	MOMENT BENDING-Y	MOMENT BENDING-Z
1	1	.0600	8725.35316	-1430.16708				153180.75047
		.0700	12664.84784	-1797.00389				192336.51047
		.0800	24053.27142	-2161.53177				240222.36433
		.0900	43356.98487	-2518.60535				296635.37468
		.1000	70862.44642	-2864.27420				361274.21343
		.1100	106510.32299	-3197.09506				433702.24482
		.1200	149416.06705	-3521.87047				513224.47178
		.1300	198403.42266	-3845.55657				599044.91582
		.1400	252198.98556	-4175.79228				690330.35481
		.1500	309460.33900	-4520.71504				786227.89283
		.1600	366804.74981	-4888.77120				885882.31944
		.1700	423837.82756	-5288.52525				988452.88860
		.1800	480181.56765	-5728.47133				1093129.17236
		.1900	545501.22876	-6216.85121				1199145.67678
		.2000	599530.53542	-6761.48176				1305794.94513
		.2100	649094.74525	-7369.59551				1412438.91600
		.2200	693131.17795	-8047.69882				1518518.35072
		.2300	730706.86634	-8801.43642				1623560.19275
		.2400	761033.05870	-9635.50603				1727182.77255
		.2500	783476.37347	-10553.55500				1829098.82162
		.3000	766830.80282	-16452.59758				2309566.56450
		.3500	549657.55820	-24361.07553				2750488.81632
		.4000	210788.86299	-33616.87578				3182928.89021
		.4500	-134020.82769	-43314.99013				3606690.22445
		.5000	-392057.43703	-52710.28238				4232013.32822
		.5500	-535510.45681	-61494.80448				4883284.08788
		.6000	-604982.21129	-69839.57659				5575750.16722
		.6500	-680522.32145	-78226.10141				6254439.64621
		.7000	-839189.11306	-87158.95063				6879207.69555

Fig. 5-5. Example Computer Output for Member Stresses.

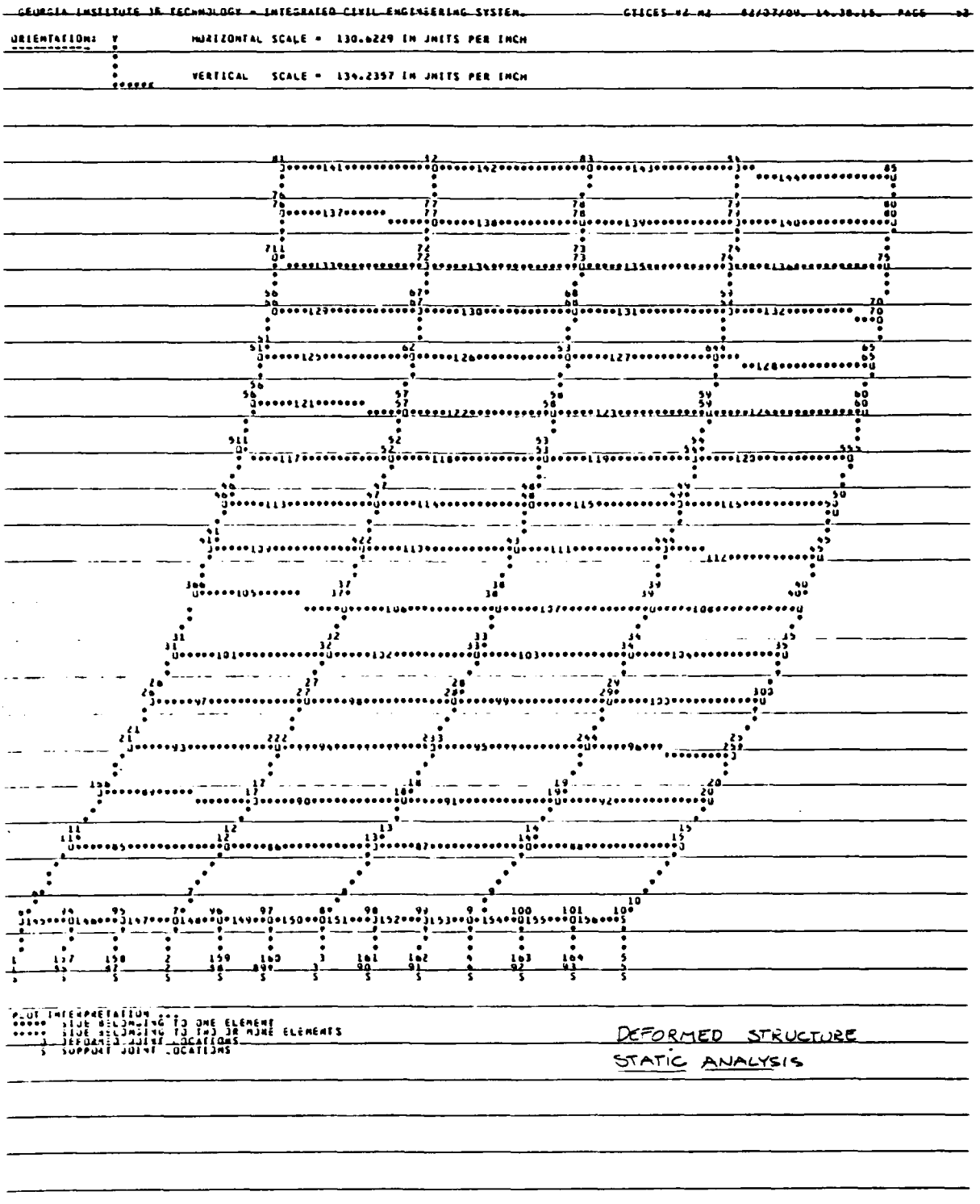

Fig. 5-6. Deformed Structure Static Analysis.

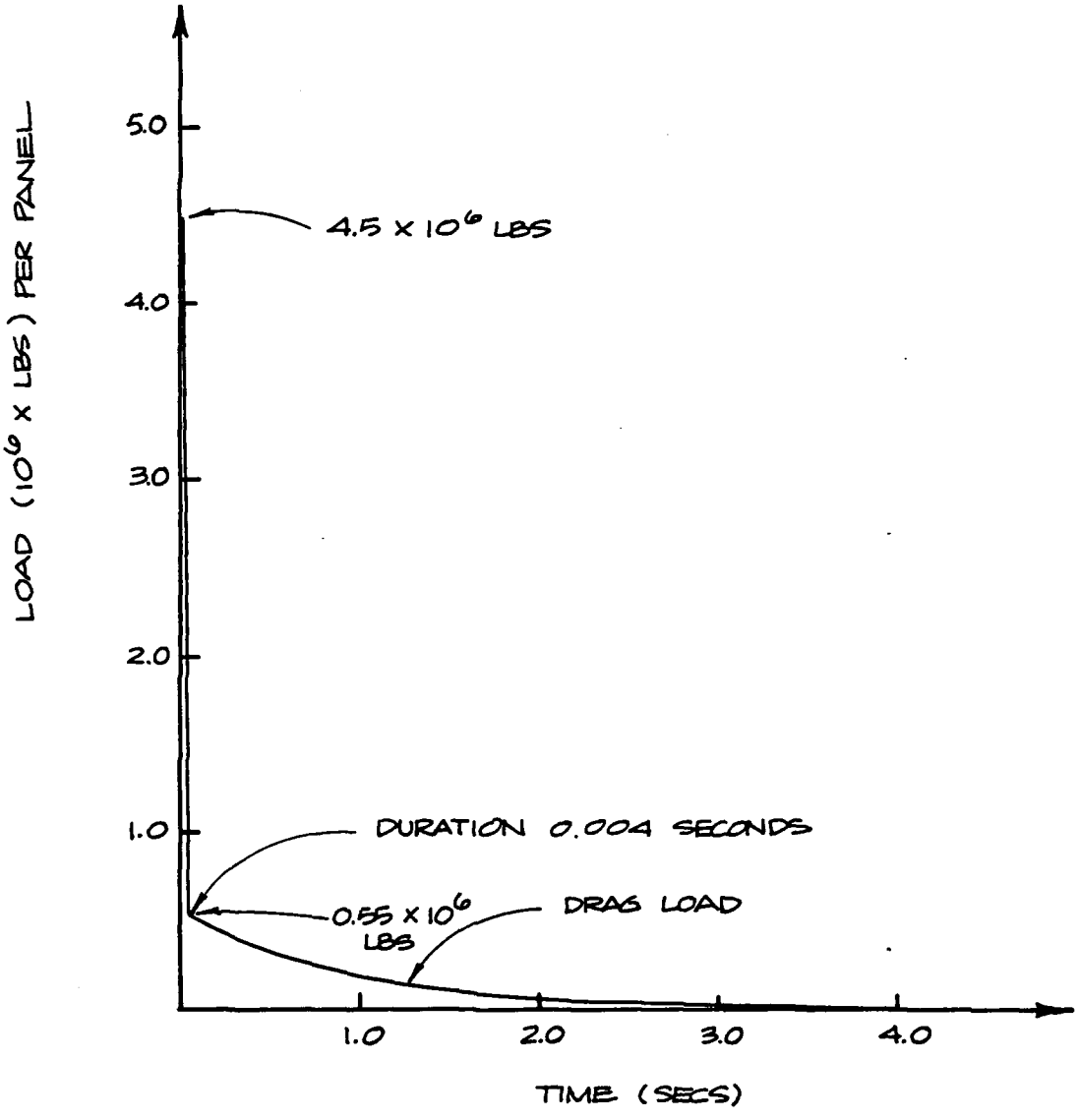

Fig. 5-7. Blast Load Input Function.

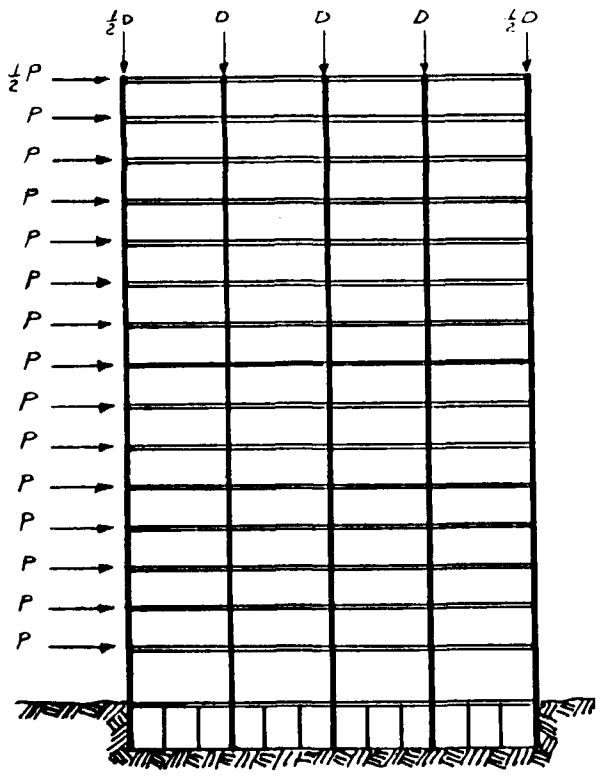

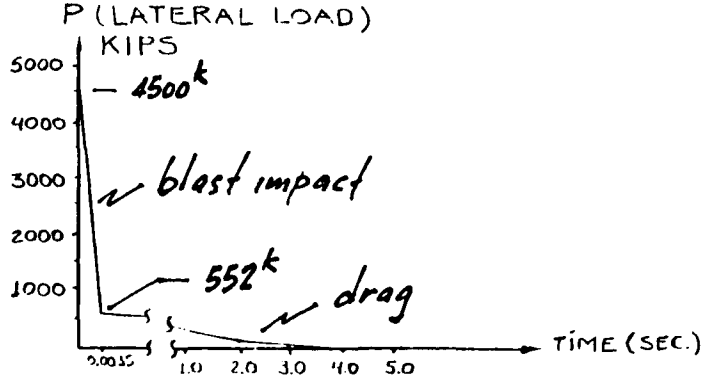

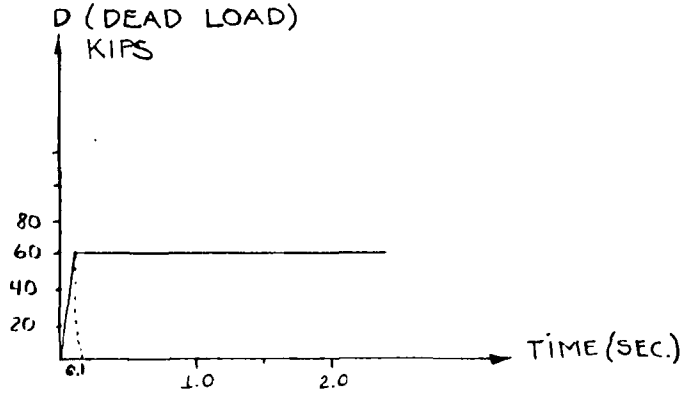

Fig. 5-8. Load History and Distribution on Structure.

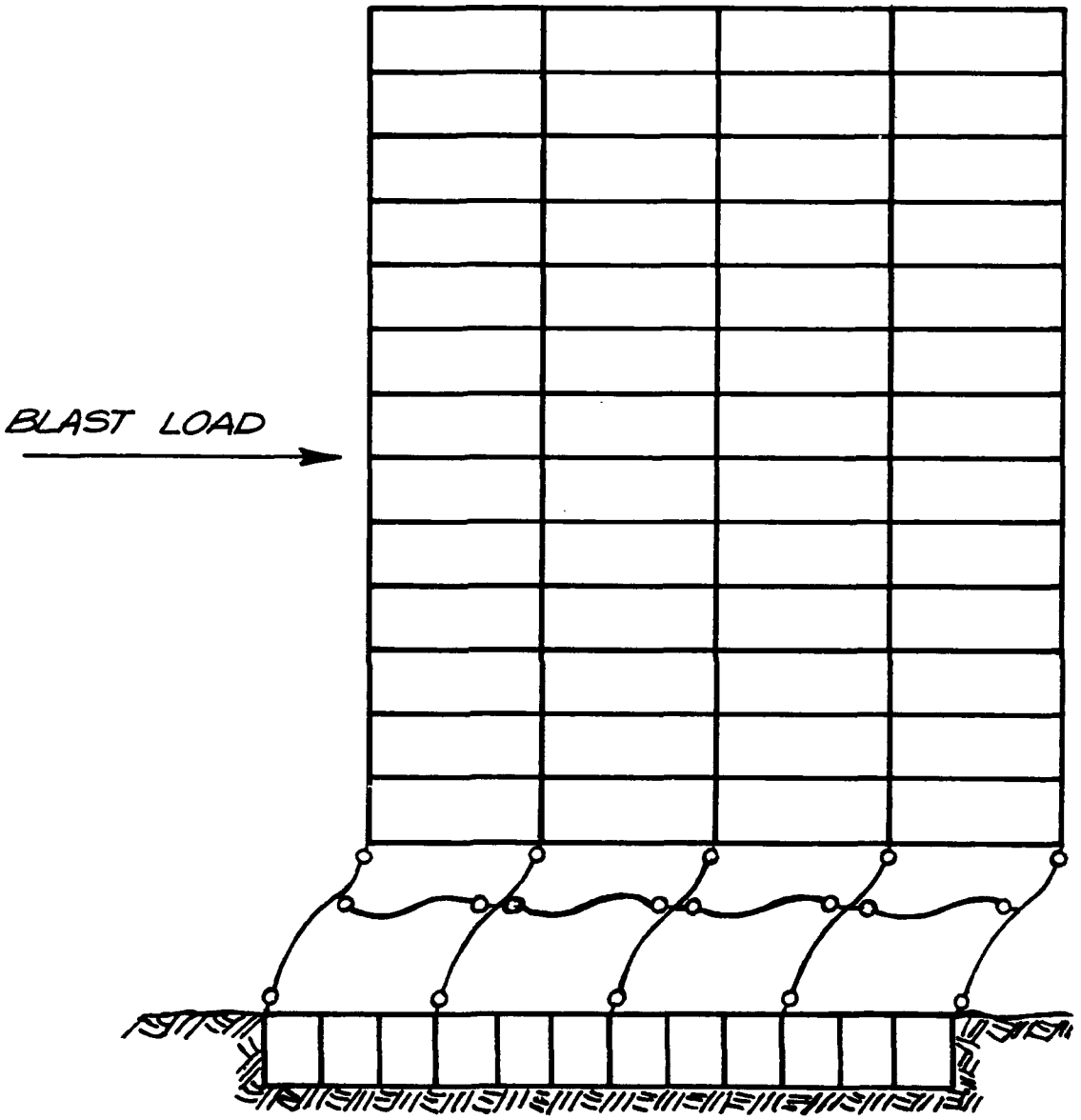

Fig. 5-9. Collapse Mechanism.

mass, velocity, acceleration and applied forces. Figures 5-10 and 5-11 show the horizontal displacement of the structure vs time. The lower two floors are severely distorted while the upper floors move more or less as a unit without appreciable structural damage. During this phase the only damage mechanism to the shelter is the blast loading itself as the columns above are yielding. Figure 5-12 shows a graphic history of each phase of the structure's behavior.

COMPUTER TIME HISTORY FOR SHELTER ELEMENTS

The more detailed results of the computer analysis provide the history of the individual member actions in a typical bay of the basement shelter. Referring back to the general member code or numbering scheme in Figure 5-4, the load-time curves for the columns, shore struts, and shelter ceiling beams are given in Figures 5-13, 5-14, 5-15, and 5-16. It should be noted that these member reactions do not include the effect of the 40 psi vertical overpressure loading on the shelter ceiling. From the previous approximate analysis, this 40 psi pressure does not fail the slab. It is, however, effective in canceling out the indicated tension forces in the shoring struts. (These were modeled as pinned-end links for the analysis, but in reality they could not take tension.) The computer indicated 30 kips, and this is completely canceled by an order of 150 kips compression due to the blast overpressure.

SUMMARY OF ANALYSIS CONCERNING EFFECTS ON SHELTER SPACE

There are two important results, one very encouraging with respect to the safety of the basement shelter area and the other, rather discouraging. Taking the encouraging aspect first, the failure mode of the frame is by yield mechanisms in the first and second story and then fracture or collapse of the first story columns at their ductility limit. The failure moments, axial loads, and shears developed by these first story columns are not sufficient to cause any significant damage to the beams, slabs, and columns of the upgraded basement shelter area. All of these shelter members, and the shoring members, have reserve strength at the point of the first story frame failure.

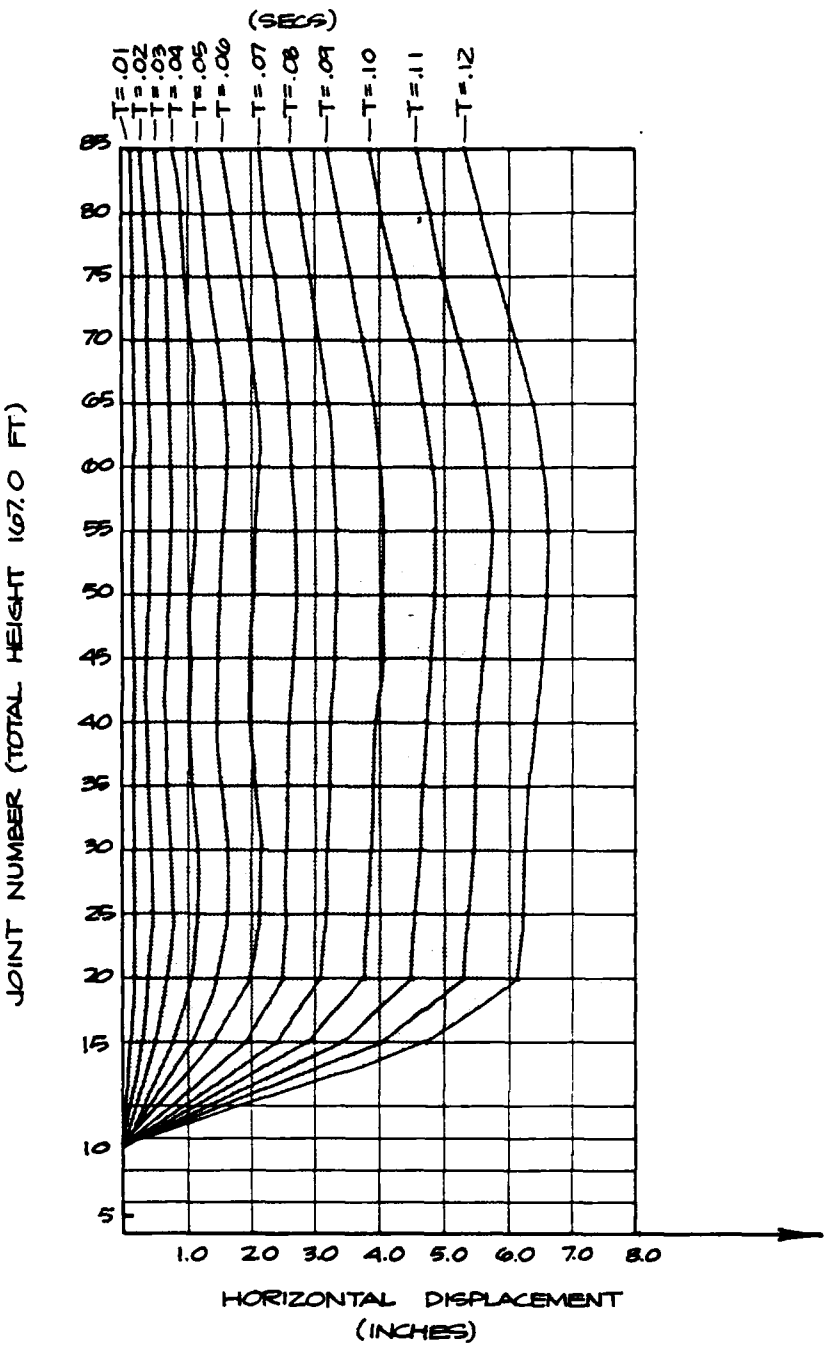

Fig. 5-10. Early Time History (to t = 0.12 sec).

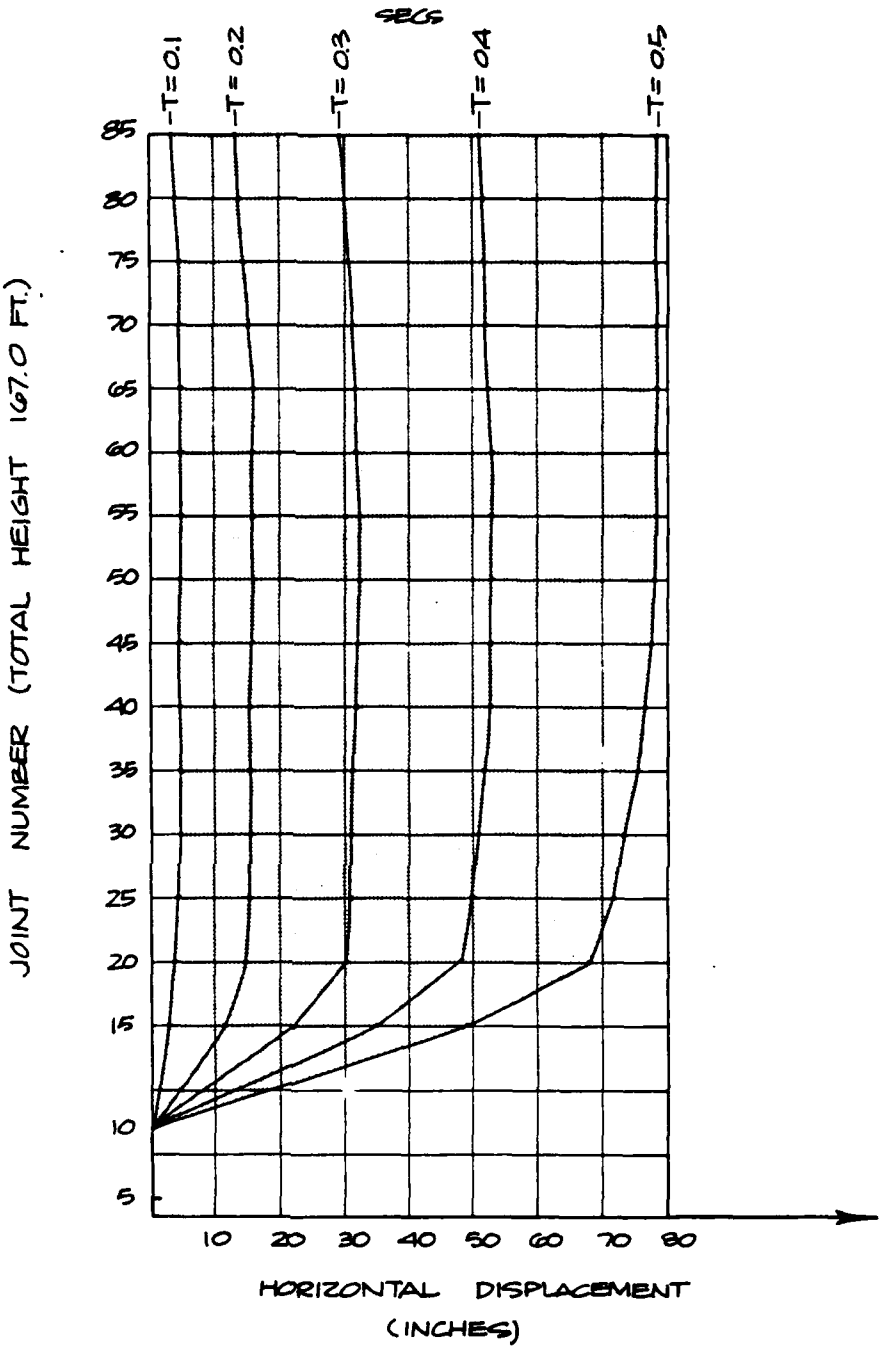

Fig. 5-11. Extended Time History (to t = 0.5 sec).

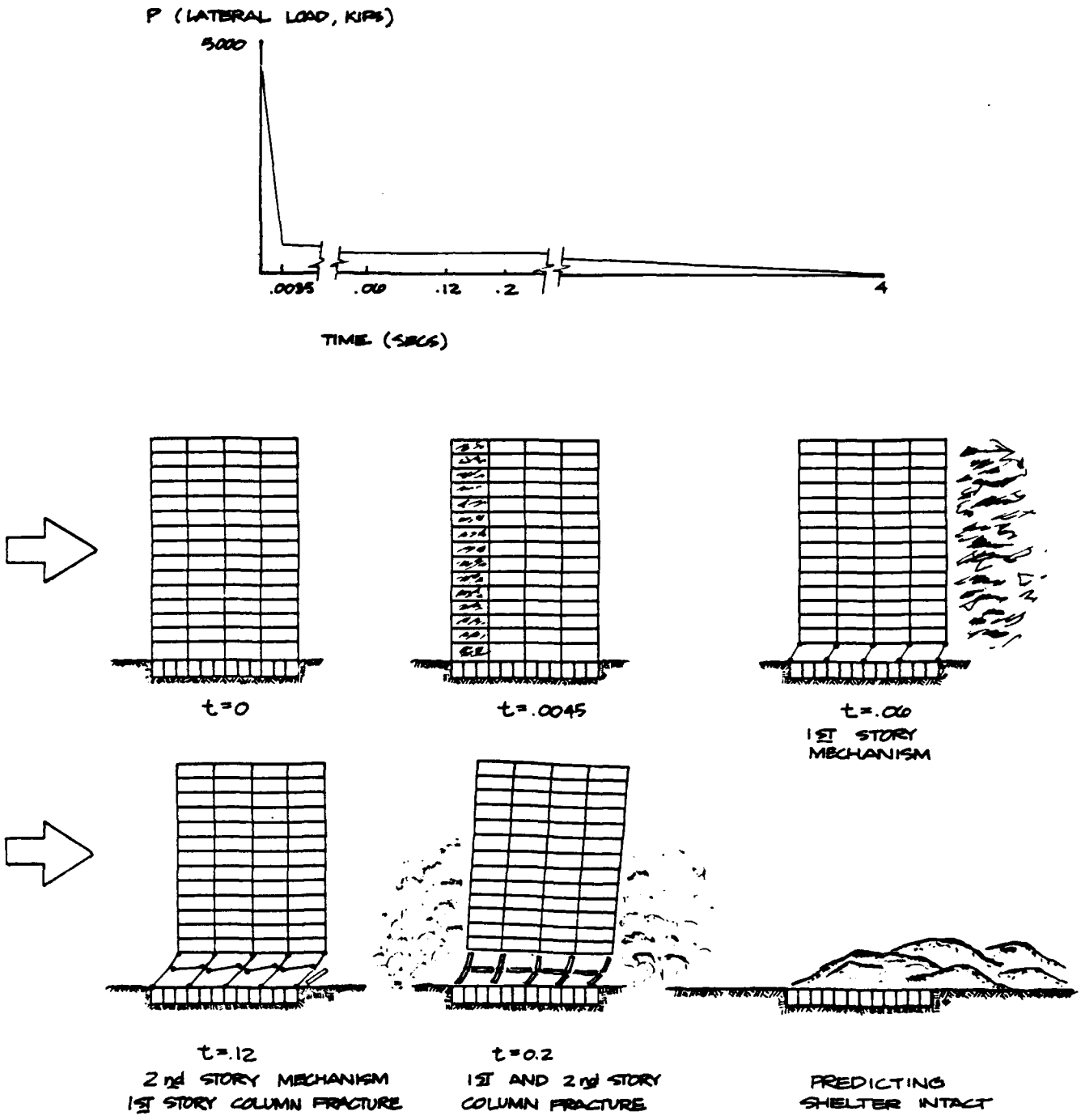

Fig. 5-12. Peachtree Building, Phases of Structural Failure.

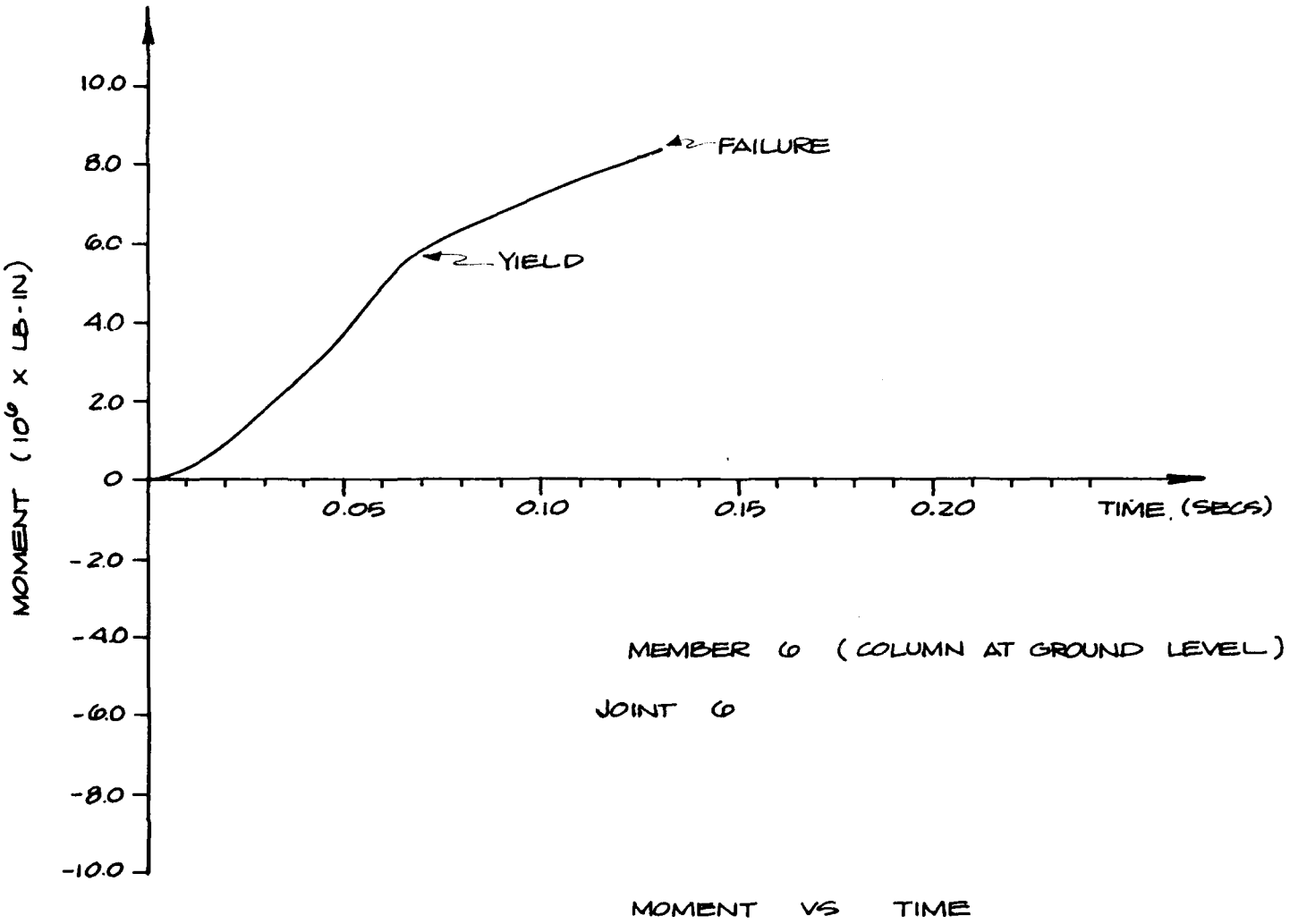

Fig. 5-13. Member Time History.

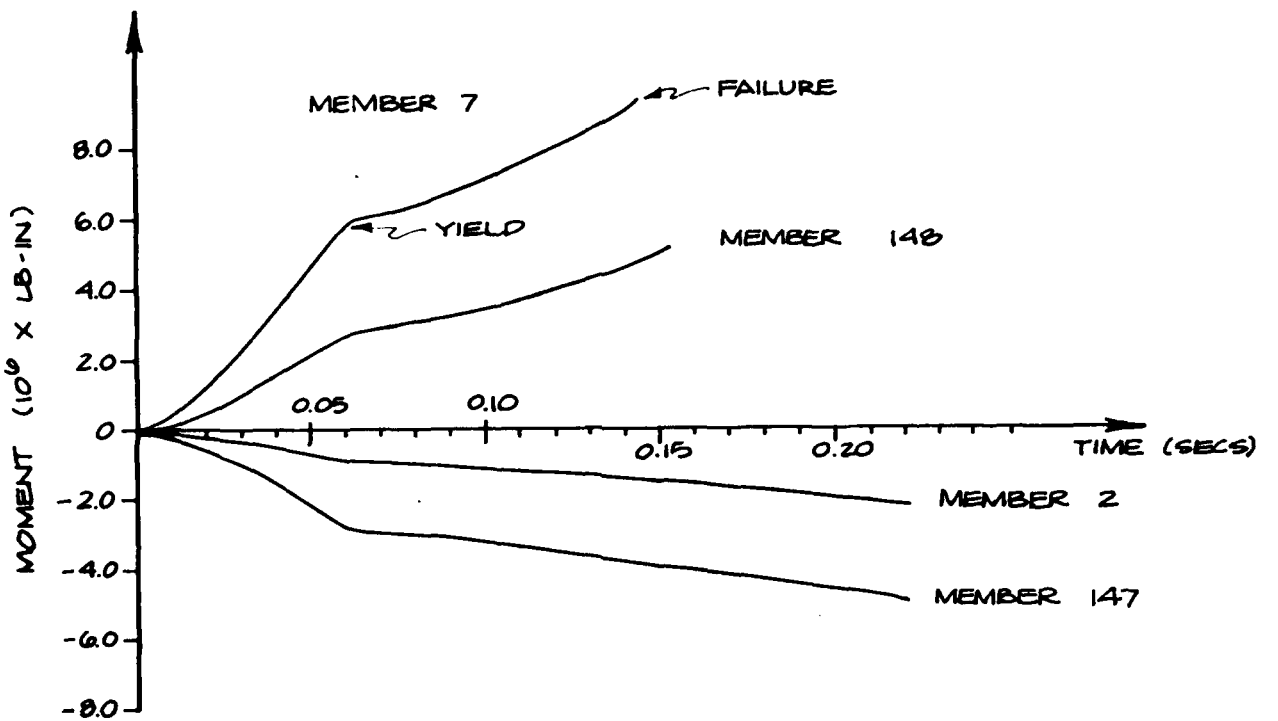

MOMENT VS TIME AT JOINT 7

Fig. 5-14. Representative Member Time Histories.

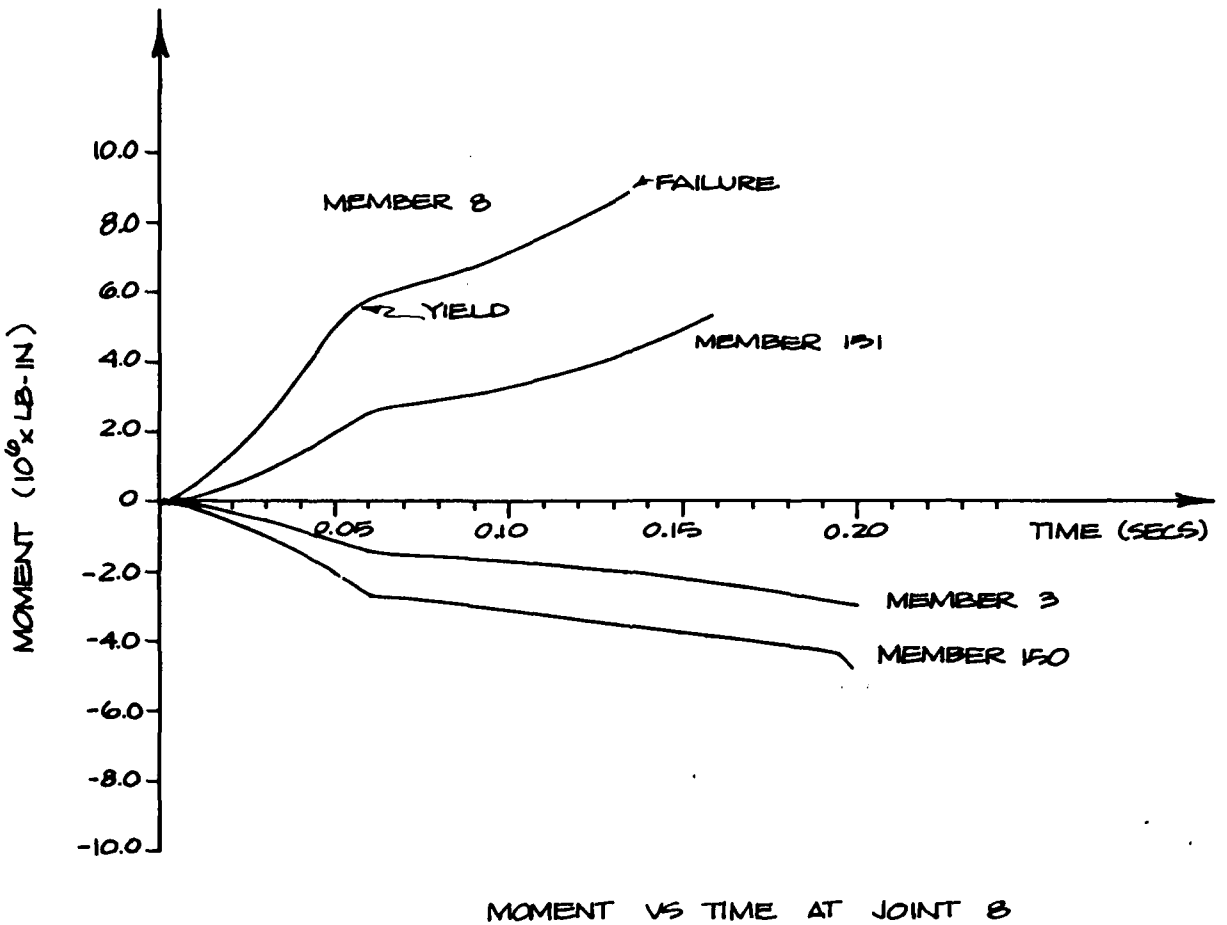

Fig. 5-15. Representative Member Time Histories.

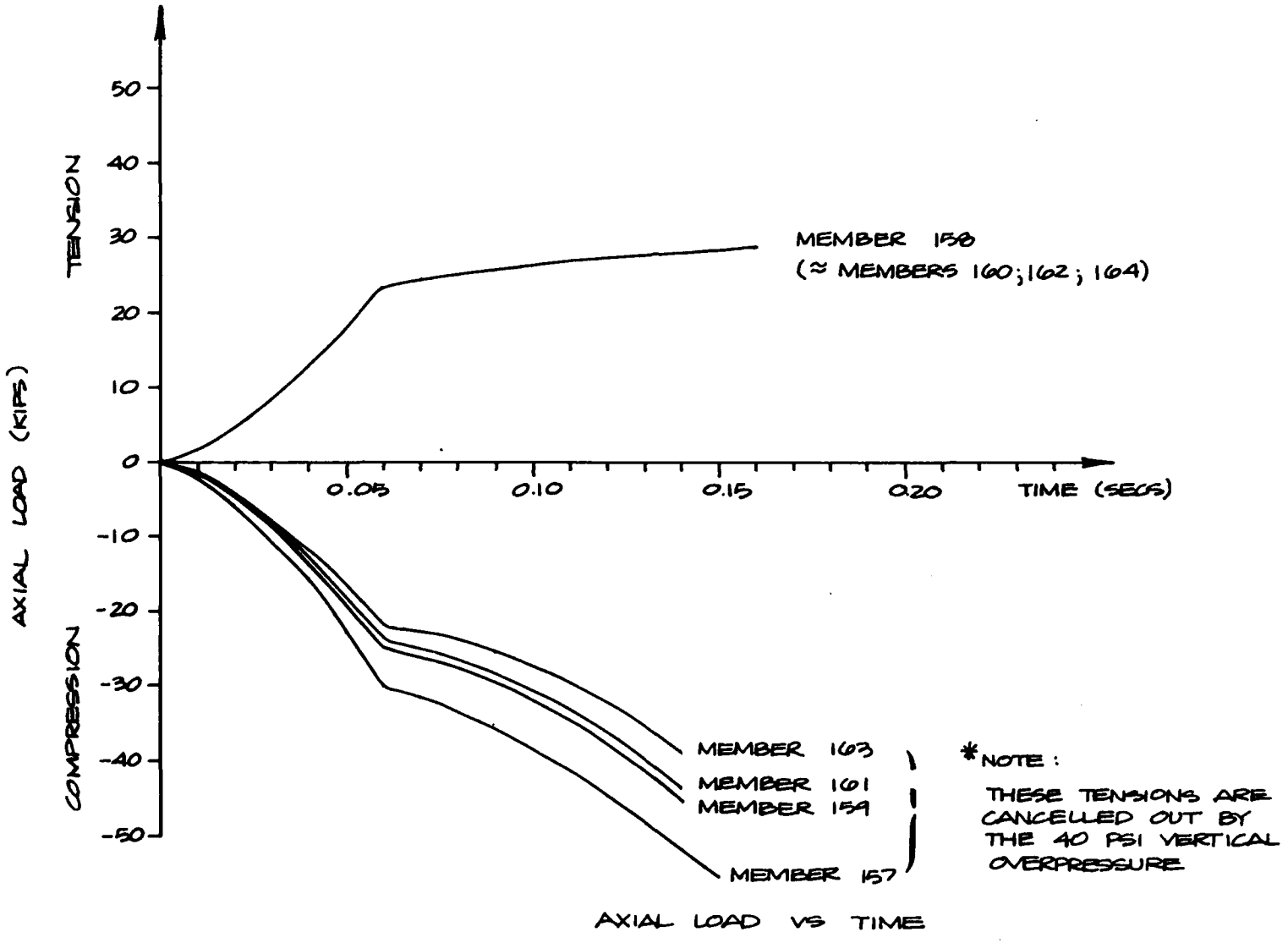

Fig. 5-16. Representative Member Time Histories.

The discouraging aspect of shelter survivability is as follows: the first and second story mechanisms, and the first story column failures, take place very rapidly without time for the upper stories to settle down "softly" onto the shelter slab. For the very probable case of brittle column failure, it is quite possible that the entire building could have virtually free fall for at least a height equal to the first story. This falling building mass might be cushioned somewhat by the failure mechanisms of the first and second stories. The impact zone could be over most of the shelter area since the blast force and its imparted velocity to the building at the time of collapse is not sufficient to carry the building beyond the shelter plan area. The impact force of the nearly intact upper story portion of the building could well exceed the upgraded shelter slab capacity. This result definitely needs further verification, for other frames, and for three-dimensional frame models, and from field observations obtainable from building demolition experience. Some representative numerical calculations are given below.

DEBRIS DEPTHS AND BASEMENT AREA SURVIVAL

The frame response depicted in Figure 5-12 indicates the formation of plastic hinges in approximately 60 milliseconds. Total time frame for building failure and collapse of the first two stories occurs at 0.2 seconds. The loading impulse on the building is sustained for 4 seconds, causing the building to collapse both vertically and horizontally.

As stated in the preceding section, the shelter survives the lateral displacement and failure of the columns at the first floor plastic hinge locations (see Figure 5-17). In addition, the shelter basement ceiling is impacted by the falling debris from the building collapse and must sustain the weight of the debris plus the related impact load forces. The 15 stories result in a total debris weight at an equivalent 120 psf for each floor and 12 psf for contents:

$$132 \text{ psf} \times 15 \text{ stories} = 1{,}980 \text{ psf}, \quad \text{or} \quad 14 \text{ psi}$$

Impact of the falling debris is estimated at two times the static weight of the debris, or 28 psi.

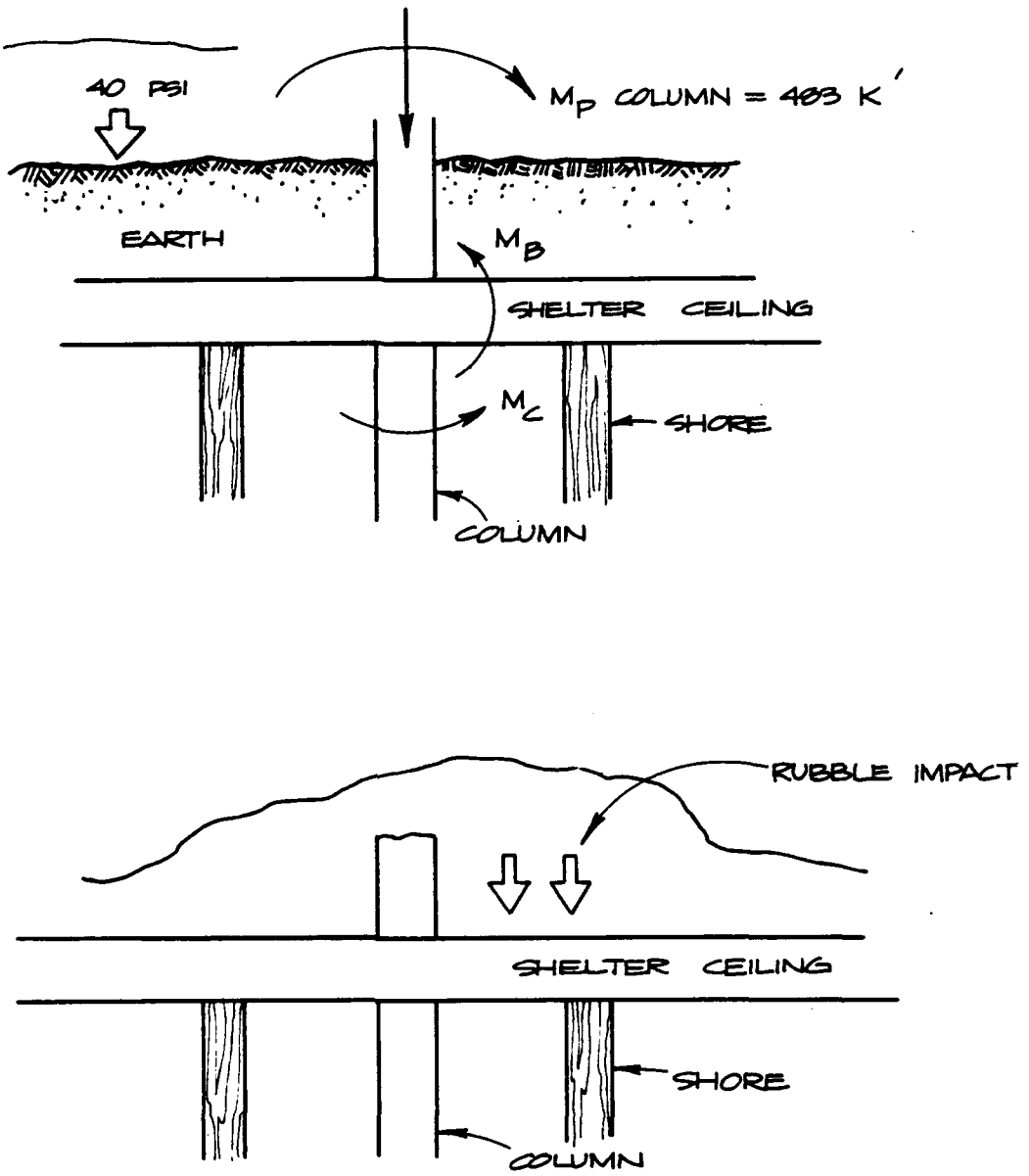

Fig. 5-17. Conditions at Shelter Ceiling Due to Building Frame Failure.

A rough estimate of punching capacity of the shored floor system is 240 kips per shore, and an 8x8 shore would not fail below approximately 300 kips. If the impact load from the falling debris occurred in conjunction with the total static debris load (not likely), total load on a shore would be approximately 180 kips, and therefore not cause punching failure. Note that this loading does not include any punching effects that could be due to falling columns impacting vertically on the slab. This type of punching has not been observed in our experience with the demolition of concrete frame buildings; however, it does occur in steel frames.

Total collapse time for a 15-story building is on the order of 7 to 10 seconds. Thus, the blast wave forces acting on the shelter ceiling have passed prior to impact of the building debris or the debris static weight.

The recovery of the shelterees is another matter. Based on our experience in building demolition with CDI, expected debris depths are 20 inches (0.5 m) per story. Thus, 15 stories' debris depth would approximate an equivalent 7.5 meters, or 24.5 feet. This debris would result from both the building analyzed and from all adjacent buildings of equivalent height.

Also, the environmental problems of dust and other air contamination effects after the blast event are not covered by this report and definitely need further study.

Section 6
SUMMARY AND CONCLUSIONS

This report presents the results of a program to develop a theoretical analysis of the effects of frame response on basement shelters in tall buildings. The objective was to determine the effect on a upgraded basement key worker shelter of the aboveground portion of the structure being subjected to a blast wave (30 to 50 psi) that would destroy the building.

This program investigated both steel and reinforced concrete frame structures with the most emphasis on poured-in-place reinforced concrete beam, slab, and girder type framing and the poured-in-place flat-slab and flat-plate type of construction. These types are very common in the National Shelter Survey inventory of upgradable structures.

A prediction technique was developed using both hand and computer analysis. This technique was tested using a previously explosively demolished 15-story cast-in-place reinforced structure, the Continental Life Building in Atlanta, Georgia. The results of this analysis indicated that the upgraded basement would have survived even though the aboveground portion of the structure was exposed to 50 psi.

Large portions of the debris landed on the shelter roof so that serious questions remain as to the advisability of using such structures as shelters because of the possible problems of entrapment of the shelterees. Other problems that need to be addressed are the large amounts of dust created in the collapse process and the possibility of fire in the debris pile.

It also should be noted that the primary work in this program was on reinforced concrete structures, where the punching effects of falling columns do not appear to be a problem. Based on the experiences of an explosive demolition contractor,

Controlled Demolition, Inc., this appears to be a serious problem in steel framed structures. It is recommended that future work in this area thoroughly investigate the collapse of steel frames both theoretically and in conjunction with building demolitions. Also, as was noted in Section 4, very little information is available on the load imparted to a frame by failing walls at pressures above 15 psi. Tests at the higher pressures of interest (30 to 50 psi) need to be conducted.

REFERENCES

1. Tansley, R.S., and R.D. Bernard, **Shelter Upgrading Manual: Key Worker Shelters,** SSI Report No. 8012-7, Scientific Service, Inc., Redwood City, CA May 1981.

2. Tansley, R.S., B.L. Gabrielsen, and G.J. Cuzner, **Upgrading of Existing Structures Phase III, Shelter Design Options,** SSI Report No. 8012-6, Scientific Service, Inc., Redwood City, CA, May 1981.

3. Murphy, H.L., **Upgrading Basements for Combined Nuclear Weapon Effects: Predesigned Expedient Options,** Stanford Research Institute, Menlo Park, CA, October 1977.

4. Beck, J.E., **Summary of Dynamic Analyses of Selected NSS Buildings,** SRI International report for the U.S. Federal Emergency Management Agency, July 1980.

5. Gabrielsen, B.L, G. Cuzner, and R. Lindskog, **Blast Upgrading of Existing Structures,** SSI Report No. 7719-4, Scientific Service, Inc., Redwood City, CA, January 1979.

6. Gabrielsen, B.L., R.S. Tansley, and G. Cuzner, **Upgrading of Existing Structures Phase II,** SSI Report No. 7910-5, Scientific Service, Inc., Redwood City, CA, June 1980.

7. Sozen, M.A., W.L. Gamble, H. Flug, **Flexural Strength of Reinforced Concrete Slab With External Applied In-Plane Forces and Strength of Slabs Subjected to Multiaxial Blending and Compression,** University of Illinois (DAHC-20-67-C-0136).

8. Huff, W.L., **Collapse Strength of a Two-Way Reinforced Concrete Slab Contained Within a Steel Frame Structure,** Weapons Effects Laboratory (DAHC-20-68-W-0192).

9. Wiehle, C.K., **Evaluation of Existing Structures,** Stanford Research Institute, Menlo Park, CA (DAHC-20-71-C-0292).

10. Wiehle, C.K., **Blast Response of Five NFSS Buildings,** Stanford Research Institute, Menlo Park, CA (DAHC-71-C-0292).

11. Wilton C., K. Kaplan, and B.L. Gabrielsen, **The Shock Tunnel: History and Results,** SSI 7618-1, Scientific Service, Inc., Redwood City, CA, March 1978.

12. Wiehle, C.K., J.L. Bockhalt, **Existing Structure Evaluation; Two-Way Action Wall,** Stanford Research Institute, Menlo Park, CA (DAHC 20-67-C-0136).

13. Coulter, G.A., **Blast Loading of Objects in Basement Shelter Models,** Ballistic Research Laboratory, Aberdeen Proving Ground, MD (DAHC-20-70-C-0310).

14. Coulter, G.A., **Blast Loading In Shelter Models - Basement and Mine Shelters,** Ballistic Research Laboratory, Aberdeen Proving Ground, MD (DAHC-20-70-C-0310).

15. Melichar, J., **The Propagation of Blast Waves Into Chambers,** Ballistic Research Laboratory, Aberdeen Proving Ground, MD (DAHC-20-67-W-0153).

16. Coulter, G.A., **Blast Loading in Existing Structures Basement Mode,** Ballistic Research Laboratory, Aberdeen Proving Ground, MD (DAHC-20-70-C-0310).

17. Melichar, J.F., **The Air-Blast-Induced Environment Within Civil Defense Blast-Slanted Shelters,** URS Corporation, San Mateo, CA (DAHC-20-67-C-0136).

18. Gabrielsen, B., C. Wilton, and K. Kaplan, **Reponse of Arching Walls and Debris from Interior Walls Caused by Blast Loading,** URS 7030-23, Scientific Service, Inc., Redwood City, CA, February 1975.

19. Melichar, J.F., **Air-Blast-Induced Aerodynamic Effects in Blast-Slanted Basement Shelters,** URS Research Company, San Mateo, CA (DAHC-20-67-C-0136).

20. Longinow, A.K., G. Ojdrovich, and L. Bertram, **People Survivability: Direct Effects Environment and Related Topics,** IIT Research Institute Chicago, IL (DAHC-20-68-C-0126).

21. Longinow, A.K., A.Weidermann, S. Citko, **Debris Motions and Injury Relationships in an All Hazard Environment,** IIT Research Institute, Chicago, IL (DAHC-01-74-C-0251).

22. Smith, J.B., E.W. Cousins, R.M. Newman, **Fire Hazard to Fallout Shelter Occupants: A Classification Guide,** Factory Mutual Research Corporation (OCD-PS-64-40).

23. Waterman, T.E., **Shelter Habitability in Existing Buildings Under Fire Exposure,** IIT Research Institute, (OCD-PS-64-200).

24. Wilton, C., K. Kaplan, B.L. Gabrielsen, **Blast/Fire Interaction, Blast Translation and Toxic Gases,** URS 7239-11, Scientific Service, Inc., Redwood City, CA, July 1976.

25. **GTSTRUDL User's Manual,** GTICES Systems Laboratory, Georgia Institute of Technology, Atlanta, GA, October 1981.

26. Tolman, D.F., R.O. Lyday, and E.L. Hill, **Statistical Classification Report: Estimated Characteristics of NFSS Inventory,** RTI 436-717, Research Triangle Institue, Research Triangle Park, NC, December 1973.

27. Tansley, R.S., and J.V. Zaccor, **Testing of Shelter Design and Industrial Hardening Concepts at the MILL RACE Event**, SSI 8115-4, Scientific Service, Inc., Redwood City, CA, January 1982.

28. Beedle, Lynn S., **Plastic Design of Steel Frames**, John Wiley & Sons, Inc., New York, London, Sidney, 1958.

29. Wilton, C., B. Gabrielsen, and P. Morris, **Structural Response and Loading of Wall Panels**, URS 709-11, URS Research Company, San Mateo, CA, July 1971.

30. Glasstone, Samuel, and Philip J. Dolan (eds), **The Effects of Nuclear Weapons**, Third Edition, U.S. Department of Defense and the U.S. Department of Energy, Washington, DC, 1977.

31. **American Institute of Steel Construction (AISC) Manual of Steel Construction**, 8th edition, American Institute of Steel Construction, Chicago, IL.

32. **Concrete Reinforcing Steel Institute (CRSI) Handbook**, Concrete Reinforcing Steel Institute, Chicago, IL, 1980.

APPENDIX A

APPLICABLE CONCEPTS OF PLASTIC ANALYSIS

APPLICABLE CONCEPTS OF PLASTIC ANALYSIS

INTRODUCTION

In order to best show how plastic analysis can be applied to frame response, it is appropriate to introduce some of the basic concepts. Ref. A-1, "The Plastic Design of Steel Frames" by Lynn S. Beedle, published in 1958, is one of the pioneering works on plastic design in framed structures and is still one of the fundamental books on this subject. This text will be used as one of the principal references in this discussion. The primary concept used in plastic design is taking advantage of the ductility of a material. Figure A-1 is an idealized plot of stress vs strain for steel. When elastic design concepts are used with a typical steel structure the allowable stresses are on the order of 20,000 psi for the A7 steel; obviously when a structure is operating under service load conditions it is desirable to keep the stress at or below such a stress level. However, when a structure is loaded up to the yield stress, 34.1 ksi in this particular case, it does not mean that the structure is going to collapse, but merely that the steel has reached its yield stress; one may continue to stretch or distort the structure and it will still remain intact, but will be permanently distorted. The area under the stress-strain curve is a measure of the energy absorption capacity of the material; as can be seen from this figure, the energy under the elastic portion is small compared to the area under the entire curve. In fact the curve shown in Figure A-1 is only the first 10% of the entire stress-strain curve. The entire curve is plotted on Figure A-2 and puts some perspective on the tremendous ductility of steel.

By way of contrast, Figure A-3 shows the stress-strain curve for plain concrete in compression. Here an ultimate compression strain of about 0.3% occurs as opposed to a value of 20% or more for steel. It should be mentioned that, although concrete is far less ductile than steel, in real world structures the full ductility of steel is generally not realized. The joints are assembled with bolts and welds, there are dimensional restraints, and the gross distortions are generally limited to the region of the curve shown in Figure A-1. That is, perhaps the first 1% to 3% of the distortion is really available for energy absorption of a structure prior to failure.

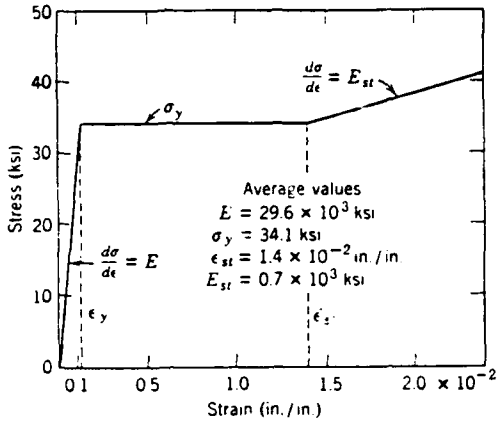

Fig. A-1. Stress-Strain Curve of A7 Structural Steel Idealized.

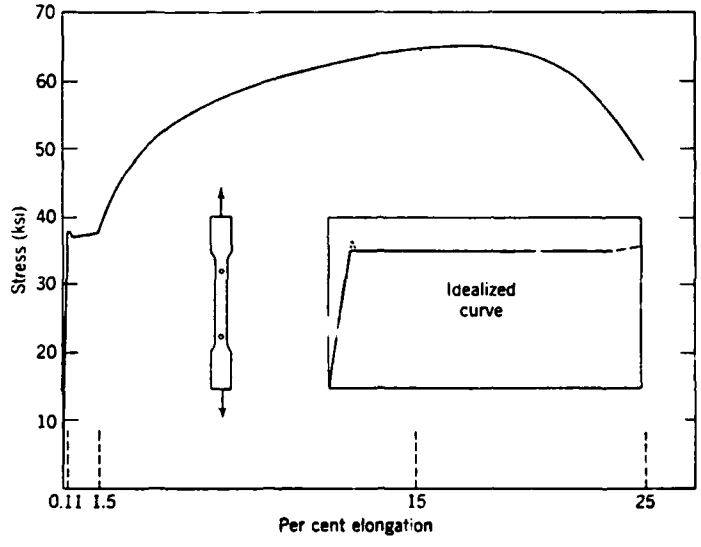

Fig. A-2. Complete Stress-Strain Curve for Structural Steel.

Source: Beedle, "Plastic Design of Steel Frames," Ref. A-1.

Steel and reinforced concrete beam behavior is shown by the curves in Figure A-4. Here M is the applied moment, M_y is the yield moment for that particular cross section or beam, M_p is the ultimate plastic moment, ϕ is the rotation angle of the joint in the zone of plastic deformation in the beam and ϕ_y is rotation at yielding of the outer fiber of a steel beam or of the reinforcing steel in the concrete beam. The particular plot shows two curves for steel, one for a round cross section and one for a wide-flange cross section, and the ratio of M_p to M_y. This is known as the shape factor; typically in rectangular sections the shape factor is 1.5, and in wide-flange sections it is equal to 1.12 to 1.14, or a 12% to 14% increase from yield moment to ultimate plastic moment in capacity in a wide-flange section. The ϕ to ϕ_y axis is a measure of ductility and in a typical reinforced concrete beam the ductility is usually in the range of 3 to 6, sometimes greater for doubly reinforced, carefully designed beams; but in most buildings encountered across the country this range of 3 to 6 for ductility is not typical. The effect of this plastic or nonlinear section behavior on the total structure behavior will be discussed below.

The following definitions are important to the understanding of plastic analysis:

(1) **A plastic hinge is a zone of yielding due to flexure in a structural member.** Although its length depends on the geometry and loading, in most of the analytical work it is assumed that all plastic rotation occurs at a point. At those sections where plastic hinges are located, **the member acts as if it were hinged, except with a constant restraining moment, M_p.**

(2) **Plastic hinges form at points of maximum moment.** Thus in a framed structure with prismatic members, it would be possible for plastic hinges to form at point of concentrated load, at the end of each member meeting at a connection involving a change in geometry, and at the point of zero shear in a span under distributed load.

(3) The plastic moment M_p equals $F_y Z$, where Z is the plastic section modulus.

(4) The shape factor ($f = Z/S$) is one measure of reserve strength beyond the elastic limit (S = section modulus).

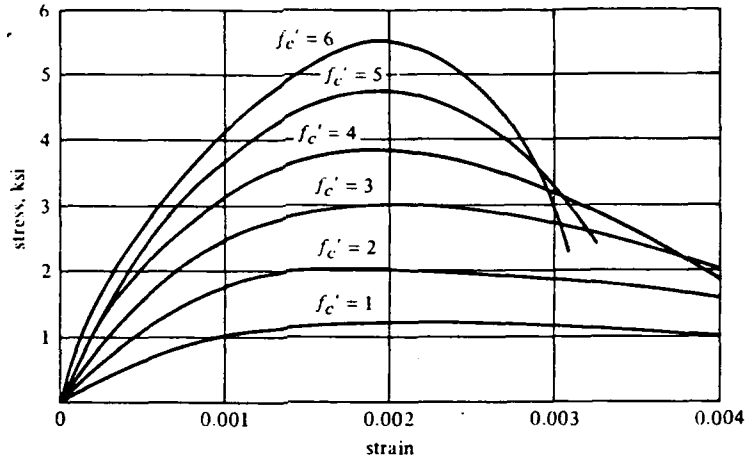

Fig. A-3. Typical Concrete Stress-Strain Curve, Short-Term Loading.
Source: McCormac, "Design of Reinforced Concrete," Ref. A-2.

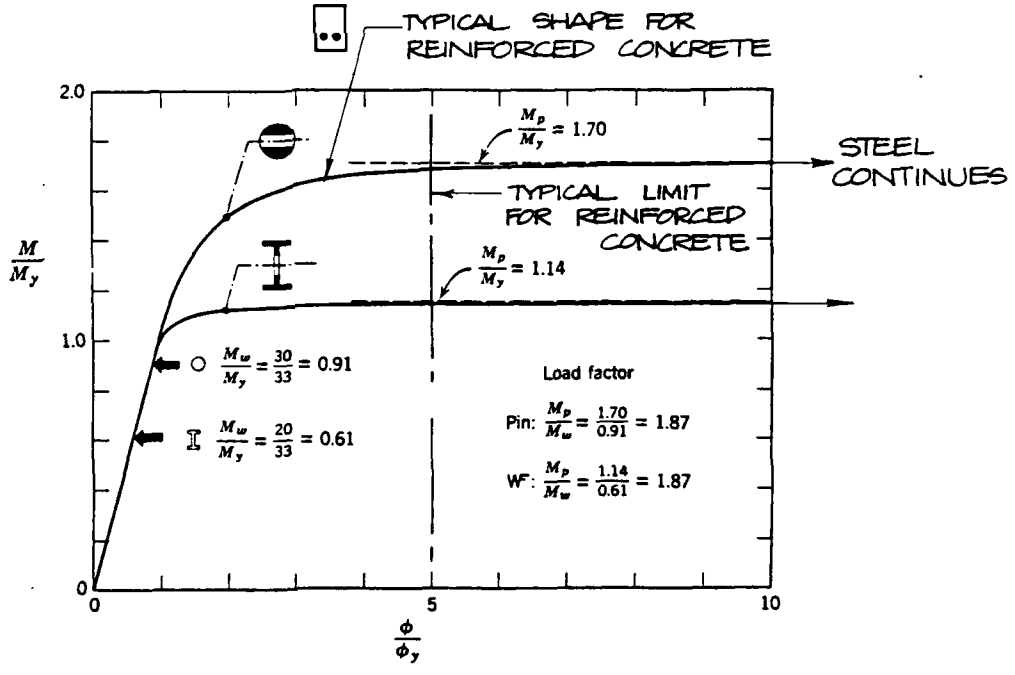

Fig. A-4. The Maximum Strength of a Round Pin Compared With That of a Wide Flange Beam.
Source: Beedle, "Plastic Design of Steel Frames," Ref. A-1.

The effect of plastic hinging on the behavior of structures can most easily be illustrated by a simple example, see Figure A-5. As the load P is applied to this simple beam at midspan, the load would increase in a linear manner until the outer fiber reaches yield. This would be in the range of classical elastic design procedure. As the structure is continually loaded beyond the yield point, it does not fail and collapse, but the yielding progresses from the outer fibers of the beam section toward the centroid of the beam until the entire section has either gone into the plastic domain or fracture occurs, as in the case of reinforced concrete. The upper picture of the rectangular section in Figure A-5 can also be represented as the normalized M-ϕ curve, Figure A-6. Figure A-6 is the normalized M/M_y vs ϕ/ϕ_y curve for a rectangular section of a steel beam. This, however, is very nearly identical to that of reinforced concrete. The point labeled (1) on the curve for the case of concrete would be the cracking moment in concrete when the first initial tension cracks form; point (2) on the curve would be the M_u value commonly used in the design of concrete structures prior to applying a safety factor; and point (3) in a concrete beam would be analogous to the so-called M_n, or the ultimate strength of the concrete beam near $\phi/\phi_y = 4$. Point (4) illustrates the immense ductility of a steel beam in this mode of bending, whereas the concrete beam will more than likely fracture somewhere between points (3) and (4). Individual resistance functions or M_ρ values are described under Subtask 3B (see Section 4).

Figure A-7 is a plot of M versus ϕ for a typical wide-flange section of steel. Here note that the shape factor is small; that is, there is only a 14% difference between point of yielding and the point of full plastic cross section.

The full impact of the plastic hinge concept is not really appreciated without the idea of a mechanism of failure and/or the moment redistribution that occurs in a continuous or indeterminate structure when it is loaded to failure. Figures A-8 and A-9 illustrate a simple beam with fixed ends, uniformly loaded. As the load is increased, the first fibers to yield will be at the ends of the beam A and B; these are shown in Figure A-8 as ends A-B on the M-ϕ plots. At the time that they are in this idealized picture, they provide a constant plastic moment, but the center of the structure is still well into the elastic domain; that is, its stresses are less than one half the way to yield, hence there is no danger whatsoever of the structure

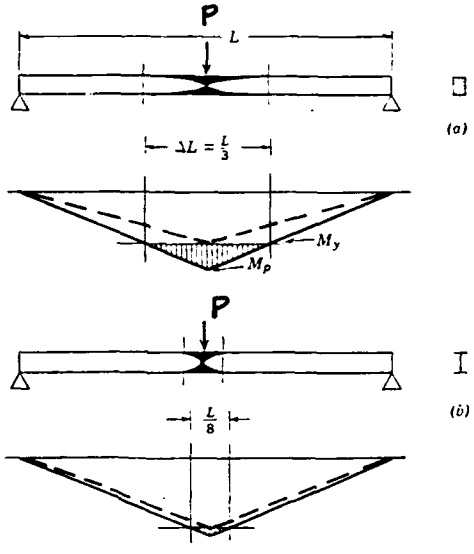

Fig. A-5. Theoretical Length of Yielded Portion of (a) Rectangular and (b) WF Beam With Central Concentrated Load.

Source: Beedle, "Plastic Design of Steel Frames," Ref. A-1.

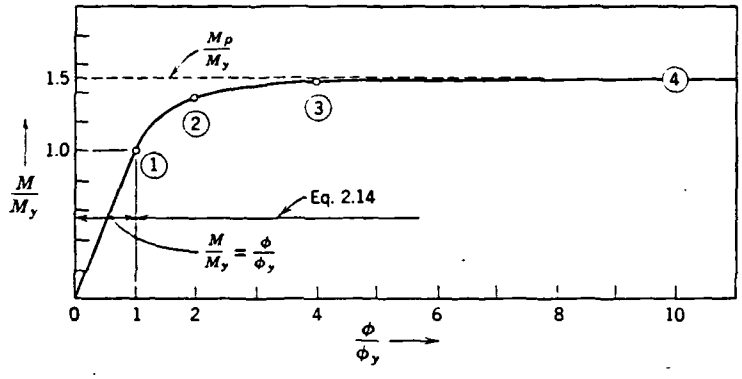

Fig. A-6. Nondimensional Moment-Curvature Relationship for Rectangular Beam.

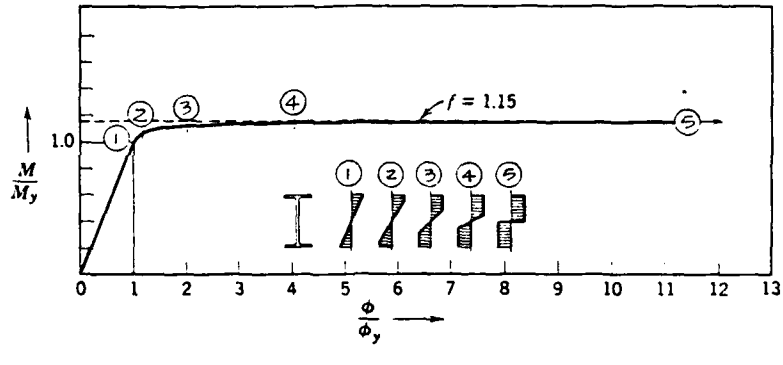

Fig. A-7. Nondimensional Moment-Curvature Relationship for Wide Flange Beam.

Source: Beedle, "Plastic Design of Steel Frames," Ref. A-1.

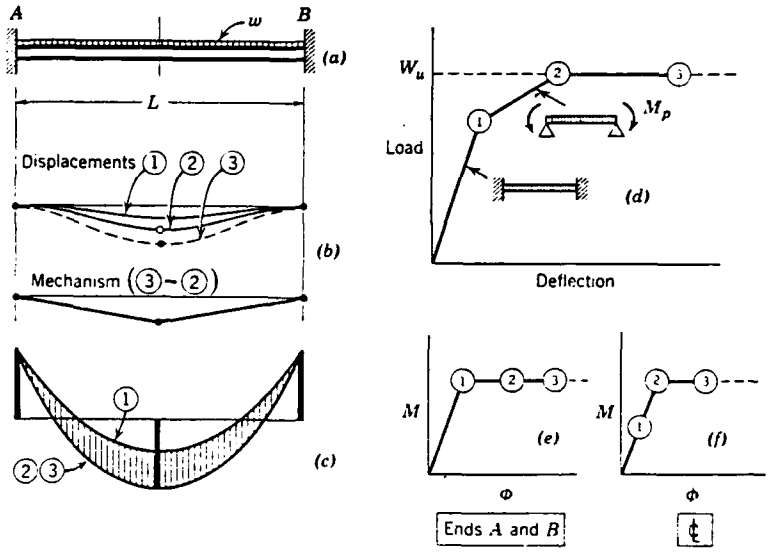

Fig. A-8. Redistribution of Moment in a Fixed-Ended Beam With Uniformly Distributed Load.

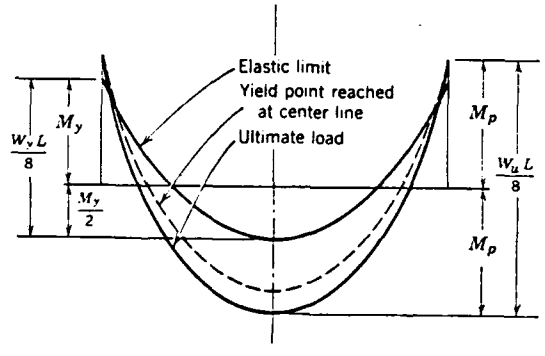

Fig. A-9. Moment Diagram at Various Stages of Loading for Fixed-Ended Beam With Uniformly Distributed Load.

Source: Beedle, "Plastic Design of Steel Frames," Ref. A-1.

collapsing. It will, therefore, require a continual increase of load to develop a hinge in the middle of the beam in order to achieve collapse; i.e., a mechanism shown by the heavy dark lines of (c) in Figure A-8. Figure A-9 shows the sequential increase of moment from the elastic to the first yield at the end, to the first yield at the center, to the development of a mechanism or hinges at all three points and collapse. This collapse load is approximately 1.52 times yield load for a wide flange section and 1.85 for a solid rectangular section.

It is interesting to compare these results with elastic theory where one would predicate failure load at first yielding, when in fact for a wide-flange beam to collapse requires 52% more load beyond yield. By contrast, if a rectangular section were bent and taken to collapse, one would have to increase the load 85% beyond yield to develop full plastic hinges at all three points and thus develop a mechanism of failure or collapse. Since most civil structures or buildings are made with wide-flange beams, the maximum reserve capacity one would generally encounter in a beam of this type would be the 52% number. In fact this is seldom realized, in that the beam connections have limitations, and as will be seen in more complex structures, there is a smoothing or a tendency of the structure to behave in the most expedient way to collapse; i.e., to form a lower bound on collapse strength nearer to that predicted by elastic theory. In concrete structures the extra strength from first yield to a collapse mechanism is not large. This is because the concrete moment capacity is controlled by steel, so that the steel placed in a concrete beam is selected to match or nearly match the actual load moment value at that section; hence there is little excess strength, but greater redundancy in reinforced concrete structures. In both concrete and steel structures the code attempts to reduce the overdesign by allowing a redistribution of moments; that is, the code allows one to allocate a portion of the high negative moment to the positive moment region, thus reducing excess structural capacity, and approximating formation of a mechanism.

To this point the ideas surrounding plastic behavior of structures have been discussed. In order to increase the potential for this type of analysis it is important to add some theorems of plastic analysis. Formal proof, discussion, etc., concerning these theorems can be found in several references such as Hodge (Ref. A-3) and Moy (Ref. A-4).

The Uniqueness Theorem: For any set of conditions of loads and strengths there is but one way (one mode) to collapse the structure and satisfy the four following conditions.

1) **Kinematic Conditions:** Enough plastic hinges to form a mechanism of collapse.
2) **Equilibrium:** Statics must be satisfied for all parts of the loaded structure.
3) **Yield Limits** must be observed; the absolute value of the moment must be equal to or less than capacity everywhere in the structure ($M \leq M_p$).
4) **The Dissipation Condition:** There must be positive work at every plastic hinge. The direction of the load bending moment must be in the direction of rotation.

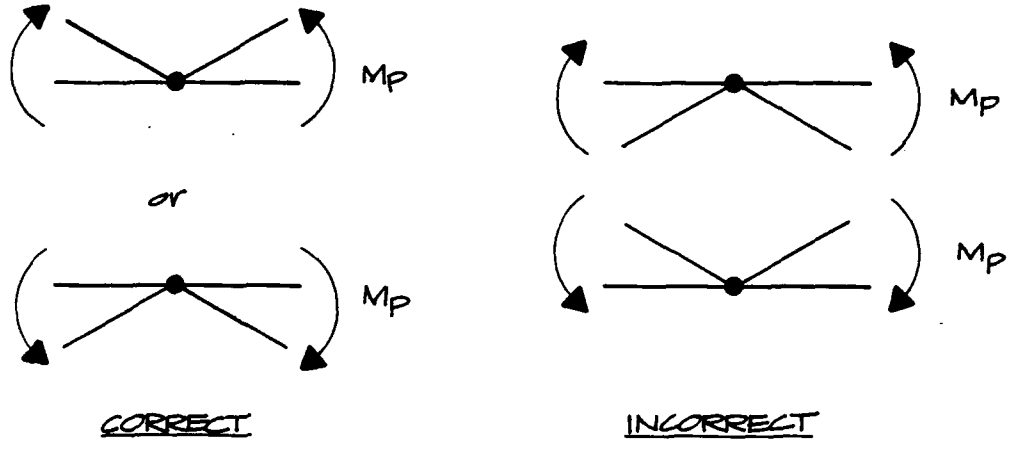

Upper Bound Theorem: is, simply stated, the violation of Item 3 of the Uniqueness Theorem, i.e., exceeding the moment $M > M_p$ (overshoot) somewhere in in the structure.

Lower Bound Theorem: is the violation of Item 1 of the Uniqueness Theorem, that is, insufficient number of hinges to form the kinematic conditions for collapse.

Independent Mechanisms: If p is the number of possible plastic hinges, r is the redundancy or degree of indeterminancy of the structure, and m is the number of

independent mechanisms, then

$$m = p - r$$

where $r = 3n - 3b - n_r - s$

and n = number of joints

b = number of members

n_r = number of support conditions, and

s = special conditions such as built-in hinges

For a more complete discussion, see Wilbur and Norris (Ref. A-5).

A two-span beam with plastic section capacity M_p will be used to illustrate the use of these theorems, see Figures A-10 and A-11.

Consider Mode 1 (see Figure A-11):

Work in = Work out

$$P(1) = M_p (\phi_A + \phi_B) + M_p \phi_B$$

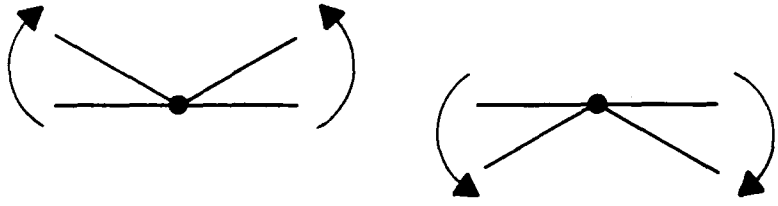

Uniqueness (1) = kinematics satisfied

Uniqueness (2) = to be verified

Uniqueness (3) = to be verified

Uniqueness (4) = dissipation satisfied

Solving

$$P = M_p (2/\ell + 2/\ell) + M_p 2/\ell$$

$$P = 6 M_p/\ell$$

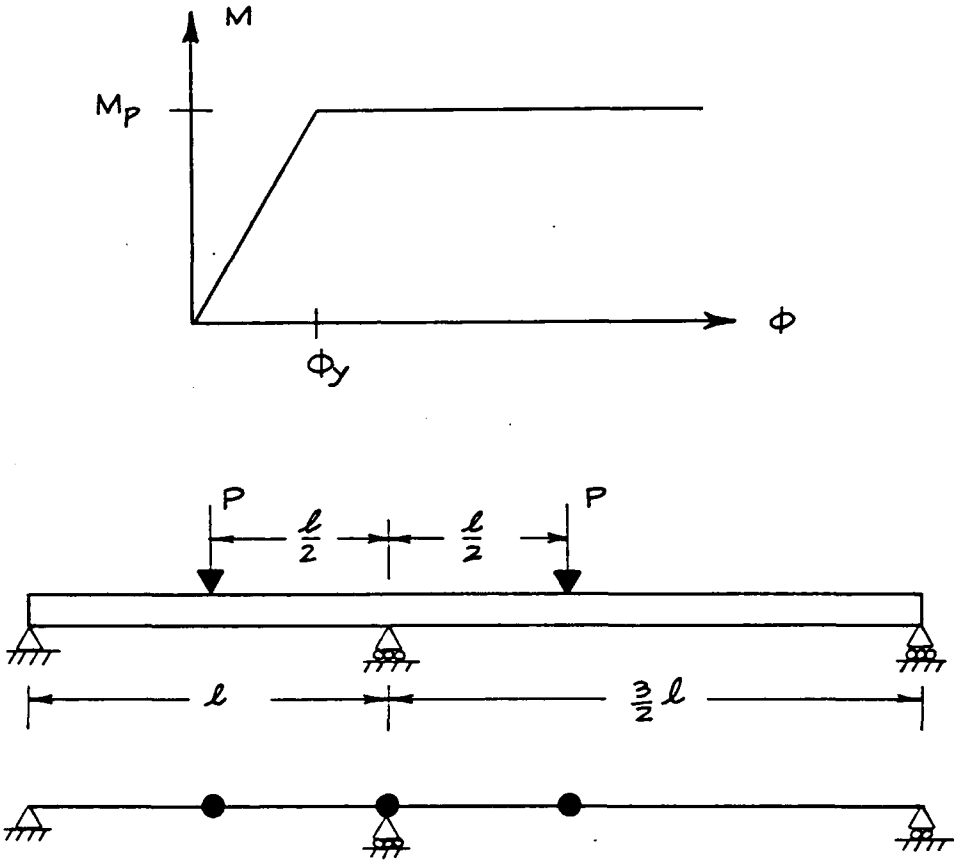

p = 3 possible hinges

r = 1 degree indeterminate

m = 2 independent mechanisms

Fig. A-10. Example Two-Span Beam.

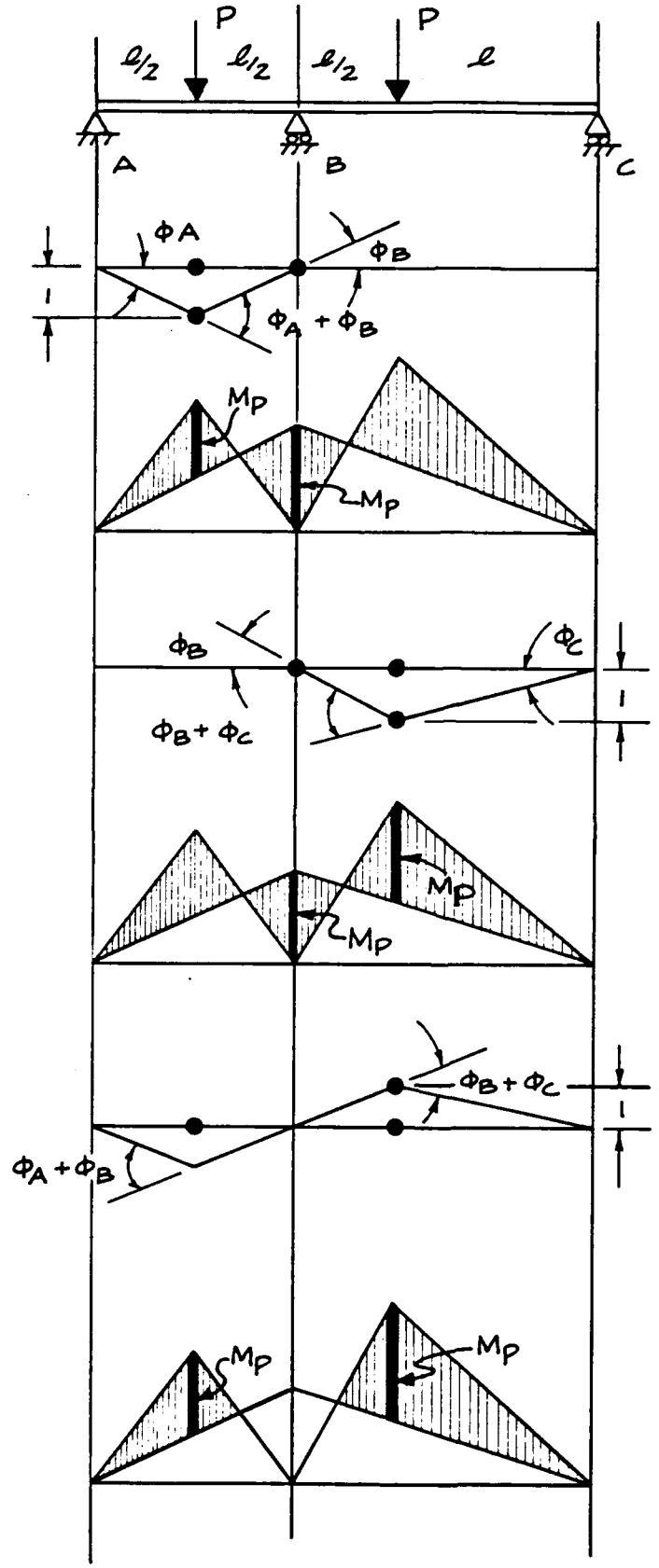

MODE 1

$\phi_A = 2/\ell = \phi_B$

Moment diagram for Mode 1

MODE 2

$\phi_B = 2/\ell$, $\phi_c = 1/\ell$

Moment diagram for Mode 2

"POSSIBLE" MODE 3

Possible moment diagram for Mode 3

Fig. A-11. Failure Modes for Two-Span Beam Example.

This is either a solution or an upper bound.

To satisfy equilibrium the moment diagram must be as shown

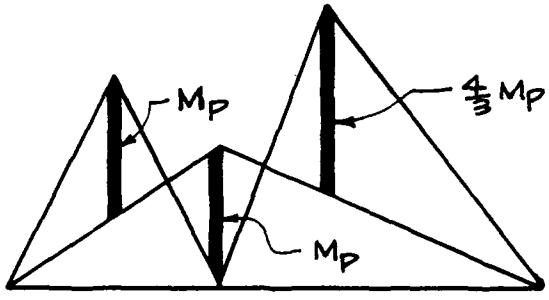

Hence we have an Upper Bound solution and have violated condition (3), i.e., exceeded capacity.

Upper bound solution

$$P = 6M_p/\ell$$

The lower bound solution can be found by reducing all moments by 3/4, and this creates a violation of condition (1) for kinematics. Hence, we know then the true solution is greater than

$$3/4(6\ M_p/\ell) = 9/2(M_p/\ell)$$

and we know

$$9/2(M_p/\ell) < P < 6M_p/\ell$$

from a single solution of the problem.

Consider Mode 2 (see Figure A-11):

work in = work out

$$P(1) = M_p\ (\phi_B + \phi_C) + M_p\ (\phi_B)$$

$$P = M_p\ (2/\ell + 1/\ell) + M_p\ 2/\ell$$

$P = 5M_p/\ell$, which is either an upper bound or the solution.

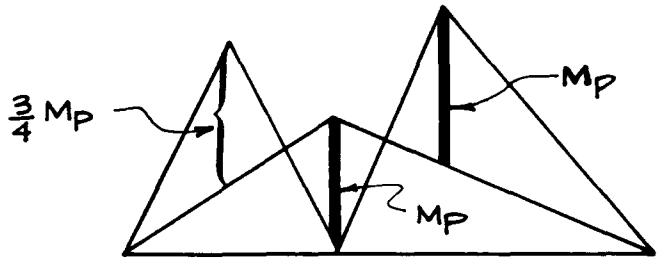

Equilibrium Moment Diagram

Therefore the Mode 2 solution satisfies

Uniqueness (1) - kinematics

Uniqueness (2) - equilibrium

Uniqueness (3) - $|M| \leq M_p$ everywhere

Uniqueness (4) - dissipation

Therefore $P = 5M_p/\ell$ is the solution.

Consider "possible" Mode 3 (see Figure A-11):

The uniqueness theorem part (4) requires a positive work or energy dissipation.

O.K. LEFT SPAN
$+\Phi$, $+M$

NO GOOD
$+M$, $-\phi$

Hence Mode 3 is inadmissible, as it violates the uniqueness theorem.

The power of the foregoing theorems and arguments for our particular problem of "Frame Collapse" is very great indeed. Any assumed mode that satisfies (1) kinematics and (4) dissipation, will provide the upper and lower bound solutions. Further, if these bounds are reasonably close there is little rational reason for attempting to find the "exact" solution. The loading conditions under blast effects

have a wide range of possibilities and variations. The actual resistance functions (plastic moment and ductility) have great variability, plus the unknowns of actual construction and design variabilities are also present. All of these variabilities lead to the realization that reasonably close bounds can provide a satisfactory estimate of the collapse load.

To illustrate the foregoing, the following frame is presented.

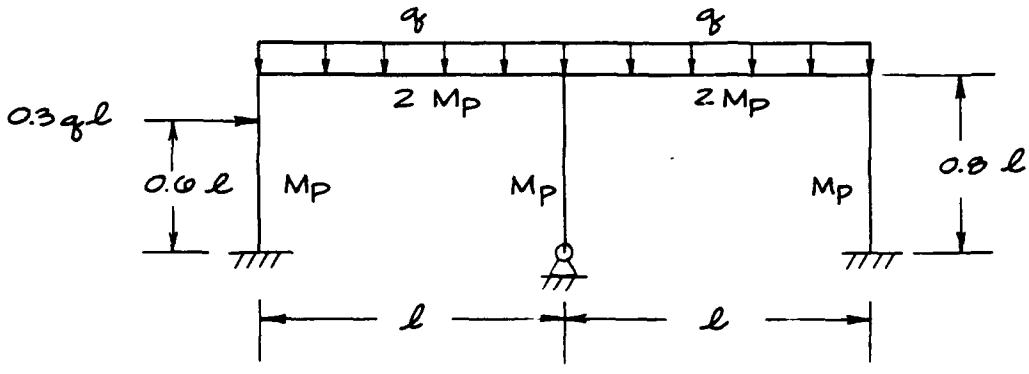

THE BASIC FRAME

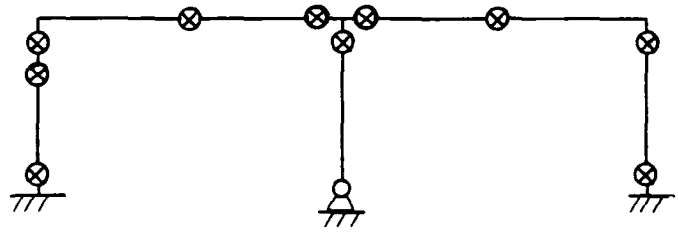

⊗ POTENTIAL HINGE LOCATIONS

Hence

h = 10 hinges

r = 5 redundancies

m = 5 independent mechanisms

The five independent mechanisms are shown in Figure A-12.

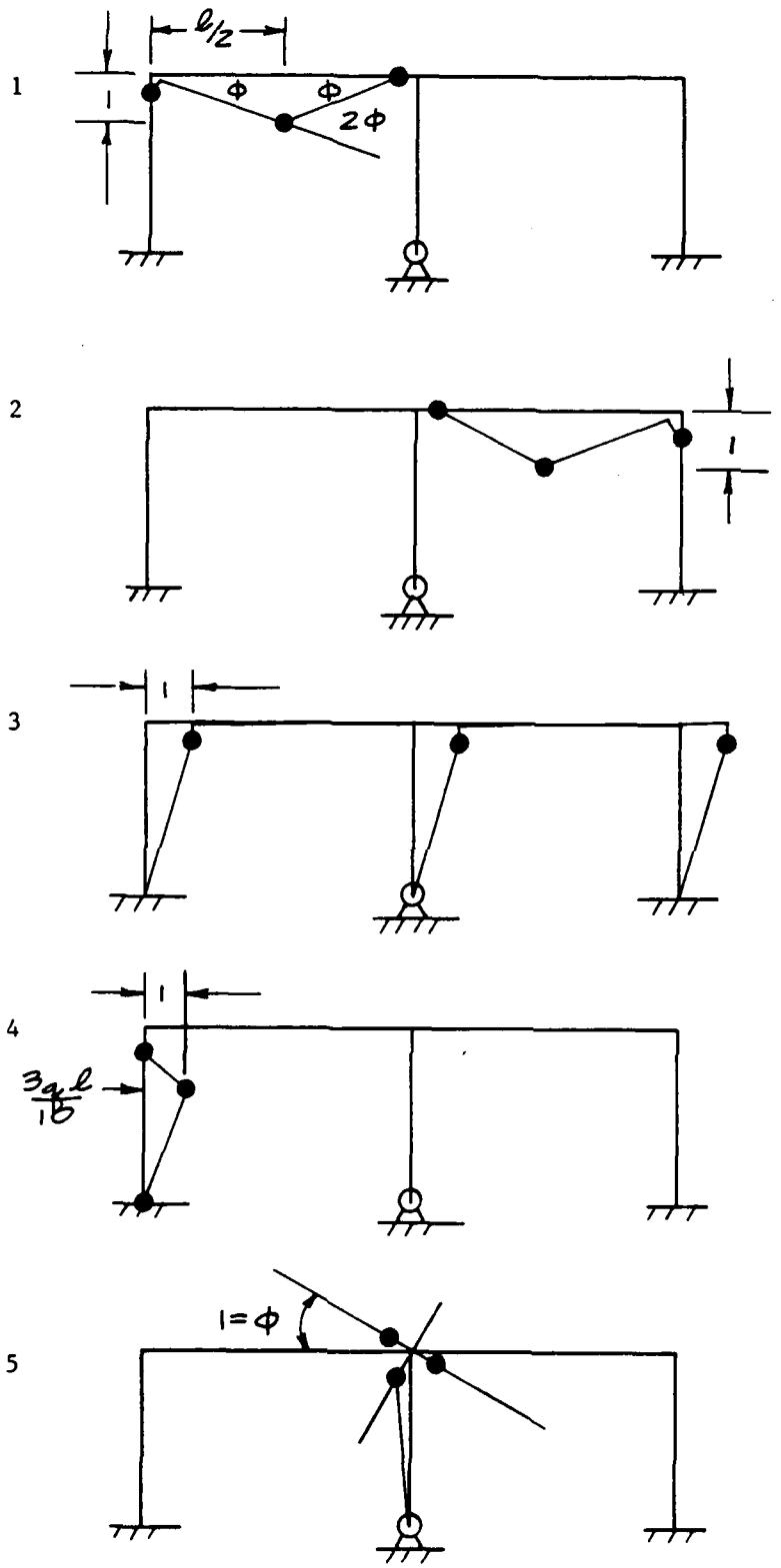

Fig. A-12. Independent Mechanisms.

The Solution (see Figure A-12)

(1) $q = (28M_p)/\ell^2$

is either a solution or upper bound.

(2) Same as mode 1 $q = (28M_p)/\ell^2$

Upper bound or solution

(3) Side sway $q = (27.8\ M_p)/\ell^2$

Upper bound or solution

(4) Column Mode $q = (44.4\ M_p)/\ell^2$

Upper bound or solution

(but obviously a very high bound)

(5) Hinge Mechanism

(Degenerate Mechanism) No energy dissipation

If we look at number (3), we find

$$q = (27.8\ M_p)/\ell^2$$

and this is either an upper bound or a solution. Solving for the equilibrium required by this solution we find an overshoot of $1.75\ M_p$.

Hence $27.80/1.75 = 15.9 < q\ \ell^2/M_p <$ 27.80

Lower bound Upper bound

This very first approximation boxes the answer by 25%. Going through several solutions, we find the solution is a combination of Modes 2, 3, and 5 plus one-third of Mode 4:

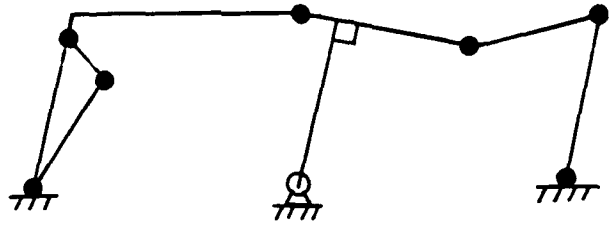

$q = (23.8\ M_p)/\ell^2$

which took five more solutions and looked promising. But adding Mode 1

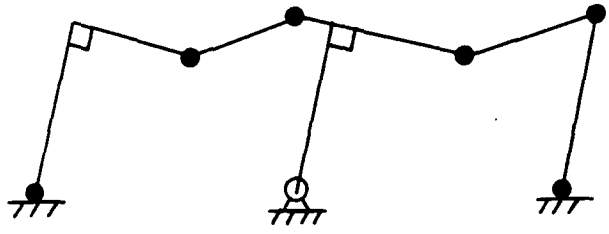

produces $q = (23.53\ M_p)/\ell^2$

and a 10% overshoot, of the M_p moment diagram, or

$$23.53/1.10 = 21.40 < q\ \ell^2/M_p < 23.53$$

and finally, success is achieved with

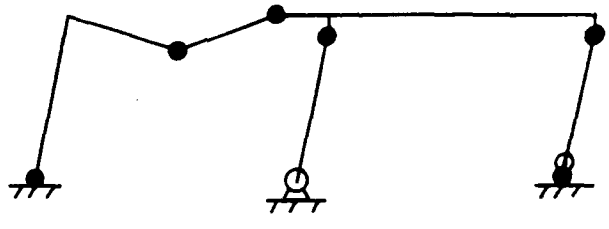

and $q = (22.83\ M_p)/\ell^2$

which is little different from the median of the first attempt. Hence, the bounds approach a very strong technique of estimating the correct failure load.

REFERENCES

A-1 Beedle, Lynn S., **The Plastic Design of Steel Frames**, John Wiley & Sons, New York, London, Sydney, 1958.

A-2 McCormac, Jack C., **Design of Reinforced Concrete**, Harper & Row Publishers, New York, 1978.

A-3 Hodge, Philip G., Jr., **Plastic Analysis of Structures**, McGraw-Hill, 1959.

A-4 Moy, Stuart S.J., **Plastic Methods for Steel and Concrete Structures**, Halsted Press, 1981.

A-5 Wilbur and Norris, **Elementary Structural Analysis**, McGraw-Hill, 1976.

APPENDIX B

COMPUTER ANALYSIS FUNDAMENTALS

COMPUTER ANALYSIS FUNDAMENTALS

Computer codes designed to solve static analyses of structures require the idealization of the two- or three-dimensional structure as an assemblage of finite elements connected at joints. The technique divides a structure into small elements with easily defined stress and deflection characteristics. Corners and, in some instances, midpoints of these elements are the locations known as grid points or nodes where deflections are calculated through the use of known stiffness properties, applied loads, and boundary conditions or displacement constraints. This finite element method is based on arrays of large matrix equations that appear complicated; however, the method is based on fundamentally simple concepts involving basic stiffness and deflection equations.

A model must be constructed that accurately represents the structural stiffness and displacement constraints and provides for the application of equivalent loadings. The input data are processed and the computer output provides nodal displacement, member forces, reactions, and stresses. Most large-scale commercial programs also have post-processing routines to allow the selection of specific output data. Stress contour plots can be generated for various sections through the model. Deformed shape plots are also available which show model displacements that are greatly exaggerated for clarity.

The computation of dynamic structural behavior requires the solution of the dynamic equations of equilibrium. These equations may be written in the following matrix form:

$$[M]\{\ddot{X}\}^{**} + [C]\{\dot{X}\}^{**} + [K]\{X\} = \{F(t)\} \qquad (1)$$

** $\ddot{X} = \frac{\partial^2 X}{\partial t^2}$ and $\dot{X} = \frac{\partial X}{\partial t}$

where t represents time.

where [M], [C], and [K] are matrices representing the mass, damping, and stiffness of the structure respectively. The vectors $\{\ddot{X}\}$, $\{\dot{X}\}$, and $\{X\}$ represent the accelerations, velocities, and displacements of the joint degrees of freedom. The vector $\{F(t)\}$ represents the dynamic, time-varying applied forces. Eq. 1 states that the sum of the inertial, damping, and elastic resistance forces of the structure must be equal to the applied loads at each point in time.

Each unrestrained joint degree of freedom in the structure is represented by an equation in matrix Eq. 1. In many instances, the forces acting at some of the degrees of freedom are small and do not significantly influence the behavior of the structure. The equations representing these degrees of freedom may be eliminated in order to reduce the total degrees of freedom of the structure prior to solution. Two techniques are used for reducing the dynamic degrees of freedom. These techniques are called STATIC and GUYAN CONDENSATION. To understand the difference between STATIC and GUYAN CONDENSATION, consider the undamped partitioned form of the Eq. 1.

$$\begin{bmatrix} M_{DD} & M_{DC} \\ M_{CD} & M_{CC} \end{bmatrix} \begin{Bmatrix} \ddot{X}_D \\ \ddot{X}_C \end{Bmatrix} + \begin{bmatrix} K_{DD} & K_{DC} \\ K_{CD} & K_{CC} \end{bmatrix} \begin{Bmatrix} X_D \\ X_C \end{Bmatrix} = \begin{Bmatrix} \{F_D\} \\ \{F_C\} \end{Bmatrix} \qquad (2)$$

The subscripts C and D in the above equation denote the degrees of freedom to be condensed and the dynamic degrees of freedom to be retained for solution respectively.

Both STATIC and GUYAN CONDENSATION assume that there is a linear transformation between the dynamic degrees of freedom and the condensed degrees of freedom:

$$\begin{aligned} \{X_C\} &= [T]\ \{X_D\} \\ \{\ddot{X}_C\} &= [T]\ \{\ddot{X}_D\} \end{aligned} \qquad (3)$$

where $[T]$ is the transformation which is independent of time. Using Eq. 3, both the dynamic and condensed displacements and accelerations may now be written as a function of only the dynamic degrees of freedom:

$$\begin{Bmatrix} [X_D] \\ [X_C] \end{Bmatrix} = \begin{bmatrix} [I] \\ [T] \end{bmatrix} \{X_D\} \tag{4}$$

and

$$\begin{Bmatrix} \{\ddot{X}_D\} \\ \{\ddot{X}_C\} \end{Bmatrix} = \begin{bmatrix} [I] \\ [T] \end{bmatrix} \{\ddot{X}_D\} \tag{5}$$

where $[I]$ is the identity matrix.

Substituting Eq. 4 and 5 into Eq. 2 and premultiplying by $\left[[I]\ [T]^T\right]$ to preserve symmetry yields:

$$\begin{aligned} &\left[[I]\ [T]^T\right] \begin{bmatrix} [M_{DD}] & [M_{DC}] \\ [M_{CD}] & [M_{CC}] \end{bmatrix} \begin{bmatrix} [I] \\ [T] \end{bmatrix} \{\ddot{X}_D\} + \\ &\left[[I]\ [T]^T\right] \begin{bmatrix} [K_{DD}] & [K_{DC}] \\ [K_{CD}] & [K_{CC}] \end{bmatrix} \begin{bmatrix} [I] \\ [T] \end{bmatrix} \{X_D\} = \left[[I]\ [T]^T\right] \begin{Bmatrix} \{F_D\} \\ \{F_C\} \end{Bmatrix} \end{aligned} \tag{6}$$

Performing the indicated operations in Eq. 6 results in the following two equations:

$$\begin{aligned}&\left[M_{DD}\right] + [T]^T \left[M_{CD}\right] + \left[M_{DC}\right][T] + [T]^T \left[M_{CC}\right][T] \left\{\ddot{X}_D\right\} + \\ &\left[K_{DD}\right] + [T]^T \left[K_{CD}\right] + \left[K_{DC}\right][T] + [T]^T \left[K_{CC}\right][T] \left\{X_D\right\} \\ &\qquad = \left\{F_D\right\} + [T]^T \left\{F_C\right\}\end{aligned} \tag{7}$$

and

$$\left[M_{CD}\right]\left\{\ddot{X}_D\right\} + \left[M_{CC}\right]\left\{\ddot{X}_C\right\} + \left[K_{CD}\right]\left\{X_D\right\} + \left[K_{CC}\right]\left\{X_C\right\} = \left\{F_C\right\} \tag{8}$$

Using Eq. 8 and further assuming that the inertial forces do not affect the relationship between $\{X_D\}$ and $\{X_C\}$ (i.e., they may be neglected), Eq. 8 may be solved for $\{X_C\}$ in terms of $\{X_D\}$, neglecting $\{F_C\}$ since it does not affect the free vibration problem:

$$\left\{X_D\right\} = -\left[K_{CC}\right]^{-1}\left[K_{CD}\right]\left\{X_D\right\} \tag{9}$$

Thus,

$$[T] = -\left[K_{CC}\right]^{-1}\left[K_{CD}\right] \tag{10}$$

Substituting Eq. 10 into Eq. 7 results in the following condensed equations of motion.

$$[M]^*\left\{\ddot{X}_D\right\} + [K]^*\left\{X_D\right\} = [F]^* \tag{11}$$

where

$$\begin{aligned}[M]^* = &\left[M_{DD}\right] - \left[K_{DC}\right]\left[K_{CC}\right]^{-1}\left[M_{CD}\right] - \left[M_{DC}\right]\left[K_{CC}\right]^{-1}\left[K_{CD}\right] \\ &+ \left[K_{DC}\right]\left[K_{CC}\right]^{-1}\left[M_{CC}\right]\left[K_{CC}\right]^{-1}\left[K_{CD}\right]\end{aligned} \tag{12}$$

$$[K]^* = \left[K_{DD}\right] - \left[K_{DC}\right]\left[K_{CC}\right]^{-1}\left[K_{CD}\right] \tag{13}$$

$$\{F\}^* = \{F_D\} - \left[K_{DC}\right]\left[K_{CC}\right]^{-1}\{F_C\} \tag{14}$$

Eq. 11 represents the condensed equations of motion for both STATIC and GUYAN CONDENSATION. The matrix $[K]^*$ in Eq. 13 is the same for both techniques. GTSTRUDL restricts the applied loadings to be applied only to the dynamic degrees of freedom (i.e., $\{F_C\} = 0$). Therefore,

$$\{F\}^* = \{F_D\} \tag{15}$$

for both methods. The form of $[M]^*$ is different in the two techniques. GUYAN CONDENSATION uses $[M]^*$ as given by Eq. 12 while STATIC CONDENSATION utilizes only $\left[M_{DD}\right]$ of Eq. 12 for $[M]^*$. A physical interpretation of the difference in the two techniques is that GUYAN CONDENSATION redistributes the mass of the structure including the mass associated with the condensed degrees of freedom while STATIC CONDENSATION considers only the mass associated with the dynamic degrees of freedom. GUYAN CONDENSATION is the recommended technique unless a very large portion of the mass of the structure is associated with only the dynamic degrees of freedom. The only advantage of STATIC CONDENSATION is reduced computational effort required to form $[M]^*$.

The vibration of an elastic structure is assumed to be harmonic in nature. The total vibration of an elastic structure may be considered to be a linear combination of the characteristic harmonic mode shapes denoted by $\{\Phi\}$. Thus, the displacement and acceleration of any characteristic mode of vibration, i, may be expressed in the following manner:

$$\{X\}_i = \{\Phi\}_i \sin \omega_i t \tag{16}$$

$$\{\ddot{X}\}_i = -\{\Phi\}_i \omega_i^2 \sin \omega_i t \tag{17}$$

where ω_i is the frequency of vibration in the i^{th} mode. The undamped equation of free vibration is

$$[K]\{X\} = -[M]\{\ddot{X}\} \tag{18}$$

Substituting Eqs. 16 and 17 into 18 yields,

$$[K]\{\Phi\}_i = \omega_i^2 [M]\{\Phi\}_i \tag{19}$$

Eq. 19 is therefore an eigenvalue problem in nonstandard form in which the eigenvalues are the squares of the frequencies and the eigenvectors are the vibrational modes associated with the frequencies. Considering all possible frequencies and mode shapes, Eq. 19 may be written as

$$[K][\Phi] = [\Omega][M][\Phi] \tag{20}$$

where $[\Omega]$ is diagonal containing the eigenvalues on the diagonals in order of increasing magnitude. The matrix $[\Phi]$ contains the eigenvectors stored columnwise in an order corresponding to the eigenvalues in $[\Omega]$. The matrix $[\Omega]$ is often called the spectral matrix while $[\Phi]$ is called the modal matrix.

Eq. 20 must be transformed to standard eigenvalue form ($[D][\Gamma] = [\Omega][\Gamma]$) in order to compute the eigenvalue and eigenvector solution. An orthogonal similarity transformation is used for the transformation in order to preserve symmetry in $[D]$. The eigenvalues of the original equation are invariant under this transformation while the eigenvectors are transformed. For lumped mass, the transformation assumes a new eigenvector basis such that

$$[\Phi] = [M]^{-\frac{1}{2}}[\Gamma] \tag{21}$$

where

$$[M] = [M]^{\frac{1}{2}}[M]^{\frac{1}{2}} \tag{22}$$

The matrix $[M]^{\frac{1}{2}}$ is defined to be the square root of all elements in $[M]$. Since $[M]$ is a diagonal matrix for lumped mass, $[M]^{\frac{1}{2}}$ is the square root of only the diagonal elements. The matrix $[M]^{-\frac{1}{2}}$ in Eq. 21 is a diagonal matrix where the diagonal elements are one over the square root of the diagonal elements in $[M]$. Therefore,

$$[\Gamma] = [M]^{\frac{1}{2}} [\Phi] \tag{23}$$

Substituting Eq. 21 into 20 yields

$$[K] [M]^{-\frac{1}{2}} [\Gamma] = [\Omega] [M] [M]^{-\frac{1}{2}} [\Gamma] \tag{24}$$

Now, substituting Eq. 22 into Eq. 24 produces

$$[K] [M]^{-\frac{1}{2}} [\Gamma] = [\Omega] [M]^{\frac{1}{2}} [M]^{\frac{1}{2}} [M]^{-\frac{1}{2}} [\Gamma] \tag{25}$$

Multiplying by $[M]^{-\frac{1}{2}}$ and realizing that $[M]^{\frac{1}{2}} [M]^{-\frac{1}{2}}$ is equal to the identity matrix yields

$$[D] [\Gamma] = [\Omega] [\Gamma] \tag{26}$$

where $[D]$ is symmetric and is defined as

$$[D] = [M]^{-\frac{1}{2}} [K] [M]^{-\frac{1}{2}} \tag{27}$$

Eq. 26 is the eigenvalue problem in standard form. Again, the eigenvalues in $[\Omega]$ have remained invariant under the transformation while the eigenvectors have been transformed using Eq. 23.

If the response of a structure due to a transient loading is desired as a function of time, a time history analysis must be performed. For the time history analysis a modal superposition method is used. The modal superposition method requires the solution of Eq. 19 for the frequencies and mode shapes. The mode shapes, $[\Phi]$, can be shown to be orthogonal with respect to the mass and stiffness matrices. The mode

shapes may be normalized to produce the following results:

$$[\Phi]^T [M] [\Phi] = [I] \tag{28}$$

When normalized according to Eq. 28, the mode shapes are said to be "normalized to unit mass". When the mode shapes are normalized to unit mass, the following relation is also valid:

$$[\Phi]^T [K] [\Phi] = [\Omega] \tag{29}$$

Eqs. 28 and 29 permit the equations of motion to be uncoupled in a dynamic analysis. Prior to uncoupling, the equation of motion in physical (structure) coordinates is given by

$$[M] \{\ddot{X}\} + [C] \{\dot{X}\} + [K] \{X\} = \{F(t)\} \tag{30}$$

The accelerations, velocities, and displacements in Eq. 30 are transformed to a different coordinate system:

$$\{\ddot{X}\} = [\Phi] \{\ddot{U}\}; \quad \{\dot{X}\} = [\Phi] \{\dot{U}\}; \quad \text{and} \quad \{X\} = [\Phi] \{U\} \tag{31}$$

where $[\Phi]$ is the modal matrix normalized to unit mass as presented in Eq. 28. The vectors $\{\ddot{U}\}$, $\{\dot{U}\}$, and $\{U\}$ in Eq. 31 are the accelerations, velocities and displacements respectively of the structure in what is defined as the normal coordinate system.

Substituting Eq. 31 into Eq. 30 and premultiplying by $[\Phi]^T$ yields

$$[\Phi]^T [M] [\Phi] \{\ddot{U}\} + [\Phi]^T [C] [\Phi] \{\dot{U}\} + [\Phi]^T [K] [\Phi] \{U\} = [\Phi]^T \{F(t)\} \tag{32}$$

Substituting Eqs. 28 and 29 into Eq. 32 yields

$$\{\ddot{U}\} + [\Phi]^T [C] [\Phi] \{\dot{U}\} + [\Omega] \{U\} = [\Phi]^T \{F(t)\} \tag{33}$$

Note that Eq. 33 will be completely uncoupled if $[\Phi]^T [C] [\Phi]$ is a diagonal matrix.

The inclusion of damping in Eq. 33 creates some difficulty. There are few theoretical means for determining the damping, and experimental investigations have produced data for only a small number of existing structures. The analyst can, however, usually assess a percentage of critical damping for each mode of interest. This percentage of critical damping for each mode i is called the damping ratio for mode i. This simplification allows Eq. 33 to be completely uncoupled, and a separate equation written for each mode i:

$$\ddot{U}_i + 2\eta_i\omega_i\dot{U}_i + \omega_i^2 U_i = f_i(t) \qquad (34)$$

where

$f_i(t)$ is the loading at the i^{th} normal coordinate, $= \Phi_i^T F(t)$,
η_i is the damping ratio for the i^{th} mode, and
ω_i is the frequency associated with the i^{th} mode.

Eq. 34 may now be solved since it is a linear differential equation. GTSTRUDL uses the Duhamel Integral solution which is exact except that the loading is assumed to be piecewise linear between integration points.

The modal superposition method requires that the eigenproblem be solved first and, if damping is present, damping ratios must be specified.

ANALYSIS PROCEDURE FOR A BUILDING STRUCTURE UNDER BLAST LOADING

The object of this computer-assisted analysis is to predict when failure of a multi-story building occurs because of the effects of a time-varying blast load and also to indicate what the collapse mechanism of the structure will be. Normally, the first step in any usual structural analysis would be the application of a static load in the direction of the blast load. However, unless a correlation can be found, based on previous experience or other criteria, between the blast load and the statically applied (pseudo-static) load, this method proves to be highly

unsatisfactory. In order to best predict response it is thus necessary to apply the blast load forcing function to the structure as a truly time-varying load, and determine the resulting behavior of the structure as a time-varying function.

Dynamic analyses are usually conducted within the range of elastic behavior of the system under consideration. A collapsing structure is outside of this range for the obvious reason that collapse does not occur in the elastic domain. Prior to collapse of a structure several behavioral phases must be satisfied. Initially, the structure behaves elastically until moments and forces are generated in structural components to cause local yielding, i.e., localized behavior outside the elastic range of the structural material. Plastic hinges are formed in individual members, which will now resist a constant moment only, independent of increased bending strain, except for a small increase due to what is normally referred to as strain hardening. If a sufficient number of plastic hinges have formed to cause the structure to behave as a mechanism, collapse is imminent. In the analysis two distinct structural behavior patterns were considered: first, elastic behavior until a sufficient number of columns and beams had reached the limits of their elastic range to cause the structure to develop a failure mechanism; second, plastic behavior until total collapse of the failure mechanism occurs at the fracture deformation end of the plastic range.

The plastic behavior was modeled using a reduced modulus of elasticity for those structural members that reached the limit of their elastic behavior. External moments equal to the plastic hinge moments were applied at those joints where a plastic hinge had formed as part of the failure mechanism. This unique method of modeling pseudo-plastic behavior retains stability of the structure, even though a mechanism has formed, and also provides a means of representing the strain hardening of the structural material. To retain continuity of behavior in the transition between the elastic and the plastic phase, the plastic phase was started with initial conditions of displacement and velocity equal to those displacements and velocities at the end of the elastic phase, see Figure B-1.

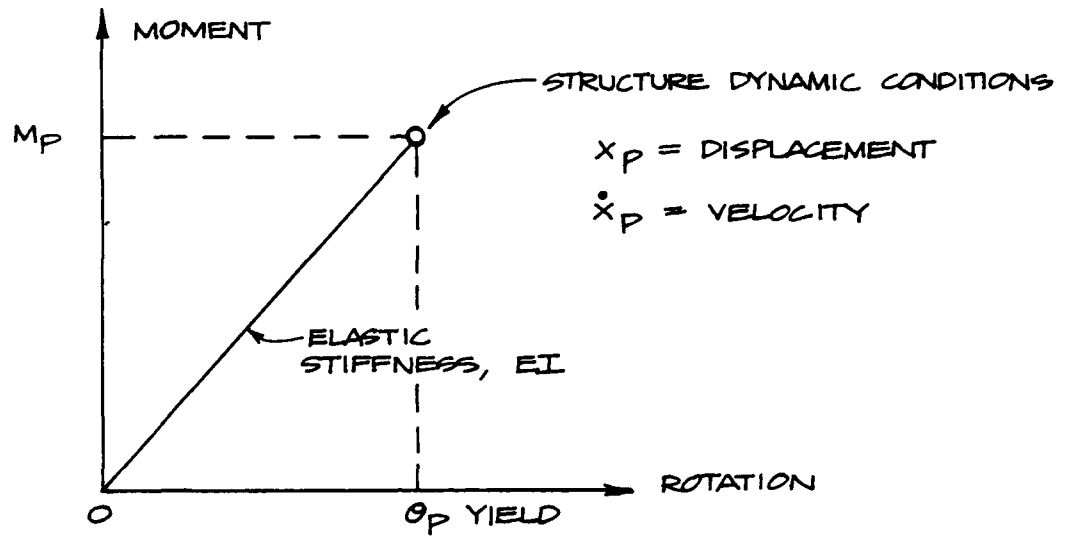

ELASTIC PHASE

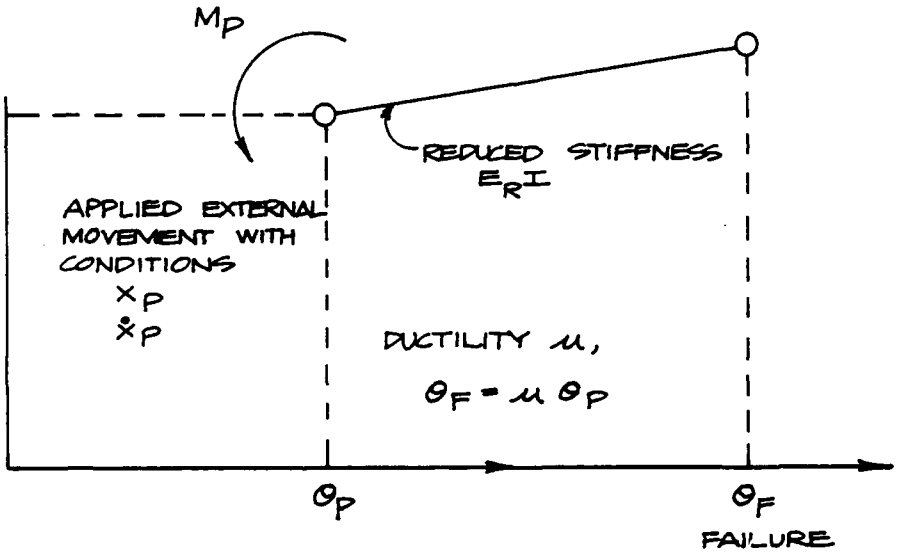

PSEUDO-PLASTIC PHASE

Fig. B-1. Computer Model for Elasto-Plastic Behavior.

REPRESENTATION OF DUCTILITY AND ELEMENT FAILURE CRITERIA

In Section 4 - Subtask 3b, the element strength and recommended ductility features (ratio of failure deformation to yield deformation) were given for both steel and reinforced concrete structural members. In order to incorporate these properties into the computer model, it is necessary to express the failure criteria in terms of bending moments rather than member section deformations (rotational angles). This is because the basic computer output is in terms of element forces (moments) rather than deformations.

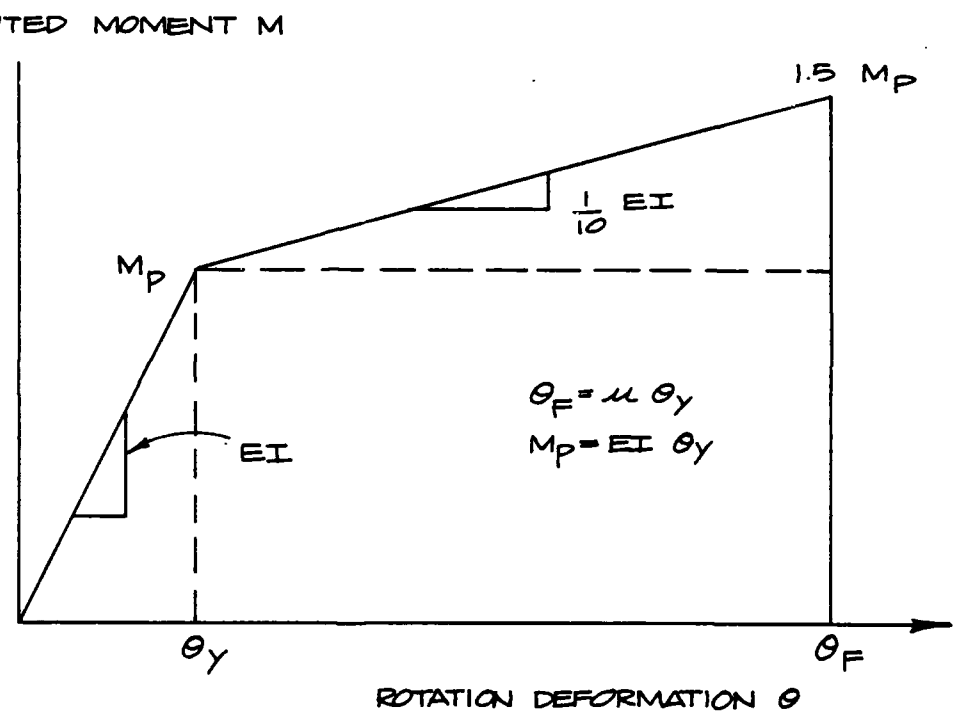

For example, if member failure is defined by a moment of 1.5 M_p in the inelastic (1/10 EI) portion of member deformation, then this corresponds to a ductility given by

$$0.5\ M_p = 0.5\ EI\ \theta_y = 1/10\ EI\ (\mu\ \theta_y)$$

or

$$\mu = 5$$

APPENDIX C

DEBRIS GENERATED LOADS

DEBRIS GENERATED LOADS

The ability to predict debris generated loads depends greatly upon the predicted strength of exterior and interior walls*. According to this reference, debris prediction and the resulting loads are only valid for accurate predictions of wall and partition strength. Data concerning building response to blast may be qualitatively useful when classified in terms of light, moderate, and severe damage, but do not reflect any information on debris production or distribution. Thus, data from shock tunnel tests and the Nevada weapons tests were used to construct debris charts. These charts predict the percent of building material that will become debris at various incident overpressures for a specific type of construction.

The intended use of these charts is to provide additional data to develop floor loadings that will affect the frame response. In the case of complete collapse, the frame response, combined with debris, will load the roof of the basement shelter. For any event less than that to cause total collapse, the following general scenario applies for a multi-story steel or reinforced-concrete frame structure, with many frangible walls, having the same general proportions as the Peachtree Building.

The exterior wall facing the blast will, upon failure, transfer its horizontal and vertical energy to the floor below through friction and/or collision with interior partitions and objects. The exterior walls on the back side, if failed, will fall onto an adjacent site. At 40 psi incident overpressure, and for a blast of long duration, considerable debris from interior and exterior walls may leave the site as well. However, up to a point, long duration blast waves will also greatly increase the drag loading -- thereby increasing the structural damage and the production of debris. Therefore, considering total wall weight as debris for more than 3 psi overpressure is conservative.

---

* Edmunds, James E., **Structural Debris and Building Damage Prediction Methods**, URS 686-5, URS Research Company, Burlingame, CA, June 1968.

The vertical energy imparted to the floor below can be expressed as the weight of the element times the height through which it falls. However, the resulting force is very small compared to existing vertical forces, especially when the weight of the exterior wall is considered to be approximately evenly distributed over the floor area. The horizontal force vector generated by the debris can be determined from the drag loading expressed as

$$F(t) = C_d\, q(t)\, A$$

The dynamic pressure pulse, q(t), acts on the exposed debris in the same manner as on the exposed frame with a area A and a drag coefficient C_d. If the coefficient of friction, μ, times the debris weight exceeds F(t) above, the debris will not move. As long as F(t) is greater than the debris weight times μ, the debris will slide across the floor generating a horizontal force on the floor, generally until it is carried out. Assuming μ is independent of velocity (i.e., nearly constant), the maximum horizontal force generated by debris will be

$$F_{max} = \text{weight} \cdot \mu_s$$

for a duration less than t_+. Table C-1 shows the approximate values of μ_s for different surfaces.

TABLE C-1: STATIC COEFFICIENTS OF FRICTION OF DRY MATERIALS

Material	μ_s
Concrete to concrete	0.8
Concrete to steel	0.4
Debris on concrete	0.6

The procedure to determine the debris generated frame loading is to first find the incident overpressure and duration for a given weapon (see Section 4, Subtask 3A) then, determine weight of wall material assuming that it becomes debris. Use

Table C-2 for a given building type and determine the volume of structural materials. This volume times the unit weight gives the weight of the structural debris. The contents (interior partitions, etc.) can also contribute significantly. Therefore, determine volume of contents from the type of occupancy in Table C-3 and multiply by 60 lbs per ft^3 to obtain contents weight, and add this to the weight of structural debris for total debris weight. Multiply total weight (walls and contents) by the appropriate coefficient(s) of friction (from Table C-1) and add this to the structural frame. Mathematically this procedure is expressed as:

$$\text{Frame Loading} = V_c \cdot w(\text{wt/ft}^3) + KA_p\mu_s$$

where V_c is volume of structural content

w is the weight per unit volume of structural material

K is a contents coefficient from Table C-3

A_p is the plan area, and

μ_s is coefficient of friction from Table C-1.

Of course, this expression is for one story; the same procedure can be used for each story in a multi-story building.

DEBRIS LOADING DATA

In Subtask 3A (see Section 4) available research establishes the failure of exterior walls due to blast pressures at the range of 5 to 15 psi. In the computer analysis this 100% debris weight is represented by an increase in the assigned gravity load (or dead load) on the structure model.

The corresponding friction drag force of the moving debris action on the building frame and floor slabs is represented by the use of a high "conservative" drag coefficient C_d in the evaluation of the drag pressure portion of the blast loading function.

TABLE C-2.

STRUCTURE VOLUME VS BUILDING TYPE

BUILDING TYPE	VOLUME FORMULA*
1. Wood Frame Residential	$V_c = A_p \cdot$ height
a. 1st floor slab on ground	$[0.55 + (N-1)(0.525)]A_p$
b. 1st floor on std. joists	$[0.7 + (N-1)(0.525)]A_p$
2. Steel Frame Industrial	
a. Light W/CI sheathing	$0.02\ A_p$
W/CA sheathing	$0.087\ A_p$
b. Heavy W/CI sheathing	$0.037\ A_p$
W/CA sheathing	$0.095\ A_p$
3. Load-Bearing Masonry with or without reinforcing - Combustible interior framing	$0.12\ V_c$
4. Reinforced Concrete Shear-Wall	
a. W/lt. interior panels	$0.07\ V_c$
b. W/masonry interior panels	$0.12\ V_c$
5. Multistory Steel and Reinforced Concrete Frame with Earthquake Design	
a. W/lt. interior panels	$0.07\ V_c$
b. W/masonry interior panels	$0.11\ V_c$
6. Multistory Steel and Reinforced Concrete Frame (non-earthquake design)	
a. W/lt. interior panels	$0.063\ V_c$
b. W/masonry interior panels	$0.10\ V_c$

* These formulae reflect solid volume of material (i.e., no void-void ratio = 0). The void ratio (usually taken as unity) is best applied after summation of contributory volumes. This minimizes the number of calculations required for making debris volume or debris depth estimates.

TABLE C-2 (contd)

STRUCTURE VOLUME VS BUILDING TYPE

BUILDING TYPE	VOLUME FORMULA*
7. Light Reinforced Concrete Shear-Wall (single story)	
a. Concrete roof w/lt. interior panels	0.07 V_c
b. Concrete roof w/masonry interior panels	0.075 V_c
c. Mill roof w/lt. int. panels	0.037 V_c
d. Mill roof w/masonry interior panels	0.05 V_c

LEGEND:

V_c contained volume

A_p plan area

S&P stucco exterior plaster interior

W&P wood exterior plaster interior

W all wood

CI corrugated iron

CA corrugated asbestos

TABLE C-3

BUILDING CONTENTS LOADS AND VOLUME FACTORS

OCCUPANCY	PSF TOTAL	VOLUME FACTOR K ($V = KA_p$)*
		TOTAL
1. Apts. and Residential	5	0.625
2. Auditoriums and Churches	1.5	0.25
3. Garage		
a. Storage	15	0.75
b. Repair	11	0.55
4. Gymnasium	0.5	0.09
5. Hospitals	3	0.375
6. Hotels	5	0.625
7. Libraries	26	0.75
8. Manufacturing		
a. Comb. Mdse. fabrics, furniture	18	1.8
b. Incombustible	11	0.55
9. Offices	12	1.2
10. Printing Plant		
a. Newspaper	23	0.9
b. Books	60	1.7
11. Schools	11	1.6
12. Storage		
a. Gen. Mdse.	35	6
b. Special	**	
13. Stores		
a. Retail Dept.	12	2
b. Wholesale	16	2.7
14. Restaurant	3.5	0.6

* V = Volume in cubic feet = KA_p

A_p = Plan area in square feet

It is most appropriate here to note a lack of research information. Specifically, all of the exterior wall blast research is in the range of 1 psi < p_o < 10 psi loading. The area of interest in this research is in the range of 30 psi $\leq$ p_o $\leq$ 50 psi, and it is most difficult to extrapolate and forecast wall-frame interaction forces and the resulting debris drag load effects in this high pressure range. There is certainly a need for both analysis and testing research to bridge this knowledge gap for high blast pressure effects on debris and debris-structure interaction.

DISTRIBUTION LIST

(One copy unless otherwise specified)

Federal Emergency Management Agency
Attn: Assistant Associate Director
for Research
National Preparedness Programs
Directorate
Washington, D.C. 20472 (60)

Dr. Michael A. Pachuta
Industrial Protection Division
National Preparedness Programs
Federal Emergency Management Agency
Washington, D.C. 20472

Mr. Phillip M. Smith
Associate Director
Natural Resources & Commercial
Services
Office of Science and Technology Policy
Executive Office Building
Washington, D.C. 20500

Defense Technical Information Center
Cameron Station
Alexandria, VA 22314 (12)

Mr. Carl Wiehle
Defense Intelligence Agency
Attn: CKW DB-4C2
Washington, D.C. 20301

Director, Defense Nuclear Agency
Attn: Technical Library
Washington, D.C. 20305

Director, Defense Nuclear Agency
Attn: Mr. Tom Kennedy
Washington, D.C. 20305

Assistant Secretary of the Army (R&D)
Attn: Assistant for Research
Washington, D.C. 20306

Director, Army Materials and Mechanics
Research Center
Attn: Technical Library
Watertown, MA 02172

Chief of Engineers
Department of the Army
Attn: ENGEME-RD
Washington, D.C. 20314

Director, U.S. Army Ballistic Research
Laboratory
Attn: Document Library
Aberdeen Proving Ground, MD 21005

Mr. William Taylor
Ballistic Research Laboratory
Aberdeen Proving Ground, MD 21005 (2)

Director, U.S. Army Engineer
Waterways Experiment Station
Attn: Document Library
P.O. Box 611
Vicksburg, MS 39180

Mr. W.L. Huff
USAE Waterways Experiment Station
P.O. Box 631
Vicksburg, MS 39180

Chief of Naval Research
Washington, D.C. 20306

Commanding Officer
U.S. Naval Civil Engineering Laboratory
Attn: Document Library
Port Hueneme, CA 93041

Civil Engineering Center AF/PRECET
Attn: Technical Library
Wright-Patterson Air Force Base
Dayton, OH 45433

Air Force Weapons Laboratory
Attn: SUL Technical Library
Kirtland Air Force Base
Albuquerque, NM 87117

Air Force Weapons Laboratory
Civil Engineering Division
Kirtland Air Force Base
Albuquerque, NM 87117

Mr. Lewis V. Spencer
National Bureau of Standards
Room C313 - Building 245
Washington, D.C. 20234

Mr. Samuel Kramer, Chief
Office of Federal Building Technology
Center for Building Technology
National Bureau of Standards
Washington, D.C. 20234

Dr. Barry Bowman
Lawrence Livermore National Laboratory
University of California
Box 808,
Livermore, CA 94550

Oak Ridge National Laboratory
Attn: Librarian
P.O. Box X
Oak Ridge, TN 37830

Emergency Technology Division
Oak Ridge National Laboratory
Attn: Librarian
Oak Ridge, TN 37830

Los Alamos Scientific Laboratory
Attn: Document Library
Los Alamos, NM 87544

Dr. Clarence R. Mehl
Division 1112
Sandia National Laboratories
Box 5800
Albuquerque, NM 87185

GARD, Inc.
7449 N. Natchez Ave.
Niles, IL 60648

Mr. C. Wilton
Scientific Service, Inc.
517 East Bayshore
Redwood City, CA 94063 (2)

Mr. Richard Laurino
Center for Planning and Research
2483 E. Bayshore Road, Suite 104
Palo Alto, CA 94303

Mr. Fred Sauer
Physics International Company
2700 Merced Street
San Leandro, CA 94577

The Dikewood Corporation
1613 University Blvd, N.E.
Albuquerque, NM 87102

Applied Research and Associates
Attn: Cornelius J. Higgins
2601 Wyoming Blvd, Suite H-1
Albuquerque, NM 87112

Mr. Thomas E. Watermann
IITRI
10 West 35th Street
Chicago, IL 60616 (2)

Mr. Leo A. Schmidt
Institute for Defense Analyses
Program Analysis Division
400 Army-Navy Drive
Arlington, VA 22202

The RAND Corporation
Attn: Document Library
1700 Main Street
Santa Monica, CA 90401

Director,
Lovelace Foundation
5200 Gibson Blvd, S.E.
Albuquerque, NM 87108

Dr. William Chenault
Human Sciences Research, Inc.
Westgate Industrial Park
7710 Old Springhouse Road
McLean, VA 22102

Mr. Kenneth Kaplan,
30 White Plains Court
San Mateo, CA 94402

Mr. John Rempel
Center for Planning and Research
2483 E. Bayshore
Palo Alto, CA 94303

H.L. Murphy Associates
Box 1727
San Mateo, CA 94401

Mr. James Beck Associates
4216 Los Palos Avenue
Palo Alto, CA 94306

Mr. Walmer Strope
Center for Planning and Research
5600 Columbia Pike - Suite 101
Bailey's Crossroads, VA 22041

Research Triangle Institute
Attn: Robert A. Frank
P.O. Box 12294
Research Triangle Park,
North Carolina 22709 (2)

Harvey G. Ryland
Ryland Research, Inc.
5266 Hollister Avenue
Suite 324
Santa Barbara, CA 93111

Dr. John Cockayne
Senior Scientist
Science Applications, Inc.
1710 Goodridge Drive
P.O. Box 1303
McLean, VA 22101

Bell Telephone Laboratories
Attn: Mr. E. Witt
Mr. R. May
Mr. J. Foss
Whippany Road
Whippany, NJ 07981 (3)

Mr. Raymond Alger
SRI International
333 Ravenswood
Menlo Park, CA 94025

Mr. Jud Leech
BDM Corporation
1801 Randolph Road, S.E.
Albuquerque, NM 87106

Dr. Ben Sussholz
R1/2094
TRW
One Space Park
Redondo Beach, CA 90278

Mr. Anatole Longinow
IITRI
10 West 35th Street
Chicago, IL 60616

Stan Martin & Associates
860 Vista Drive
Redwood City, CA 96062

Dr. Joseph E. Minor, Director
Institute for Disaster Research
Department of Civil Engineering
Box 4089
Lubbock, TX 79409

Professor R.K. Pefley
University of Santa Clara
Santa Clara, CA 95053

THE ANALYSIS OF THE EFFECTS OF FRAME RESPONSE ON BASEMENT SHELTERS IN TALL BUILDINGS

Unclassified
October 1982

Scientific Service, Inc., Redwood City, CA
Contract EMW-C-0570, Work Unit 1128E
156 pages

This report presents the results of a program to develop a theoretical analysis of the effects of frame response on basement shelters in tall buildings. The objective was to determine the effect on an upgraded basement key worker shelter of the aboveground portion of the structure being subjected to a blast wave that would destroy the building.

Both steel and reinforced concrete frame structures were investigated, with most emphasis on poured-in-place reinforced concrete beam, slab, and girder type framing and poured-in-place flat-slab and flat plate construction. A prediction technique using both hand and computer analysis was developed and tested using a previously demolished 15-story cast-in-place reinforced structure. The analysis indicated that the upgraded basement would have survived even though the aboveground portion of the structure was exposed to 50 psi.

THE ANALYSIS OF THE EFFECTS OF FRAME RESPONSE ON BASEMENT SHELTERS IN TALL BUILDINGS
Unclassified
October 1982
Scientific Service, Inc., Redwood City, CA
Contract EMW-C-0570, Work Unit 1128E
156 pages

This report presents the results of a program to develop a theoretical analysis of the effects of frame response on basement shelters in tall buildings. The objective was to determine the effect on an upgraded basement key worker shelter of the aboveground portion of the structure being subjected to a blast wave that would destroy the building.

Both steel and reinforced concrete frame structures were investigated, with most emphasis on poured-in-place reinforced concrete beam, slab, and girder type framing and poured-in-place flat-slab and flat plate construction. A prediction technique using both hand and computer analysis was developed and tested using a previously demolished 15-story cast-in-place reinforced structure. The analysis indicated that the upgraded basement would have survived even though the aboveground portion of the structure was exposed to 50 psi.

THE ANALYSIS OF THE EFFECTS OF FRAME RESPONSE ON BASEMENT SHELTERS IN TALL BUILDINGS
Unclassified
October 1982
Scientific Service, Inc., Redwood City, CA
Contract EMW-C-0570, Work Unit 1128E
156 pages

This report presents the results of a program to develop a theoretical analysis of the effects of frame response on basement shelters in tall buildings. The objective was to determine the effect on an upgraded basement key worker shelter of the aboveground portion of the structure being subjected to a blast wave that would destroy the building.

Both steel and reinforced concrete frame structures were investigated, with most emphasis on poured-in-place reinforced concrete beam, slab, and girder type framing and poured-in-place flat-slab and flat plate construction. A prediction technique using both hand and computer analysis was developed and tested using a previously demolished 15-story cast-in-place reinforced structure. The analysis indicated that the upgraded basement would have survived even though the aboveground portion of the structure was exposed to 50 psi.

THE ANALYSIS OF THE EFFECTS OF FRAME RESPONSE ON BASEMENT SHELTERS IN TALL BUILDINGS
Unclassified
October 1982
Scientific Service, Inc., Redwood City, CA
Contract EMW-C-0570, Work Unit 1128E
156 pages

This report presents the results of a program to develop a theoretical analysis of the effects of frame response on basement shelters in tall buildings. The objective was to determine the effect on an upgraded basement key worker shelter of the aboveground portion of the structure being subjected to a blast wave that would destroy the building.

Both steel and reinforced concrete frame structures were investigated, with most emphasis on poured-in-place reinforced concrete beam, slab, and girder type framing and poured-in-place flat-slab and flat plate construction. A prediction technique using both hand and computer analysis was developed and tested using a previously demolished 15-story cast-in-place reinforced structure. The analysis indicated that the upgraded basement would have survived even though the aboveground portion of the structure was exposed to 50 psi.